Decoupling of Magnetic Resonance Signals in Time and Frequency Domain

THÈSE N^{O} 5688 (2013)

PRÉSENTÉE LE 15 MARS 2013

LABORATOIRE DE RÉSONANCE MAGNÉTIQUE BIOMOLÉCULAIRE
PROGRAMME DOCTORAL EN CHIMIE ET GÉNIE CHIMIQUE

ÉCOLE POLYTECHNIQUE FÉDÉRALE DE LAUSANNE

POUR L'OBTENTION DU GRADE DE DOCTEUR ÈS SCIENCES

PAR

Takuya Fabian SEGAWA

acceptée sur proposition du jury:

Prof. M. Chergui, président du jury
Prof. G. Bodenhausen, directeur de thèse
Prof. J.-Ph. Ansermet, rapporteur
Dr J. Keeler, rapporteur
Prof. J. Kowalewski, rapporteur

ÉCOLE POLYTECHNIQUE
FÉDÉRALE DE LAUSANNE
Suisse
2013

Wissenschaft ist Spektralanalyse.
Kunst ist Lichtsynthese.
— Karl Kraus (1874-1936)

There is nothing that nuclear
spins will not do for you,
as long as you treat them
like human beings.
— Erwin Hahn (1921-)

Acknowledgements

I would like to express my gratitude to all those who contributed in their individual ways to this thesis, but whose names do not appear on the title page.

I thank Prof. Bodenhausen for accepting me twice: First, in 2006 as an exchange student from Zurich in his group in Paris and again, in 2009 as a PhD student here in Lausanne. Geoffrey has a unique knowledge and intuition of spins: a true source of inspiration. It is the freedom of research under his supervision that makes the spirit of the *Laboratoire de Résonance Magnétique Biomoléculaire* (LRMB).

I would like to thank all members of my thesis jury for kindly accepting to be a part of my examination committee: Prof. Majed Chergui (EPFL), president of the jury, Prof. Jean-Philippe Ansermet (EPFL), Dr James Keeler (University of Cambridge, UK), and Prof. Jozef Kowalewksi (Stockholm University, Sweden).

It was Bikash Baishya with whom I had the closest collaboration during these four years. With much patience, he taught me how to work at the spectrometer and was an invaluable guide to me. My favourite projects in the last two years were rendered possible thanks to Diego Carnevale. His profound knowledge of solid-state NMR turned out to be very helpful for our liquid-state experiments. I really appreciate the privilege to have been formed by two experienced postdocs. This thesis would perhaps never have been written if Nicolas Aeby would not have gently encouraged me to continue his research on echo modulations. I can only thank him for his efforts: I am still wholeheartedly fascinated by this subject! Nicolas did not only introduce me to his experiments, but also generously shared his last project with me. When Bikash left, it was Pascal Miéville who joined me in exploring the mysteries of 360° pulses. His support was very important to me and his analytical precision brought the project forward.

Besides echoes and decoupling, I had the pleasure to look into other fields of research in our group. In the "HDR" project, I benefited from a collaboration with Mariachiara Verde, Simone Ulzega, Fabien Ferrage, and Nicola Salvi, where I learned a lot about relaxation phenomena. I found singlet NMR spectroscopy always an exciting topic and hoped to find synergies with "my" echoes. Although my contributions are minor, I am happy and honoured to be part of a "long-lived" paper, together with the experts Srinivas Chithalapalli, Aurélien Bornet,

Riddhiman Sarkar and Sami Jannin.

I would like to thank Dr. Jens Dittmer, who discovered the SITCOM effect, and Dr. Karthik Gopalakrishnan, who developed the theory, for their time to kindly answer my questions by e-mail. I particularly enjoyed the collaboration about “WASTE” with Dr. Aitor Moreno from Bruker Biospin Switzerland in Fällanden that started at the Swiss NMR Symposium in Bern.

Since I came to EPFL, Aurélien Bornet was a part of our lab, first as an undergraduate and now as a PhD student. During two years I had the joy to share an office with Puneet Ahuja, not only a scientist but a poet at heart. Riddhiman, a gifted spectroscopist, was the most senior graduate student when I joined the group. He could often help me, when I felt lost in the complexity of NMR. I always enjoyed talking in German to Vroni Vitzthum, without doubt the most sportive lab member. Marc Caporini, a postdoc from the US, was a reliable source of good mood in the lab. I enjoyed numerous discussions and tennis matches with Sami Jannin, an impressively fast learner in sports and science with inspiring ideas and questions. Furthermore, I was happy to meet Simone Cavadini, Paul Vasos, Roberto Buratto, Jonas Milani, AJ Perez-Linde, Shutao Wang, and Daniele Mammoli, during these four years on the other side of the Röstigraben.

The most expensive equipment is valueless without people who maintain or know how to use the machines. It is Martial Rey, our indispensable electronic engineer, who keeps all the spectrometers running. He is always there to solve an urgent problem and thus makes our experiments possible. Recently, it was Pascal who joined Martial and helps users with spectroscopic challenges; a great enrichment for our group and the institute. I would like to thank Vladan Jankovic for filling our magnets week after week with liquid nitrogen.

Another essential part in the background of daily research is played by the administration. Thanks to Béatrice Bliesener (before: Christine Kupper) and Anne Lene Odegaard, we can simply focus on research. The heart of our building BCH is the “magasin” with its always friendly équipe. Together with Patrick Favre, Frédéric Gumy and Donald Zbinden in our corridor, they provide the good atmosphere.

The money for the precious machines, the beautiful buildings, the chemicals and of course my salary is coming from the Swiss tax payers. I am grateful to live and study in a country that generously enables fundamental research such as this doctoral thesis.

Zum Schluss möchte ich meiner Familie danken, die immer für mich da ist. Meinem Bruder Satoshi, meiner Mutter Lisa und meinem Vater Tomihiro, sowie meiner Freundin Aline gebührt mein tiefster Dank.

Lausanne, February 2013 Takuya Segawa

Abstract

Nuclear magnetic resonance (NMR) was discovered in the first half of the 20th century. Today, neither analytical chemistry *without* NMR spectroscopy nor medical diagnostics *without* magnetic resonance imaging (MRI) could be imagined. A magnetic resonance signal decays with a time constant T_2, the transverse relaxation time. This parameter contains a great deal of information about structure and dynamics of the molecule, where the observed nuclear spin is located. A method to measure T_2 is the so-called spin echo, discovered by Erwin Hahn in 1950. Usually, the spin echo can generate an exponential decay of the signal and T_2 can be extracted. But if the indirect spin-spin interaction, the J-coupling, connects nuclear spins of the *same* isotope, the echo signal is modulated. The present work discusses novel methods to quench these *echo modulations*. This enables one, on the one hand, to measure the transverse relaxation in *homonuclear* spin systems. On the other hand, this *decoupling* technique can simplify NMR spectra by making splittings due to J-couplings disappear. These two processes can be seen to be equivalent, since the *Fourier transform* of a oscillating time signal corresponds to a line splitting of the frequency signal. To measure T_2's of protons (the nuclei of the most abundant hydrogen isotope ^{1}H) or molecules isotopically enriched in carbon-13, we use a "train of echo pulses" with a *moderate* amplitude of the irradiated radio-frequency. To decouple various nuclear spins in a ^{1}H NMR spectrum, we use a selective radio-frequency irradiation. These experiments are performed as Fourier transform spectroscopy, introduced by Ernst and Anderson in 1966. Based on the same pulse sequence, we measure so-called "spin tickling" experiments, described by Freeman and Anderson in 1962. All lines in the spectrum *split* that share a common energy-level with the irradiated resonance. "Tickling" and decoupling are complementary and belong both to the category of double resonance NMR experiments.

Key words:
magnetic resonance; NMR spectroscopy; J-coupling; decoupling; transverse relaxation; spin tickling; Fourier double resonance

Zusammenfassung

Kernspin-Resonanz (kurz NMR, aus dem Englischen von *Nuclear Magnetic Resonance*) wurde in der ersten Hälfte des 20. Jahrhunderts entdeckt. *Weder* die NMR Spektroskopie für die Analytik in der Chemie *noch* die Magnetresonanz-Tomographie (kurz MRI, aus dem Englischen von *Magnetic Resonance Imaging*) in der Medizin sind heute wegzudenken. Ein Magnetresonanz-Signal zerfällt mit der Zeitkonstante T_2, der transversalen Relaxationszeit. Dieser Parameter enthält viele Informationen über Struktur und Dynamik des Moleküls, in dem sich der gemessene Kernspin befindet. Eine Methode um T_2 zu messen ist das sogenannte Spin-Echo, entdeckt durch Erwin Hahn im Jahr 1950. Normalerweise führt das Spin-Echo zu einem exponentiellen Zerfall des Signals und T_2 kann abgelesen werden. Aber falls die indirekte Spin-Spin Wechselwirkung, die J-Kopplung, Kernspins des *gleichen* Isotops verknüpft, erscheint das Echo-Signal moduliert. Die vorliegende Arbeit setzt sich mit neuen Möglichkeiten auseinander diese *Echo Modulationen* zu unterdrücken. Dies ermöglicht einerseits die transversale Relaxation in *homonuklearen* Spin-Systemen zu messen. Auf der anderen Seite kann diese *Entkopplungs*-Technik NMR Spektren vereinfachen, indem sie die Linienaufspaltung aufhebt. Diese beiden Vorgänge können als äquivalent angesehen werden, da die *Fourier-Transformation* eines oszillierenden Zeitsignals einer Lininenaufspaltung des Frequenzsignals entspricht. Um T_2 von Protonen (Atomkerne des häufigsten Wasserstoffisotops ^{1}H) oder in Molekülen angereichert mit dem Isotop Kohlenstoff-13 zu messen, verwenden wir einen "Zug von Echo-Pulsen" mit einer *moderaten* Amplitude der eingestrahlten Radiofrequenz. Um verschiedene Kernspins in einem ^{1}H NMR Spektrum zu entkoppeln, verwenden wir eine selektive Radiofrequenz-Einstrahlung. Diese Experimente werden als Fourier-Transformations-Spektroskopie durchgeführt, die 1966 von Ernst und Anderson eingeführt wurde. Mit der gleichen Pulssequenz führen wir sogenannte "Spin-Tickling" (*tickling* heisst kitzeln auf Englisch) Experimente durch, die 1962 von Freeman und Anderson beschrieben wurden. Alle Linien im Spektrum werden *aufgespalten*, die ein Energieniveau mit der bestrahlten Resonanz teilen. "Tickling" und Entkopplung sind komplementär zueinander und gehören beide zur Kategorie der Doppelresonanz-NMR-Experimente.

Schlüsselwörter:
Magnetresonanz; NMR Spektroskopie; J-Kopplung; Entkopplung; Transversale Relaxation; Spin-Tickling; Fourier-Doppelresonanz

Contents

1 Introduction

1.1 Objectives of this thesis

This doctoral thesis is entitled *Decoupling of Magnetic Resonance Signals in Time and Frequency Domain*. It discusses strategies to remove, on the one hand, modulations stemming from J-couplings in a time-domain signal and, on the other hand, to collapse corresponding multiplets in a nuclear magnetic resonance (NMR) spectrum. All our experiments are performed in isotropic liquid solutions and therefore, throughout this thesis, decoupling refers to the removal of the effects of *scalar* J-couplings. The *anisotropic* dipolar couplings, averaged out in liquids but dominant in solid-state NMR spectra, are not discussed. We focus our attention on "homonuclear" decoupling and develop methods to decouple for example protons from each other. This is a greater challenge than "heteronuclear" decoupling. A carbon-13 spectrum that is free of splittings to the attached protons can be generated by continuously irradiating the protons with a radio-frequency (*rf*) field. In this setting, we are not interested to see the proton spectrum at the same time; this is fortunate, since the proton signals are "destroyed" by the continuous-wave (CW) irradiation. This illustrates the dilemma of homonuclear decoupling: How can we decouple spins, when we want to observe their signals at the same time?

In nuclear magnetic resonance, the term *decoupling* is often used for experiments that simplify spectra by adding up all transitions of a multiplet to a singlet at the frequency of the chemical shift. Ray Freeman emphasizes in *Spin Choreography* [1] (on page 2) the distinction between *coupling* (a fixed physical interaction) and *splitting* (the quantity observed in the spectrum). Only the *splittings* can be changed, for example by radio-frequency irradiation, but also by chemical exchange or relaxation effects. Consequently, "de-splitting" would have been more appropriate than "de-coupling".

In this thesis, we use *decoupling* not only for frequency-domain spectra but also for time-domain signals. It is a decay, modulated by the coupling constant J, that leads after Fourier transform [2], to a doublet split by J. In contrast to chemical shifts, *heteronuclear* couplings or inhomogeneities of the magnetic field, only modulations from *homonuclear* couplings cannot

be removed by an echo and lead to *echo modulations*. These oscillations of the decay make the measurement of the transverse relaxation time T_2 difficult.

Our decoupling work is based on two fundamental NMR pulse sequences: the *spin echo* [3] and the *spin-lock* sequence [4, 5]. To measure transverse relaxation, usually one of these two sequences is applied. We use Erwin Hahn's spin echo in the form of a pulse train, as proposed by Carr and Purcell [6] and modified by Meiboom and Gill [7], known as the CPMG sequence. To adapt the echoes to our "homonuclear challenge", we use radio-frequency amplitudes of a *moderate* strength. This variant of the echo train was proposed by Dittmer and Bodenhausen in 2006 [8] and can generate decays *without* echo modulations. The decoupling effect can be explained by the interchange of three product operators and is different to the case of *selective* echoes. In this thesis, we apply this *moderate-amplitude CPMG sequence* to measure transverse decay rates in systems of protons or ^{13}C-enriched molecules, normally made impossible by echo modulations.

To generate a decoupled spectrum, an echo sequence is *not* an option, since all chemical shifts are refocused. A selective continuous-wave irradiation can be used to lock one spin, collapse it into a singlet, but not affect the chemical shifts in the spectrum [9]. We use the corresponding pulse sequence in Fourier transform (FT) spectroscopy [10] and propose a *polychromatic* version that can decouple several spins in a single scan.

By simulating the time evolution of the density operator [11], we see that not only the *moderate-amplitude CPMG sequence*, but also the *selective spin-lock* is confined within three product operators. Both *triads* share the in-phase I_x and antiphase magnetization $2I_yS_z$. The CPMG has the multiple-quantum coherence $2I_yS_y$ and the spin-lock the longitudinal two-spin order $2I_zS_z$ as a third operator.

Last but not least, we promote "spin tickling" [12] as a Fourier transform NMR experiment. *Tickling* and *decoupling* are generated by the same pulse sequences; it is only the *rf* amplitude that is weaker for spin tickling. In contrast to decoupling, a single resonance is irradiated for tickling. This will cause all spectral lines that share a common energy-level to *split*.

1.2 Organization of this thesis

This thesis is organized in four chapters. The first one is the present compact *Introduction*, where the goals and the structure of the thesis are presented. Before, an *Abstract* in English (on page vii) as well as a German *Zusammenfassung* (on page ix) were given.

The introduction of the basic theory, applications, history and language of NMR goes beyond the scope of this PhD thesis. Instead, I would like to refer to textbooks that helped me during the last years to better understand the very fascinating and complex field of magnetic resonance. For a beginner, the text by Keeler [13] is an ideal introduction. If the focus is set on the application of the "product operator formalism", the booklet by Hore, Jones and Wimperis [14] is a must. Levitt's *Spin Dynamics* [15] is probably the broadest NMR textbook of the newest generation. Besides its emphasis on biomolecules, *Protein NMR Spectroscopy* by Cavanagh, Fairbrother, Palmer, Rance, and Skelton [16] dedicates many pages to general aspects in NMR spectroscopy. And, there is Freeman's *Spin Choreography* [1] which is full of inspiration and almost written like a novel. For an even deeper involvement with the subject, the three *Principles*, by Abragam [17], by Slichter [18] and by Ernst, Bodenhausen and Wokaun [19] may be consulted.

The two main chapters of the thesis are divided into a *time-domain* part (chapter 2) and a *frequency-domain* part (chapter 3), resulting together in a Fourier transform pair.

The time-domain chapter 2 is entitled *Measuring Transverse Relaxation despite Echo Modulations*. Decays free of modulations from J-couplings are generated to extract transverse relaxation rates $R_2 = 1/T_2$. The *Introduction* of section 2.1 sketches briefly the history of echo modulations starting from the very beginning of NMR spectroscopy, and gives an overview of methods that can quench these modulations. Then, we focus on the multiple-refocusing sequence using a moderate radio-frequency amplitude, the method of our choice, and discuss its theory and a present a basic experimental recipe. The first experiments are performed in *Scalar-coupled protons*, presented in section 2.2. We extract transverse relaxation rates R_2 of various protons in the oligopeptide cyclosporin A, before continuing our measurements in the small protein ubiquitin, using a two-dimensional detection scheme. In section 2.3, we turn to *Scalar-coupled carbon-13 nuclei* and introduce an off-resonance version of our experiment to obtain unmodulated decays. In section 2.4, we discuss the surprising results obtained with *Trains of 360° pulses*, in stead of the conventional 180° echoes. And to conclude chapter 2, we make *A comparison of different methods* to measure T_2 in protons in section 2.5. We would like to highlight the difference between an effective locking *or* refocusing of the J-evolution in theory and experiments. Since the measured rate can be accelerated by the antiphase term $2I_yS_z$, we think about experimental methods to directly measure the decay of the antiphase magnetization.

The frequency-domain chapter 3 is dedicated to *Fourier Double Resonance*. Double resonance is an old NMR technique that adds a second radio-frequency field to introduce a perturbation. The probably best known double resonance experiment is decoupling. The first part of chapter

3, *Polychromatic homonuclear decoupling* in section 3.1, presents a method to decouple at several frequencies in a proton spectrum. In the second part in section 3.2 we promote a complementary double resonance technique called *Fourier spin tickling*. In lieu of collapsing lines as decoupling does, "tickling" splits all resonances that are connected to the irradiated line.

In the last chapter 4 *Conclusions and Outlook*, we would like to bring together our results from time and frequency domain and underline the similarities of the methods used in both domains.

A list of *Abbreviations and Acronyms*, essential in the field of NMR, can be found on page 79, the *Bibliography* starts on page 81 and the *Curriculum Vitae* is on page 91.

A large part of this thesis is based on articles published in peer-reviewed scientific journals. For the sake of clarity, the references are given in the titles of the corresponding sections or subsections.

2 Measuring Transverse Relaxation despite Echo Modulations

In this chapter, methods to measure transverse relaxation rates $R_2 = 1/T_2$, when they are obscured by echo modulations, are presented. We use the classical multiple echo sequence in the style of Carr, Purcell, Meiboom and Gill (CPMG)[6, 7], but reduce the radio-frequency (*rf*) amplitude of the refocusing pulses to a moderate strength as proposed by Dittmer et al. [8]. With this *moderate-amplitude CPMG sequence*, we measure T_2's of protons in a small peptide (cyclosporin A) as well as in a protein (ubiquitin). For the carbon-13 three-spin system in ^{13}C-enriched alanine, we explore the off-resonance effects of this sequence to measure T_2's. Replacing the 180° pulses by 360° pulses on an amide proton in cyclosporin, we record unmodulated decays; an effect we could not fully explain so far. In the last section of this chapter, we evaluate different methods to measure T_2's in protons and discuss the possibility to measure the relaxation of the antiphase component.

2.1 Introduction [20]

2.1.1 Echo modulations

Brief history Modulations of echo signals are as old as spin echoes themselves. When Erwin Hahn discovered the spin echo [3], he observed not only smooth decays, but also signals with a beat pattern on top of the echo envelope. This behavior appeared for proton signals of an organic molecule, namely ethanol. At that time not yet understood, it was the first observation that led to the discovery of the scalar J-coupling [21].

A spin echo compensates for the inhomogeneity of the static magnetic field (e.g., imperfect shimming) and can limit the effects of molecular diffusion through field gradients. Thus, only relaxation is left to cause losses of transverse magnetization. A spin echo also refocuses evolution of chemical shifts and heteronuclear couplings.

Spin echo sequences offer a convenient means to measure transverse relaxation, although difficulties arise when *homonuclear* couplings cause modulations. Protons in most molecules,

and carbon-13 nuclei in systems that are isotopically enriched, fall into this category. The main purpose of this chapter is to present methods that can quench such modulations and yield oscillation-free decays, so that one can obtain a reliable measure of transverse relaxation rates. From this perspective, J-modulations must be seen as a nuisance, but of course, one may also adopt the opposite point of view. The Fourier transform of J-modulated echoes is known as a J-spectrum [1], showing only splittings due to couplings, without chemical shifts.

Quenching J-modulations in the time domain is analogous to decoupling multiplets in the frequency domain: both aim at simplifying the signals, albeit at the expense of a loss of information about couplings. The main difference is that both shifts and couplings are eliminated in echo decays, while in a decoupled spectrum, chemical shifts should be preserved rather than refocused. This is why homonuclear decoupling is such a challenge.

Carr and Purcell [6] made two crucial refinements to Hahn's original echo sequence. First they introduced a 180° pulse for refocusing. Hahn had used two 90° pulses, the first for excitation, and the second for refocusing. Refocusing with a 180° pulse is the simplest and most effective way to generate a spin echo. Secondly, Carr and Purcell proposed a sequence with multiple echoes that are evenly spaced. In experiments with a single refocusing pulse

$$90° - \tau - 180° - \tau \tag{2.1}$$

(Figure 2.1 top, "method A" in the parlance of Carr and Purcell), the delay τ is varied. In experiments with multiple refocusing pulses (Figure 2.1 bottom, "method B"), the delay τ is constant, but more refocusing units ($\tau - 180° - \tau$) are appended to increase the overall echo train duration $2n\tau$. Method B allows one to measure a complete relaxation decay in a single experiment (if signal measurement halfway between two 180° pulses is possible), while method A must be run again for each different interval 2τ. An important advantage of multiple echo sequences is the great reduction in the effects of translational diffusion. Carr and Purcell showed that a single echo measurement is affected by diffusion in an inhomogeneous field, while multiple echoes quench most of the effects of diffusion, due to the shorter intervals 2τ during which free evolution occurs. We shall see below that this quenching is not limited to diffusion, but also works for chemical exchange.

In the original work of Carr and Purcell, all pulses had the same phase. An improvement due to Meiboom and Gill [7] contains a 90° phase shift between the excitation pulse and all subsequent refocusing pulses. It can be shown that for all even-numbered echoes, some pulse imperfections are partially compensated (as described in Ref. [22] by Freeman and Hill, an excellent book chapter about echo modulations and measuring T_2). This sequence was baptized CPMG, after the initials of its four inventors (Carr, Purcell, Meiboom, and Gill):

$$90°_y - [\tau - 180°_x - \tau]_{2n} \tag{2.2}$$

where n is an integer.

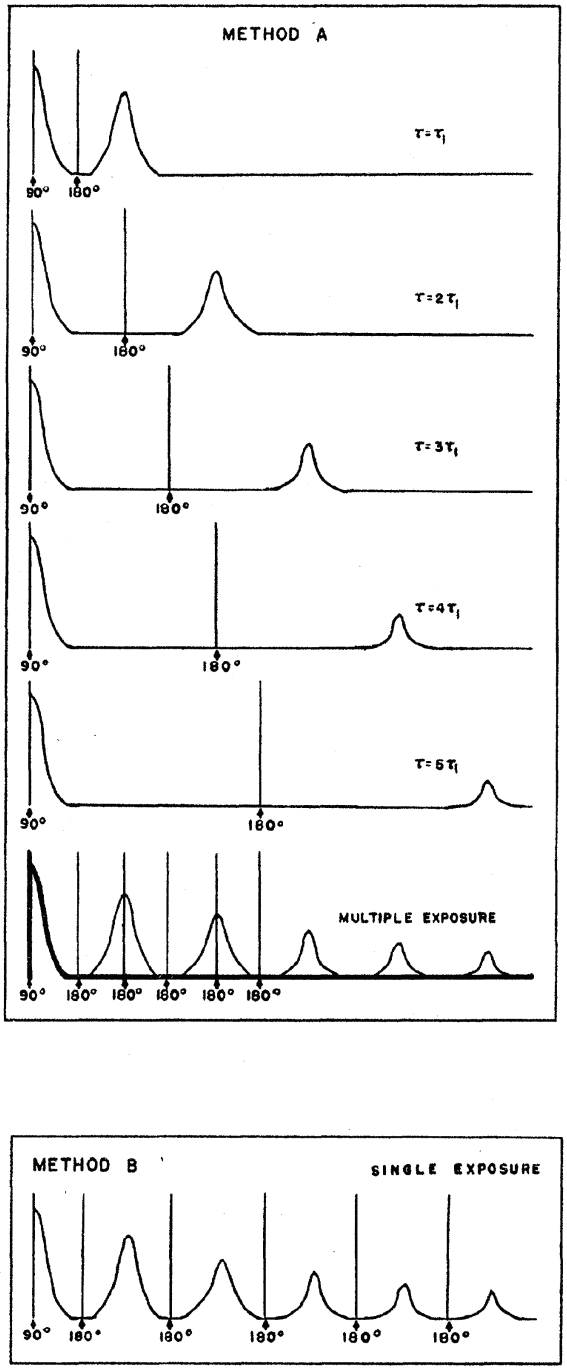

Figure 2.1: Comparison of two echo methods A and B as sketched by Carr and Purcell [6]. While method A uses a single refocusing pulse with a different τ delay for each echo, method B uses multiple echoes, separated by equal intervals 2τ. The free evolution delay τ in method A must be increased stepwise, where as in method B, it can be kept constant, what is a key advantage of multiple echo sequences. Method B was originally introduced to measure T_2 in a "single scan" and suppress the effects of diffusion. Reprinted with permission from Ref. [6]. Copyright 1954 by the American Physical Society.

Quenching echo modulations The simplest way to avoid modulations arising from homonuclear couplings is inspired by the fact that *heteronuclear* couplings are refocused and therefore do not give rise to any modulations. Only couplings between resonant spins lead to modulations of spin echoes [22]. (An exception to this rule was formulated by Kumar and Ernst [23]: non-resonant spins, if they are strongly coupled to each other, can lead to echo modulations of the resonant nucleus.) So, if one wishes to *introduce* modulations due to heteronuclear couplings, it is necessary to apply 180° pulses to both nuclei, as in "spin echo double resonance" (SEDOR) [18, 24] and "insensitive nuclei enhanced by polarization transfer" (INEPT) [25]. Conversely, to *suppress* homonuclear modulations, one can apply *selective* refocusing pulses to the spin of interest so as to leave the coupling partner(s) unaffected, as shown by Freeman and Hill [22]. The idea can be used in both single- and multiple-echo experiments. This technique needs the *rf* carrier to be set on resonance, so that the decay of each spin must be separately measured in turn. Depending on the chemical shift difference between the coupled nuclei, the selective 180° pulses may have to be rather long, in particular for protons since these have a relatively small range of chemical shifts. The effects of relaxation during protracted selective pulses are difficult to take into account, since one has to consider a mixture of longitudinal and transverse relaxation effects. If relaxation during selective pulses cannot be neglected, alternative techniques for measuring transverse relaxation should be preferred.

Magnetically equivalent spins do not show any effects of couplings between each other and therefore lead to singlets, as for the two protons in a water molecule. If a CPMG sequence is applied with a pulse repetition rate fast compared to the differences in chemical shifts, the spins do not have time to evolve under these shifts during the free precession intervals, so that they become in effect magnetically equivalent. Consequently, the J-modulations are suppressed. This method was described by Gutowsky et al. [26] and by Allerhand [27]. The former also highlighted parallels between the quenching of echo modulations and the quenching of contributions to echo decays due to chemical exchange [16]. This similarity makes it difficult to study exchange effects in homonuclear coupled systems [22]. One of the advantages of CPMG methods with high repetition rates is that they are broadband, since all pulses are non-selective. An extreme case of this sequence is found when the inter-pulse delay 2τ tends to zero, so that the 180° pulses merge into continuous-wave (CW) irradiation, an experiment known as "spin-locking" [5]. This allows one to measure transverse relaxation in homonuclear coupled systems. The time constant of the decay is denoted $T_{1\rho}$, for "longitudinal relaxation in the rotating frame", which is usually very similar to T_2 in liquids. It may be interesting to note that it is the 90° phase shift introduced by Meiboom and Gill that makes spin-locking closely related to CPMG. Without this 90° phase shift, the signal would not be locked, but would "nutate" continuously and be dephased by the inhomogeneity of the *rf* field. A protracted CW irradiation always carries the risk of heating the sample and probe. Other unwanted side effects of spin-locking may arise, for example transferring coherence in the manner of "total correlation spectroscopy" (TOCSY) [28], or bringing about a transfer of magnetization through Overhauser effects as in "rotating frame nuclear Overhauser effect spectroscopy" (ROESY)

[29].

A third method for quenching modulations in CPMG sequences, when the *rf* amplitude of the refocusing pulses is set to a *moderate* strength [8], was discovered in 2006. This effect has become known as "stabilization by interconversion within a triad of coherences under multiple refocusing" (SITCOM). While the spin I of interest, which has a chemical shift that coincides with the *rf* carrier, undergoes a series of ideal 180° rotations about the x-axis, the off-resonance spin S that plays the role of coupling partner will rotate about a tilted effective *rf* field and slightly overshoot the ideal angle of 180°. The imperfect refocusing of the coupling partner is propagated throughout the echo train, and the cumulative effect leads to decoupling. In contrast, a single echo (method A) with the same moderate *rf* amplitude generates oscillations. CPMG with moderate *rf* amplitude is a selective technique, so that the decay of each resonance I has to be measured separately (with the exception of the likewise decoupled spin S). But we would like to stress that the pulses are much "harder" than those that are required for the above mentioned *selective* refocusing. Here, the *rf* amplitude ω_1 is of the order of the frequency offset between the coupling partners ($\Omega_S - \Omega_I$). Tošner et al. showed that besides offset effects, miscalibrated refocusing pulses or inhomogeneous *rf* fields can also lead to decoupling [30]. In the next subsection 2.1.2, we shall discuss the theory in more detail.

The conditions that must be fulfilled for the three mechanisms that lead to quenching of echo modulations are summarized in Table 2.1.

Mechanism	*Selective Refocusing*	*High Pulse Repetition Rate*	*Moderate-Amplitude CPMG*
***Rf* field amplitude** $\nu_1 = \gamma B_1/(2\pi)$	$\nu_1 \ll \Omega_S/(2\pi)$	$\nu_1 \gg \Omega_S/(2\pi)$	$\nu_1 \approx \Omega_S/(2\pi)$
Pulse repetition rate $\nu_{rep} = 1/(\tau + \tau_\pi + \tau)$	$\nu_{rep} < \Omega_S/(2\pi)$	$\nu_{rep} \gg \Omega_S/(2\pi)$	$\nu_{rep} \neq \Omega_S/(2k\pi)$ (k integer)
References	Freeman and Hill [22]	Gutowsky et al. [26] Allerhand [27]	Dittmer et al. [8] Gopalakrishnan et al. [31]

Table 2.1: Mechanisms that can lead to quenching of modulations of spin echoes due to homonuclear J-couplings. The *rf* carrier ω_{rf} is set on resonance for spin I ($\Omega_I = 0$), while spin S has an offset Ω_S. Table adapted from Ref. [32] and [33].

2.1.2 Moderate-amplitude multiple refocusing sequence

Theory The principles underlying the quenching of modulations by moderate-amplitude CPMG sequences become evident when we look at simulations of the time-dependence of the relevant product operators [11]. For simplicity we assume a two spin-1/2 system IS, where the I-spin is on resonance and is coupled to the off-resonance spin S. We do not consider relaxation in the simulations, since the SITCOM effect can be fully explained by coherent pro-

cesses. Just after the initial 90°$_y$ excitation pulse, the term I_x is maximal. If we leave the system to evolve freely, the J-coupling will convert the in-phase magnetization I_x into the antiphase term $2I_yS_z$. The interconversion between I_x and $2I_yS_z$ leads to modulations of echoes and splittings in the spectra (Figure 2.2 A).[1] To quench the modulations, the interconversion must be hindered. In a CPMG sequence with "hard" pulses with intervals 2τ that are longer than the inverse of the difference in chemical shifts, i.e., if we avoid the spin-locking régime, the picture remains identical to that for free evolution: the echoes are modulated by the J-coupling.

When $2I_yS_z$ is created starting from I_x a "hard" 180°$_x$ pulse will refocus the "I_y" term and invert the "S_z" term of this bilinear operator. If both rotations are perfect, the antiphase term will continue to build up. But for a moderate *rf* amplitude, only the on-resonance "I_y" term experiences perfect refocusing, while the inversion of the off-resonance "S_z" term to "$-S_z$" partly fails, leading to the creation of some transverse components "S_y", and hence to a product $2I_yS_y$. Thus if the refocusing pulses are less "hard", a third product operator, the multiple-quantum coherence (MQC) $2I_yS_y$, comes into play. The antiphase $2I_yS_z$ product oscillates around zero, while the $2I_yS_y$ product oscillates between zero and its maximum (Figures 2.2 B, C). There are no other product operators involved, as can be verified by noting that the norm of the three coherences $N = \left(\langle I_x\rangle^2 + \langle 2I_yS_z\rangle^2 + \langle 2I_yS_y\rangle^2\right)^{1/2}$ is constant. This explains the name "stabilization by interconversion within a triad of coherences under multiple refocusing" (SITCOM). In the case of decoupling by selective spin-locking, a SITCOM effect takes place in a different triad, in which $2I_yS_y$ is replaced by the longitudinal two-spin order $2I_zS_z$ [36]. A detailed discussion of this alternative SITCOM effect will be given in section 3.1.

A similar SITCOM effect was observed earlier in a different context, when a double CPMG sequence was applied simultaneously to both I and S spins of a *heteronuclear IS* system. Surprisingly, the deleterious effects of pulse imperfections are compensated by the J-coupling [37].

When quenching echo modulations by SITCOM, one has to pay attention since the J-modulation may "come back" for certain critical conditions. Such "recoupling effects" (the expression was borrowed from the parlance of *solid-state magic angle spinning NMR*) appear for well-defined delays

$$\tau = \frac{k\pi}{\Omega_S} - \frac{\pi}{4\omega_1} \tag{2.3}$$

where 2τ is the inter-pulse delay, $\Omega_S/(2\pi)$ is the offset of the coupling partner S, $\omega_1/(2\pi)$ is the *rf* amplitude of the refocusing pulses and k is an integer [31, 32]. For "hard" pulses ($\omega_1 \to \infty$), the recoupling condition coincides theoretically with the sidebands of "delays alternating with nutation for tailored excitation" (DANTE) [1, 38, 39]. Decoupling by the addition of pulse errors on the off-resonance spin S fails when its offset Ω_S coincides with multiples of the

[1] All time evolution of product operators were simulated with mPackages, version 5.35 in Wolfram Mathematica® 7.0 [35]. The latest version of the SpinDynamica package [34], programmed by Malcolm H. Levitt, is available at www.SpinDynamica.soton.ac.uk.

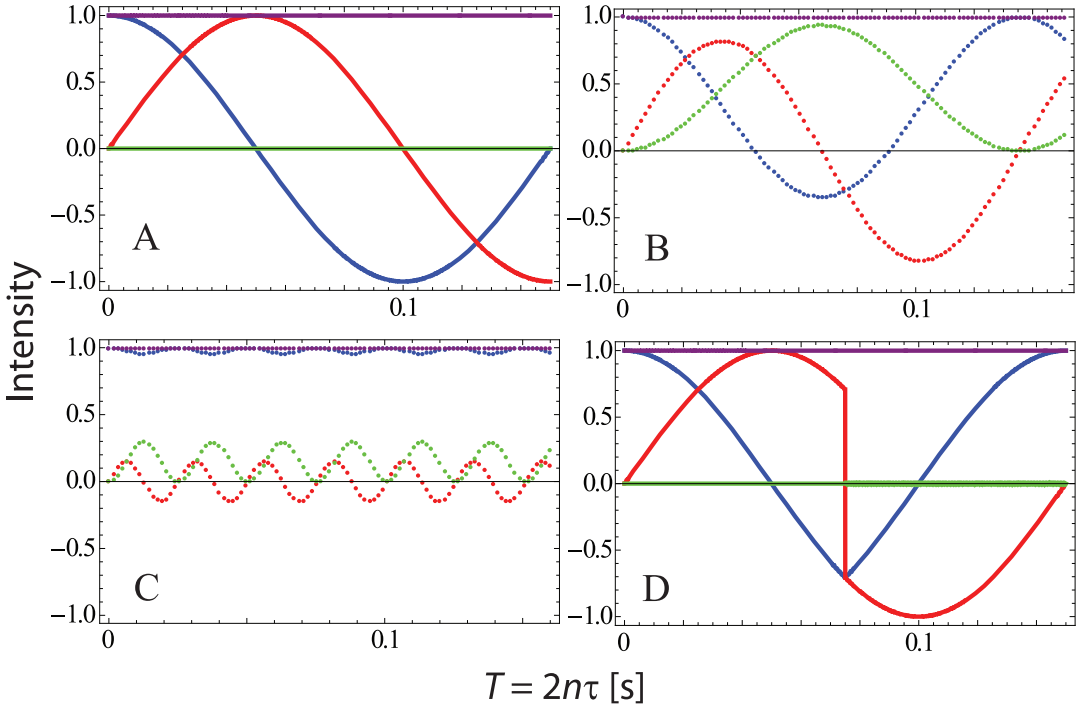

Figure 2.2: Simulations of the "stabilization by interconversion within a triad of coherences under multiple refocusing" (SITCOM) effect for a two spin-1/2 system IS, on resonance for I ($\Omega_I = 0$ Hz), with an offset $\Omega_S/(2\pi) = 1$ kHz of spin S and a coupling constant $J = 10$ Hz. The figures show the expectation values of the three coherences I_x in blue, $2I_yS_z$ in red, and $2I_yS_y$ in green. This "triad of coherences" has a constant norm $N = \left(\langle I_x\rangle^2 + \langle 2I_yS_z\rangle^2 + \langle 2I_yS_y\rangle^2\right)^{1/2}$, shown in purple. A) Free evolution after a non-selective $90°_y$ excitation pulse. B) CPMG sequence with an inter-pulse delay $2\tau = 1.5$ ms and 100 echoes with an *rf* amplitude $\omega_1/(2\pi) = 50$ kHz. C) Similar CPMG sequence, but with $\omega_1/(2\pi) = 5$ kHz. The expectation values are plotted versus the total time in seconds. The delay $2\tau = 1.5$ ms does not coincide with any recoupling condition. From A) to C), the amplitude of the modulation of I_x is attenuated, while its frequency is increased. Note in C) that while $2I_yS_y$ builds up to ca. 30%, I_x is only diminished by ca. 5%. D) Refocusing using a single block of a "perfect echo" (discussed in section 2.5). The sign of the antiphase term $2I_yS_z$ is inverted in the middle by the $90°_x$ pulse. The coherence $2I_yS_y$ is not excited in this scheme. Simulations were performed with the mPackages code (now superseded by SpinDynamica [34]) for Mathematica developed by Malcolm H. Levitt.

pulse repetition rate ν_{rep} (see Table 2.1), i.e., $\Omega_S = 2k\pi\nu_{rep}$. The only term of the triad that evolves under the offset Ω_S is the MQC $2I_yS_y$. The second term on the right-hand side of Equation 2.3 accounts for refocusing pulses of finite strength ($\omega_1 < \infty$) and leads to shifts of the recoupling conditions. The interval between two neighboring conditions $\tau(k)$ and $\tau(k+1)$ remains inversely proportional to the offset of spin S:

$$\Delta\tau = \frac{\pi}{\Omega_S} \tag{2.4}$$

The average Hamiltonian [40] for a CPMG sequence illustrates these effects, as shown by Gopalakrishnan et al. [31]:

$$\bar{\mathscr{H}} = 2\pi J[I_zS_z + \alpha(I_xS_x + I_yS_y)] \tag{2.5}$$

where α is a sinc function with a maximum of 1 and a minimum of ca. -0.2, and depends on $\Omega_S\tau_{\mathrm{CPMG}}$, where $\tau_{\mathrm{CPMG}} = \tau + \tau_\pi + \tau = 1/\nu_{rep}$, as defined in Table 2.1. When $\alpha = 1$, the Hamiltonian has the isotropic form $I \cdot S = I_xS_x + I_yS_y + I_zS_z$, and no modulations will appear, as in systems with magnetically equivalent spins. But if $\alpha = 0$, the Hamiltonian is truncated to the weak coupling form proportional to I_zS_z and full modulations will be present. This happens at the recoupling condition of Equation 2.3. Note that the term $I_xS_x + I_yS_y$ that is scaled by α is a zero-quantum Hamiltonian.

Experimental recipe A direct application of moderate-amplitude CPMG sequences is the measurement of transverse relaxation times in homonuclear J-coupled systems, when simple echoes would be distorted by modulations. This is relevant for molecules that are isotopically enriched in carbon-13 or nitrogen-15, and of course for systems with coupled protons.

The experimental recipe consists of two steps. First, one should identify the positions of recoupling conditions. This can be done using "hybrid sequences", i.e., CPMG sequences with multiple refocusing pulses that are repeated with variable inter-pulse delays 2τ. Such sequences are called "hybrid sequences" because they appear to be mixtures of Carr and Purcell's methods A and B [31]. When τ sits on a recoupling condition, the integral of the multiplet of spin I decreases. This "dip" reveals a recoupling condition. If the coupling partners and their shifts are known the recoupling conditions can be identified with simulations or with Equation 2.3 for a two-spin system. The second step is the actual measurement of the transverse relaxation time constant T_2. In the style of CPMG with a τ delay that is chosen to avoid modulations, the decay is measured by recording spectra for durations $2n\tau_{\mathrm{CPMG}}$ with integer n.

There is no analytical answer to the question of the optimal choice of the moderate *rf* amplitude $\omega_1/(2\pi)$ for the refocusing pulses. The typical empirical range is $\Omega_S < \omega_1 < 10\,\Omega_S$.

The theory of SITCOM was developed for a two-spin system. As long as the hybrid experiment offers enough "flat regions" between the "dips", there are no restrictions to applications to

more complex spin systems. Protons are ideal for this method, since their range of chemical shifts is relatively small, so that the recoupling conditions are spaced far apart, as highlighted by Equation 2.4. In section 2.2, we will show results for proton T_2's in a peptide as well as in a protein. Identifying "flat regions" is more challenging for spins like carbon-13 with larger chemical shift ranges. While in the two-spin system of ^{13}C-enriched glycine a measurement of carbon T_2's is still feasible [32], in the three-spin system of ^{13}C-enriched alanine, no satisfying delay could be found [33]. However, by moving the carrier away from the spin of interest, conditions without modulations could be identified [41]. This will be the topic of section 2.3.

2.2 Scalar-coupled protons

2.2.1 Cyclosporin A [42, 43]

For the measurements of transverse relaxation rates $R_2 = 1/T_2$ in a proton system, we looked at the cyclic undecapeptide cyclosporin A (CsA). CsA is a metabolite of a fungus whose immunosuppressive activity was discovered in a screening by Hartmann Stähelin at the Swiss pharmaceutical company Sandoz in the 1970's. The chemical structure of the active compound was determined by Rüegger et al. [44]. In a collaboration with Sandoz, Kessler and Oschkinat completed the NMR assignment of the CsA spectra [45] and the conformational analysis of the molecule [46]. CsA is still sold today as Sandimmun® by the successor company Novartis and is administered after organ transplantations or against auto immune diseases. We chose to study CsA as a test system, because it has already a fairly complex structure, but still most of the proton signals are resolved in a one-dimensional (1D) NMR spectrum.

Relaxation rates by direct proton detection The chemical structure and the numbering of the amino acids is shown in Figure 2.3 A. A thin layer chromatography (TLC) grade sample was obtained from Sigma Aldrich and dissolved in $CDCl_3$. The 1D ^{1}H spectrum displayed in Figure 2.3 B shows many well-resolved multiplets: All the four H^N protons (*o*-*r*; seven backbone amide N-atoms are methylated), all eleven backbone H^α protons (*d*-*n*), and a few non-overlapping methyl peaks (*a*-*c*), assigned with the help of Ref. [45].

In order to choose appropriate *rf* amplitudes $\omega_1/(2\pi)$, the offsets of the coupling partners were determined from a COSY spectrum. To find suitable repetition rates ν_{rep}, the integrals of the selected multiplets were recorded using the so-called "hybrid" approach (see page 12), i.e., by varying the delay τ while keeping n constant in the CPMG sequence $90°_y - [\tau - 180°_x - \tau]_{2n}$. In this manner, favorable quenching conditions can easily be identified empirically without resorting to theory or simulations. By way of example, consider the doublet of the proton $I = H^\alpha$ of MeVal11 (signal "*k*" in Figure 2.3 B). The *rf* carrier was positioned at 5.15 ppm to be resonant with this H^α proton. Since there is only one resolved coupling $^3J(H^\alpha H^\beta) = 10.9$ Hz, the system can be limited to two spins, provided one limits the observation to the H^α region. The offset of the coupling partner $S = H^\beta$ is $\Omega_S/(2\pi) = 1.5$ kHz. The ^4J couplings to the six protons of the two $C^\gamma H_3$ groups and the three protons of the NCH_3 group are not resolved. The *rf* amplitude of the refocusing pulses was $\omega_1/(2\pi) = 5.6$ kHz, corresponding to a pulse length of $\tau_\pi = 89.2$ µs and a ratio of $\omega_1/\Omega_S = 3.7$. Figure 2.4 A displays the amplitude of the integral of the multiplet obtained by Fourier transformation of the 60$^{\text{th}}$ echo ($n = 30$) as a function of τ, i.e., using the "hybrid" approach. For the 500$^{\text{th}}$ echo ($n = 250$), the ^4J couplings to the nine remote protons give rise to three other weak "dips" for $\tau = 430$, 677, and 705 µs (not shown). Figure 2.4 B shows experimental decays of the H^α proton "*k*" recorded for increasing n, using favorable τ intervals ($\tau = 500$, 750, and 825 µs; marked by square, circle, and triangle in Figure 2.4 A). All curves appear to be free of modulations and the transverse relaxation rate R_2 can be determined by simple monoexponential fits, leading to the decay rates $R_2 = 2.04$,

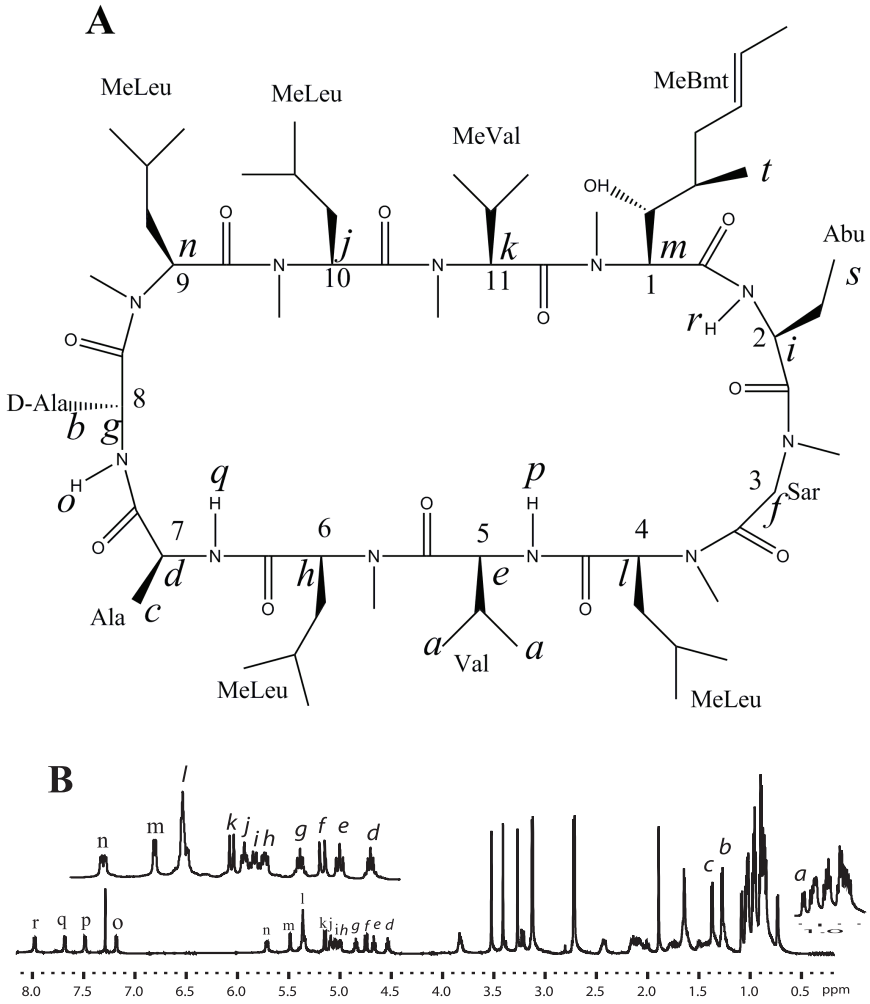

Figure 2.3: A) Chemical structure of the cyclic undecapeptide cyclosporin A (CsA) with its amino acids numbered 1 to 11. "Me" in front of the three letter amino acid code stands for "methyl", e.g., MeLeu – *N*-methyl-leucine. The abbreviations for the non-standard amino acids are: Bmt – 4-[2-butenyl]-4-methyl-threonine, Abu – aminobutyric acid, Sar – sarcosine (*N*-methylglycine). The transverse proton relaxation was determined for few selected protons labeled "*a*" to "*r*". B) Proton spectrum of CsA in $CDCl_3$ at 500 MHz (B_0 = 11.74 T) and T = 300 K. The labeled peaks in the NMR spectrum correspond to the protons highlighted in A).

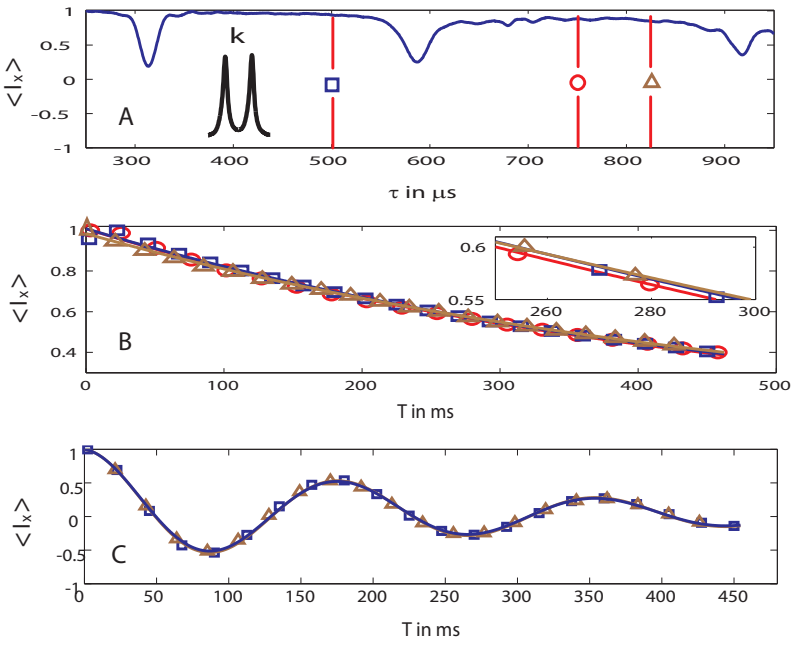

Figure 2.4: A) Amplitude of the H^{α} doublet "k" (see Fig. 2.3) of MeVal11 in CsA recorded with the hybrid experiment $90°_y - [\tau - 180°_x - \tau]_{2n}$ as a function of τ at the top of the 60$^{\text{th}}$ echo (n = 30), varying τ from 250 to 950 µs in steps of 0.5 µs. The doublet arises from the $^3J(H^{\alpha}H^{\beta})$ = 10.9 Hz. The *rf* carrier is positioned on resonance for the H^{α} proton "k" at 5.15 ppm. The offset of the coupling partner H^{β} is $\Omega_S/(2\pi)$ = 1.5 kHz. The *rf* amplitude of the refocusing pulses was $\omega_1/(2\pi)$ = 5.6 kHz (pulse length of τ_π = 89.2 µs), that is ω_1/Ω_S = 3.7. Three favorable intervals τ = 500, 750, and 825 µs, where echo modulations can be neglected are marked with a square, an open circle, and a triangle, respectively. B) Decays of the H^{α} proton "k" recorded for these favorable τ intervals as a function of the number of cycles n. The unmodulated decays were fitted with monoexponential functions. For squares, open circles, and triangles with τ = 500, 750, and 825 µs, one finds R_2 = 2.04, 2.07, and 1.94 s^{-1}, respectively. For τ = 500 µs (squares), n = 1, 10, 20, ..., 200, so that the time axis $T = n(4\pi + 2\tau_\pi)$ extended over $0 < T < 450$ ms; for τ = 750 µs (open circles), n = 1, 8, 16, ..., 144, $0 < T < 458$ ms; for τ = 825 µs (triangles), n = 1, 6, 2, ..., 120, $0 < T < 426$ ms. C) Modulated decay of the H^{α} proton "k" obtained with a single refocusing 180° pulse applied at $T/2$. A fit with an exponential function multiplied by a cosine function gives R_2 = 3.7 s^{-1}, using J = 10.9 Hz.

2.07, and 1.94 s^{-1}, respectively. These rates are compared with experiments in which echo decays were monitored with a *moderate* single refocusing 180° pulse of the same duration τ_π applied at $T/2 = n(2\tau + \tau_\pi) - \tau_\pi/2$, leading to a modulated decay (Figure 2.4 C). Fitting with a monoexponential decay multiplied by a cosine function (i.e., assuming a two-spin system with J = 10.9 Hz) gives R_2 = 3.7 s^{-1}, a clearly faster decay rate. It is difficult to define a fitting function that takes into account all unresolved ^4J couplings to the nine remote protons of the three methyl groups, since there may be several J-couplings with different magnitudes. For larger biomolecules with faster relaxation rates and broader lines, fitting both R_2 and J will be even more difficult (see subsection 2.2.2). When the main coupling $^3J(H^\alpha H^\beta)$ is quenched, long-range couplings have very weak effects. These can be quenched by using sequences with $750 < \tau < 850$ µs. The longitudinal relaxation rate of this proton was determined by an inversion recovery experiment to R_1 = 1.54 s^{-1}.

Figures of hybrid sequences, unmodulated decays, and complete tables of experimentally determined transverse relaxation rates R_2 of all the protons marked in Figure 2.3 can be found in Ref. [43]. We observed empirical correlations between R_2, R_1, and the intensities of NOESY cross peaks. These correlations are more pronounced when similar protons are compared between similar amino acid residues, for example, when comparing H^α protons in the four MeLeu residues.

Why do we obtain different results for R_2, when we use a moderate-amplitude CPMG or a single refocusing with the same moderate amplitude? Why does the latter one lead to a faster decay? In our experiments of the former type, the scalar couplings are in effect decoupled by cumulative pulse imperfections due to a large number of refocusing pulses. If the pulse repetition rates ν_{rep} were very slow, i.e., comparable to the magnitudes of typical homonuclear J-coupling constants, the evolution under the scalar couplings in the τ delays could partly convert an in-phase term I_x into an antiphase term $2I_yS_z$. The decay rates of I_x and $2I_yS_z$ are generally different [47]. The neighboring S spin could be interacting with more remote spins R through dipole-dipole interactions, or it could be subject to external random field effects, or indeed relax because of chemical shift anisotropy (CSA). The relaxation rate of the $2I_yS_z$ term would be enhanced by any one of these mechanisms. However, if J = 10 Hz, and if τ = 1 ms, the amplitude of the antiphase terms that can build up in an interval τ is limited to $\sin(\pi J\tau) = 0.03$. The fact that the echoes are not modulated indicates that the buildup of the antiphase terms is not cumulative in the course of the multiple pulse train. Contributions of antiphase terms to the average relaxation rates are therefore negligible in multiple refocusing experiments (compare Figure 2.2 C on page 11). In effect, we therefore detect the transverse relaxation rates of in-phase components $R_2(I_x)$ which are not significantly "contaminated" by $R_2(2I_yS_z)$. The use of different τ values may however lead to small variations of R_2. In experiments using a single refocusing pulse with $\nu_{rep} < J$, the scalar coupling interaction cannot be quenched, so that the decay rate is determined by the average of in-phase and antiphase relaxation rates. The scalar coupling interaction evolves on a timescale that is faster than the relaxation processes and averages the two relaxation rate constants. Typical $^3J_{HH}$ couplings are in the range of 5–10 Hz and have periods $1/J$ of 200 to 100 ms, which are

comparable to the transverse relaxation times $T_2 = 1/R_2$ of 200 to 300 ms we observed. For homonuclear spin pairs with large scalar couplings (e.g., ${}^1J_{CC}$ = 35–55 Hz), contributions of antiphase terms may play a larger role even in multiple refocusing experiments (see section 2.3).

Relaxation rates expressed in terms of spectral densities The in-phase relaxation rate of an isolated two-spin system, relaxing through the internal dipole-dipole interaction (ignoring CSA) is [16, 47]:

$$\begin{aligned} R_2(I_x) &= (d_{IS}/8)[4J_{IS}(0) + J_{IS}(\omega_I - \omega_S) + 3J_{IS}(\omega_I) + 6J_{IS}(\omega_S) + 6J_{IS}(\omega_I + \omega_S) \\ &= (d_{IS}/8)[5J_{IS}(0) + 9J_{IS}(\omega) + 6J_{IS}(2\omega)] \end{aligned} \tag{2.6}$$

where $d_{IS} = (\mu_0/4\pi)^2\hbar^2\gamma^4 r_{IS}^{-6}$ and $J_{IS}(\omega) = (2/5)[\tau_c/(1+\omega^2\tau_c^2)]$ is the spectral density associated with the fluctuations of the I–S dipolar interaction with μ_0 the permeability of free space, $\hbar$ the Planck's constant divided by 2π, γ the gyromagnetic ratio, r_{IS} the distance between spins I and S, and the τ_c the correlation time. The second line of Equation 2.6 is fulfilled for our homonuclear proton system, by assuming $J_{IS}(\omega_I - \omega_S) = J_{IS}(0)$, $J_{IS}(\omega_I) = J_{IS}(\omega_S) = J_{IS}(\omega)$, and $J_{IS}(\omega_I + \omega_S) = J_{IS}(2\omega)$. For the same system, the antiphase relaxation rate is:

$$\begin{aligned} R_2(2I_yS_z) &= (d_{IS}/8)[4J_{IS}(0) + J_{IS}(\omega_I - \omega_S) + 3J_{IS}(\omega_I) + 6J_{IS}(\omega_I + \omega_S)] \\ &= (d_{IS}/8)[5J_{IS}(0) + 3J_{IS}(\omega) + 6J_{IS}(2\omega)] \end{aligned} \tag{2.7}$$

Hence, the difference between the anti- and in-phase relaxation rates is:

$$R_2(2I_yS_z) - R_2(I_x) = -(d_{IS}/8)[6J_{IS}(\omega_S)] = -(d_{IS}/8)[6J_{IS}(\omega)] \tag{2.8}$$

In an isolated two-spin system, the antiphase term decays *slower* than the in-phase term. The difference originates from the spectral density of the coupled spin $6J_{IS}(\omega_S)$, which does not appear in Equation 2.7.[2]

In our experiments, we always obtained antiphase rates $R_2(2I_yS_z)$ that were *faster* than the in-phase rate $R_2(I_x)$. We have to look at a (slightly) more complex spin system to properly understand our results. We add a third spin R that has a dipolar coupling to spin S, but *not* to spin I. Spin R has no influence on the in-phase relaxation rate of spin I, so that we do not need to modify Equation 2.6. But spin R will change the antiphase relaxation rate $R_2(2I_yS_z)$

[2] In a private communication, Thomas Meersmann pointed out that for systems fulfilling $R_2(I_x) = R_1$, we will see $R_2(2I_yS_z) < R_1$, approaching the extreme theoretical limit $T_2 \leq 2T_1$ as discussed in Ref. [15] on p. 284.

by offering to the coupled spin S an additional relaxation pathway:

$$\begin{aligned} R_2(2I_yS_z^R) = (d_{IS}/8)[4J_{IS}(0) + J_{IS}(\omega_I - \omega_S) + 3J_{IS}(\omega_I) + 6J_{IS}(\omega_I + \omega_S)] \\ +(d_{SR}/8)[2J_{SR}(\omega_S - \omega_R) + 6J_{SR}(\omega_S) + 12J_{SR}(\omega_S + \omega_R)] \end{aligned} \tag{2.9}$$

where where $d_{SR} = (\mu_0/4\pi)^2\hbar^2\gamma^4 r_{SR}^{-6}$ and the superscript "R" in $R_2(2I_yS_z^R)$ highlights the presence of a third spin. Now, the difference between the anti- and in-phase relaxation rate becomes:

$$R_2(2I_yS_z^R) - R_2(I_x) = -(d_{IS}/8)[6J_{IS}(\omega)] + (d_{SR}/8)[2J_{SR}(0) + 6J_{SR}(\omega) + 12J_{SR}(2\omega)] \tag{2.10}$$

To simplify Equation 2.10, we may assume $r_{IS} = r_{SR}$, and therefore $d_{IS} = d_{SR}$:

$$R_2(2I_yS_z^R) - R_2(I_x) = (d_{SR}/8)[6J_{SR}(0) + 12J_{SR}(2\omega)] \tag{2.11}$$

Since the difference depends on both $J(0)$ and $J(2\omega)$, the decay of the antiphase term $2I_yS_z$ will always be faster than the decay of I_x, irrespective of the correlation time, i.e., for both slow and rapid tumbling. It is therefore the longitudinal cross relaxation (nuclear Overhauser effect) of the coupled spin S to a third spin R which accelerates the decay of the antiphase term $2I_yS_z$.

One may ask the question if such a decay rate should still be called R_2, i.e., seen as a transverse relaxation. There is no consistent nomenclature in the NMR community. Cavanagh et al. [16] for example speak of R_{2I} for the in-phase and R_{2IS} for the antiphase decay rate; Kowalewski and Mäler [48] use $R(I_x)$ and $R(2I_xS_z)$, respectively, without the subscript "2", for transverse relaxation.

In experiments with a single refocusing pulse, the buildup and relaxation of the antiphase term $2I_yS_z$ explains why the echo decays are faster. The rate measured by single refocusing experiments (Carr and Purcell's Method "A") is determined by:

$$R_2(\text{"A"}) = 1/2[R_2(I_x) + R_2(2I_yS_z)] \tag{2.12}$$

while the rate measured by multiple refocusing experiments (Carr and Purcell's Method"B") with a moderate *rf* amplitude corresponds to:

$$R_2(\text{"B"}) = R_2(I_x) \tag{2.13}$$

Our ISR spin system is representative for the observed proton "k" in MeVal11 of CsA, that

is, $H^{\alpha}(I)$, $H^{\beta}(S)$, and $H^{\gamma}(R)$, where the latter stands for one of the six methyl protons. The experimental rates were R_2(B) = 2.04 s^{-1} (τ = 500 µs), 2.07 s^{-1} (750 µs), and 1.94 s^{-1} (825 µs), respectively. Assuming that the largest error in these measurements stem from "contaminations" by the remaining antiphase term $2I_yS_z$, this will always *increase* the apparent R_2. This is consistent with the slightly lower relaxation rate R_2 = 1.94 s^{-1} at τ = 825 µs, where the quenching of long-range couplings is expected. In this case of a two-spin system, the measurement of R_2("A") and R_2("B") can be used to determine the antiphase relaxation rate $R_2(2I_yS_z)$ indirectly:

$$R_2(2I_yS_z) = 2R_2(\text{"A"}) - R_2(\text{"B"}) \tag{2.14}$$

leading to an estimate of $R_2(2I_yS_z)$ = 5.4 s^{-1}, for R_2("A") = 3.7 s^{-1} and R_2("B") = 2.0 s^{-1}. Since the direct measurement of the antiphase relaxation in a homonuclear spin system is very challenging (see Ref. [47] and section 2.5), this indirect method could be useful. And it is interesting to note that the antiphase magnetization $2I_yS_z$ decays more than two times faster than the in-phase I_x. It is the number of spins that have a dipolar interactions with the coupled spin S that increase the difference in Equation 2.14. The analysis gets difficult when more than two J-coupled spins are involved, leading to antiphase terms $2I_yS_z, 4I_yS_zS'_z, 8I_yS_zS'_zS''_z$ of increasing complexity.

Relaxation rates by indirect detection via ^{13}C Methyl resonances of peptide side chains often overlap in 1D proton spectra, as can be seen in Figure 2.3 B, thus preventing the integration of their peak amplitudes. For such overlapping proton resonances, the ^{1}H magnetization can be transferred to neighboring ^{13}C spins (which are usually resolved in ^{13}C spectra) by a refocused INEPT sequence [25, 49] applied at the top of the $2n^{\text{th}}$ echo. Figure 2.5 shows a pulse sequence that combines multiple or single refocusing of protons with refocused INEPT. The signal is observed on ^{13}C but its intensity is proportional to the proton magnetization at the top of the $2n^{\text{th}}$ echo.

The blue curve in Figure 2.6 A shows $^{13}C^{\alpha}$ signals, observed after the transfer from $^1H^{\alpha}$ to $^{13}C^{\alpha}$ in MeVal11 at the top of the 120$^{\text{th}}$ echo (n = 60), as a function of τ, i.e. using the hybrid approach. The proton *rf* carrier for ^{13}C was set at 57.18 ppm. Correlations between such pairs can easily be observed in heteronuclear single-quantum coherence (HSQC) experiments [50]. The red curve in Figure 2.6 A shows amplitudes of the same $^1H^{\alpha}$ proton in MeVal11 observed directly at the top of the 120$^{\text{th}}$ echo (the proton signal is well resolved in this case). Not surprisingly, the recoupling conditions (revealed by dips in the curves) precisely coincide in the two schemes. Thus the same scheme can be safely applied for overlapping proton resonances. The blue curve in Figure 2.6 A decays faster than the red curve. To determine R_2("B") with multiple refocusing, the best delays to avoid recoupling were found to be τ = 400 µs (squares and dots) and 800 µs (circles and triangles). Figure 2.6 B shows monoexponential fits to the experimental decay recorded for increasing n. The decays detected on ^{13}C after

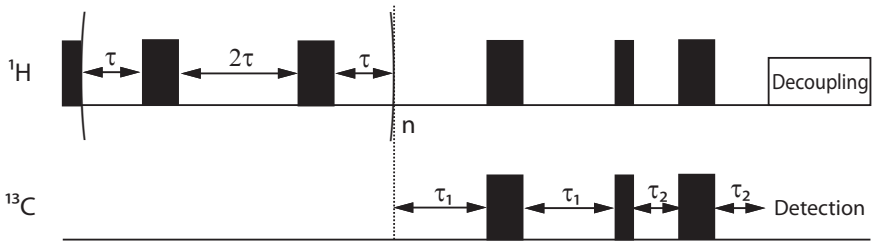

Figure 2.5: Pulse sequence that combines a CPMG spin-echo sequence with multiple refocusing pulses (Method "B") applied to protons with refocused INEPT. Narrow and wide rectangles represent 90° and 180° pulses, respectively. To identify suitable conditions (i.e., to avoid recoupling effects), the delay τ is varied while n is kept constant ("hybrid" experiments). To measure the rates R_2("B"), τ is kept constant and n is stepped. Matched delays $\tau_1 = 1/(4J_{CH})$ and $\tau_2 = 1/(6J_{CH})$ where used to achieve efficient transfer for both CH and CH_3 systems.

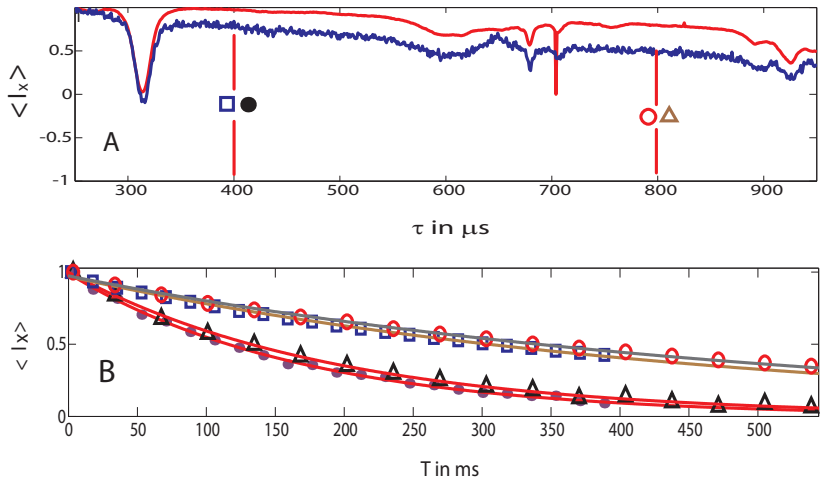

Figure 2.6: A) The blue curve displays the amplitude of the 120th echo ($n = 60$) of the H^α proton "k" as a function of τ, observed *indirectly* by transferring the magnetization of $^1H^\alpha$ to $^{13}C^\alpha$ by INEPT at the end of the echo train (see pulse sequence of Figure 2.5). The red curve shows the amplitude of the same H^α proton "k", again at the top of the 120th echo ($n = 60$), by *direct* observation of the H^α proton signal. Since the sample was not isotopically enriched, 99% of H^α protons have non-magnetic ^{12}C nuclei as neighbors. The proton *rf* carrier was positioned at 5.15 ppm to be on resonance for H^α, while the ^{13}C *rf* carrier was set at 57.18 ppm. 2 scans were acquired for the^{1}H detected scheme, while 64 scans were added up for the ^{13}C detection. Favorable intervals $\tau = 400$ µs (squares and dots) and 800 µs (circles and triangles) were chosen to avoid echo modulations. B) Experimental decays recorded with and without ^{13}C detection for increasing n, using τ intervals 400 or 800 µs. Dots and triangles correspond to decays of H^α attached to ^{13}C while squares and circles correspond to decays of the same H^α attached to ^{12}C. Dots: $R_2 = 5.91$ s^{-1}; triangles: $R_2 = 5.26$ s^{-1}; squares $R_2 = 2.2$ s^{-1}; circles: $R_2 = 1.99$ s^{-1}.

INEPT with $R_2 = 5.91\ s^{-1}$ ($\tau = 400\ \mu s$) and $R_2 = 5.26\ s^{-1}$ (800 µs) are clearly *faster* than directly measured rates $R_2 = 2.2\ s^{-1}$ ($\tau = 400\ \mu s$) and $R_2 = 1.99\ s^{-1}$ (800 µs).

The discrepancies between the relaxation rates of the two detection schemes arise from the fact that two different types of protons are selected. In our sample all isotopes are in natural abundance. Therefore, in the INEPT detection only 1% of the protons attached to a carbon-13 contribute to the decay. In direct detection however, 99% of the protons attached to carbon-12 are measured, as we did not integrate the satellite peaks. Since ^{12}C has no spin, only protons attached to ^{13}C have an additional dipolar coupling and relax faster. The difference between these two rates gives insight into the contribution of the ^{13}C-^{1}H dipolar coupling.

Further figures and decay rates of indirectly detected protons, including resonances unresolved in the ^{1}H spectrum, can be found in Ref. [43]. This method makes T_2 measurements of unresolved protons possible, but the rates from the two detection schemes remain difficult to compare since neighbors of different isotopes are selected. As we will see in the next subsection 2.2.2, this problem can be circumvented by choosing systems that are fully enriched in a single nuclear isotope.

2.2.2 Ubiquitin [51]

Our goal is to measure T_2's of protons in a protein with moderate-amplitude CPMG sequences. Since proton signals in a 1D spectrum are not resolved, we will detect the signal with a two-dimensional (2D) HSQC spectrum. We chose ubiquitin as a protein to study.

Ubiquitin was first identified in 1975 as a small 8.5 kDa protein of 76 amino acids, expressed *ubiquitously* in eukaryotic cells. When ubiquitin binds to a protein, it acts as a label for its degradation. The discovery of this ubiquitin-mediated proteolysis in the early 1980's by Aaron Ciechanover, Avram Hershko, and Irwin Rose led to their Nobel Prize in Chemistry in 2004. Ubiquitin is a popular model system in protein NMR spectroscopy. It is small, stable, commercially available with various isotope combinations and without doubt has the most studied structure and dynamics of all proteins in the NMR field [52].

The study of internal dynamics in proteins usually relies on accurate measurements of Overhauser effects $^{15}N\{^{1}H\}$, combined with longitudinal relaxation rates $R_1(^{15}N) = 1/T_1(^{15}N)$ and transverse relaxation rates $R_2(^{15}N) = 1/T_2(^{15}N)$ [16]. Recently, longitudinal rates of two-spin order terms $2N_zH_z$ [53] and transverse relaxation rates of multiple-quantum coherences $2N_xH_x$ have also been investigated [54, 55]. So far, however, measurements of longitudinal and transverse relaxation rates of *protons* in proteins have by and large remained elusive. Early attempts [56] used selective pulses to avoid echo modulations. Spin-locking experiments that focus on the $R_{1\rho}$ rates of amide H^N protons in deuterated proteins were designed [57] and extended to fully protonated samples [58]. If one uses CPMG sequences, perturbations stemming from homonuclear J-couplings can be neglected under certain circumstances [59]. Such experiments allow one to study the "dispersion" of the relaxation rates as a function of the *rf*

amplitude ($R_{1\rho}$) or the pulse repetition rate (CPMG) and are used to study chemical exchange [16]. In this context, not only the homonuclear *J*-couplings, but also dipolar couplings among protons make the analysis challenging [57].

Our experiments do not allow one to study the "dispersion" of relaxation rates as a function of pulse repetition frequency or effective *rf* amplitude, since our refocusing pulses are neither "hard" nor short enough and due to recoupling conditions, not every inter-pulse delay can be chosen. However, unlike $R_{1\rho}$ spin-locking experiments that focus on amide H^N protons, our experiments do not suffer from any TOCSY effects [28], since there can be no coherence transfer between on-resonance H^N protons and the coupling partners that experience tilted effective fields. Likewise, our approach avoids the pitfalls of unwanted ROESY effects [29, 60].

The idea of combining our CPMG sequences with INEPT is sufficient to analyze all transverse proton relaxation rates of an oligopeptide like CsA (subsection 2.2.1). It can be adapted for H^N protons by transferring their magnetization to ^{15}N spins. However, in small proteins such as ubiquitin, this strategy fails by lack of resolution and sensitivity of ^{15}N spectra.

This problem can be alleviated using heteronuclear single-quantum correlation spectroscopy (HSQC) [50, 61, 62, 63] to monitor the amplitudes of proton echoes resulting from CPMG pulse trains with moderate *rf* amplitudes applied to the protons prior to the HSQC sequence. There are many variants of HSQC, any of which can be combined with our CPMG sequences without modification of the phase cycles, etc. The proton carrier frequency was set on resonance for the protons of interest during the CPMG scheme, and switched to the water resonance prior to the HSQC sequence. Refocusing pulses with moderate *rf* amplitudes were used during the CPMG trains, leading to tilted effective fields for the coupling partners, so as to quench echo modulations. The 2D signal amplitudes were determined using NMRPipe [64]. The resulting [^{1}H, ^{13}C]-CPMG-HSQC method allows one to confirm the apparent transverse relaxation rates $R_2(^1H)$ of protons attached to ^{13}C in natural abundance in CsA that had previously been measured by CPMG-INEPT (see subsection 2.2.1). Since there were no significant differences in CsA, we switched our attention to ^{15}N-enriched (but not deuterated) ubiquitin. If homonuclear scalar couplings act during the spin-echo train (i.e., if they are not quenched), antiphase single-quantum coherences (SQC's) of the type $2H_x^N H_z^\alpha$ may appear at the end of the CPMG sequence. Such terms may be converted into $4H_x^N H_y^\alpha N_x$ at the beginning of the t_1 interval of the HSQC sequence and interfere with the desired pathways. However, if the τ delays are chosen to quench the homonuclear *J* modulations, only in-phase SQC terms such H_y^N appear at the end of the CPMG echo train, so that a normal HSQC spectrum will be obtained by gradient selection. As a sample we used ^{15}N-labeled, but not deuterated, ubiquitin at pH 7.2 in 9:1 H_2O:D_2O at 600 MHz (B_0 = 14.1 T). The assignments were taken from Cornilescu et al. [65]. Using [^{1}H,^{15}N]-CPMG-HSQC, the rates $R_2(^1H^N)$ were measured for the six residues[3] D32, G35, L50, L56, E64 and G76, and its decays are shown as red solid curves in Figure 2.7. A typical [^{1}H,^{15}N]-CPMG-HSQC spectrum is shown in Figure 2.8. The decays of ordinary spin echoes were recorded for comparison with a single refocusing 180°

[3] Using the single-letter amino acid code: D – aspartic acid, G – glycine, L – leucine, and E – glutamic acid.

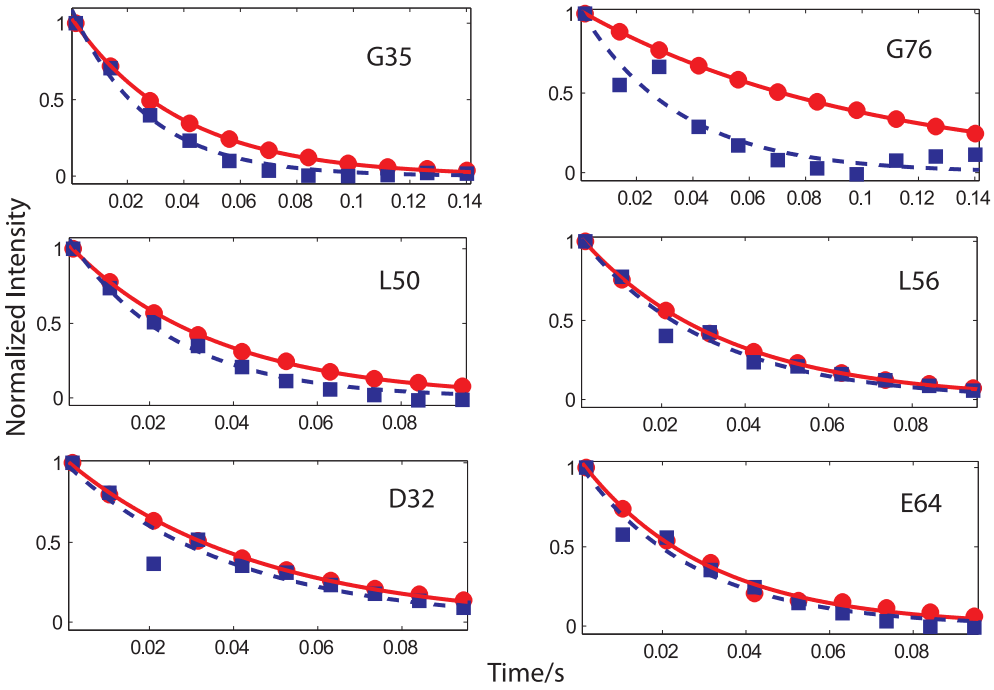

Figure 2.7: Intensities of six different H^N signals in ubiquitin obtained by [^{1}H,^{15}N]-CPMG-HSQC as a function of the duration $T = n(4\tau + 2\tau_\pi)$ of echo trains with τ = 400 µs at 300 K and 600 MHz. The increments were n = 1, 8, 16,..., 80 for G35 and G76, and n = 1, 6, 12,..., 54 for L50, L56, D32, and E64. The experimental points (red circles) were fitted with monoexponential decays (red solid curves). Blue squares show intensities of echoes that decay faster due to unresolved modulations that can be observed when using a single refocusing pulse with the same overall T intervals, also followed by [^{1}H,^{15}N]-HSQC. These values were also fitted with monoexponential decays (blue dashed curves) for comparison (Table 2.2). The proton 180° pulses in the CPMG trains and in the experiments with single-refocusing pulses had the same *rf* amplitude $\omega_1/(2\pi)$ = 6.6 kHz.

Temperature	D32	G35	L50	L56	E64	G76
285 K	**28.8**	**33.1**	**35.3**	**40.4**	**40.4**	**6.5**
	43.3	58.4	90.4	63.0	94.1	30.2
300 K	**21.8**	**26.1**	**28.4**	**29.1**	**33.0**	**9.9**
	25.1	37.9	40.0	32.6	37.0	28.9
315 K	**17.1**	**19.8**	**21.4**	**21.3**	**26.3**	**33.3**
	19.4	34.7	35.1	23.9	32.1	40.5

Table 2.2: Transverse proton relaxation rates $R_2(^1\mathrm{H}^\mathrm{N})$ (s^{-1}) in ubiquitin, measured at three different temperatures at 600 MHz. The rates in boldface were obtained from monoexponential fits of unmodulated CPMG experiments (red solid curves in Fig. 2.7), the rates in lightface stem from monoexponential fits of partly modulated echo envelopes obtained with a single refocusing pulse (blue dashed curves in Fig. 2.7).

pulse of duration τ_π applied at $T/2 = n(2\tau + \tau_\pi) - \tau_\pi/2$, followed by HSQC (Figure 2.7 blue dashed curves). The proton 180° pulse in both CPMG trains and experiments with a single refocusing have an *rf* amplitude $\omega_1/(2\pi)$ = 6.6 kHz. In contrast to CsA (compare Figure 2.4 on page 16) one cannot resolve any modulations in ubiquitin, so that evolution under the scalar coupling merely lead to faster decays (Table 2.2). This can be explained by the different correlation times τ_c. The medium-sized molecule CsA is tumbling faster and has therefore a shorter correlation time than the larger ubiquitin. Since R_2 increases with larger τ_c [18], we enter the régime of "self-decoupling". As explained by Cavanagh et al. (Ref. [16], p. 381), the *difference* between the two relaxation rates $\Delta R = R_2(I_x) - R_2(2I_yS_z)$ compared to the J-coupling determines if the spectrum gets decoupled due to relaxation effects.[4] While for $\Delta R^2 << (2\pi J)^2$, the resonance appears split in the spectrum, if $\Delta R^2 >> (2\pi J)^2$, a decoupled singlet will appear. The former case applies to CsA, with mulitplets in the spectrum and modulated single refocusing decays. Here in ubiquitin we are near coalescence, as known from chemical exchange, with $\Delta R^2 \approx (2\pi J)^2$. Therefore, if we go to systems with even higher correlation times, decoupling will become obsolete, since relaxation has already taken care of it.

All relaxation decays, with and without decoupling, were measured at three different temperatures T = 285, 300, and 315 K and the rates are listed in Table 2.2. For all residues except G76, the rates R_2 *decrease* with *increasing* temperature, as expected for exchange-free rates $R_2°$ since higher temperatures lead to shorter correlation times τ_c. The transverse relaxation rates of G76 at the end of the flexible C-terminus of ubiquitin behaves in an exceptional way. For the two lower temperatures $R_2(^1\mathrm{H}^\mathrm{N})$ of G76 decays clearly slower than the other measured amide protons. This is due to the faster local correlation time τ_c of the flexible C-terminal region that keeps $R_2(I_x)$ low. On top of this, G76 is the only residue in Table 2.2 where $R_2(^1\mathrm{H}^\mathrm{N})$ *increases* with *increasing* temperature. This can be explained by an additional contribution R_2^{ex} to the transverse relaxation $R_2°$ from the exchange of H^N proton with water. R_2^{ex} increases with temperature and will dominate the total relaxation rate $R_2 = R_2° + R_2^{ex}$ at higher temperatures.

[4] This was not correctly stated in Ref. [51], where R_2 was taken in stead of ΔR.

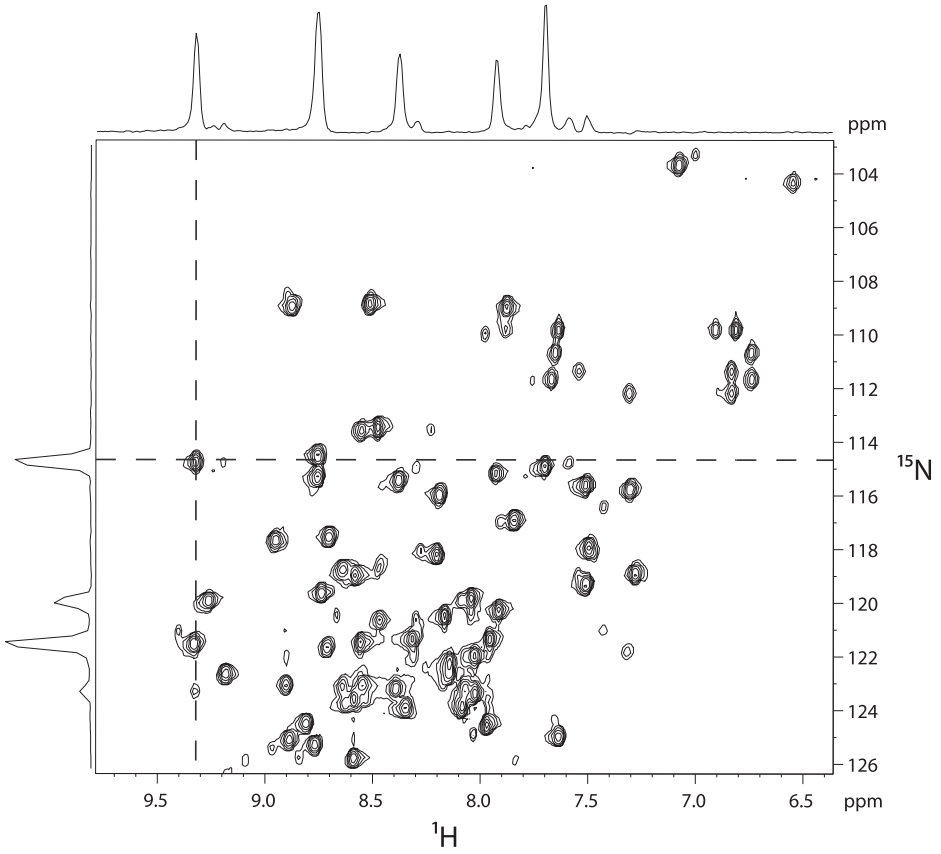

Figure 2.8: Detail of a [^{1}H,^{15}N]-CPMG-HSQC at 600 MHz (B_0 = 14.1 T) with cross sections (taken at the frequencies indicated by dashed lines) corresponding to E64 with $\delta(^1H^N)$ = 9.31 ppm and $\delta(^{15}N)$ = 114.8 ppm, with n = 1 (i.e., second echo) at T = 315 K. The number of transients was 4, the recycle delay 3.5 s, the number of points in the t_1 domain 72, and the spectral width in the indirect ω_1 dimension 26 ppm. In contrast to the ^{1}H 1D spectrum of CsA in Figure 2.3 on page 15, the proton signals appear as broad singlets and the homonuclear J_{HH}-splitting has disappeared. Since decoupling is applied on the ^{15}N channel during acquisition, the heteronuclear J_{HN}-couplings do not appear in this spectrum.

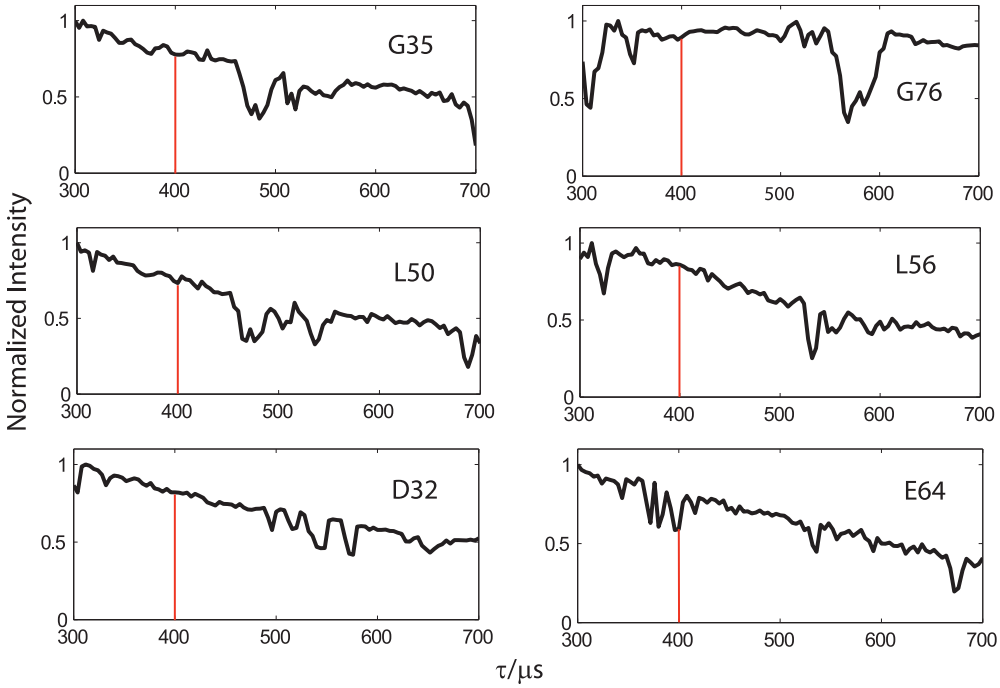

Figure 2.9: Signals of H^N protons in the backbone of ubiquitin, obtained with the "hybrid" version of [^{1}H,^{15}N]-CPMG-HSQC, where the number of refocusing pulses $2n = 40$ was kept constant, while the delay τ was incremented from 300 to 700 μs in steps of 4 μs at T = 300 K. The red vertical lines correspond to the delay τ = 400 μs used in Fig. 2.7

To verify that none of the CPMG-HSQC experiments suffered from accidental recoupling effects at unfavorable τ intervals, a few "hybrid" experiments (see page 12) were carried out in 2D fashion (Fig. 2.9). For each residue, 101 spectra were recorded with the proton carrier frequency on resonance, varying the delay $300 < \tau < 700$ µs in steps of 4 µs, while keeping the number of 180° pulses constant with $2n = 40$.

The red vertical lines in Fig. 2.9 highlight the delay $\tau = 400$ µs where all CPMG-HSQC spectra of Fig. 2.7 were recorded. Only for E64 does this coincide with a "dip" due to echo modulations arising from recoupling, which explains the weak modulations of the circles in Fig. 2.7. This leads to a significant overestimation of R_2. This problem could be circumvented by repeating the CPMG sequence with another delay to avoid all "recoupling dips", e.g., $\tau = 480$ µs. Once again, G76 stands apart not only by its slower decay rate, but also by a broader and deeper recoupling dip.

Each 2D CPMG-HSQC spectrum took about 5 min. Therefore, the screening of recoupling conditions with a hybrid experiment becomes very time consuming. There are several recent methods that allow to accelerate the acquisition time of a 2D spectrum [66], like optimized aliasing [67], band-selective optimized flip-angle short transient (SOFAST) methods [68], or by single-scan 2D [69, 70].

Other protons in ubiquitin could be studied by [^{1}H, ^{13}C]-CPMG-HSQC experiments correlating ^{1}H with ^{13}C nuclei through heteronuclear couplings $J(^1\mathrm{H}, ^{13}\mathrm{C})$, as we have done for 1D CPMG in the subsection 2.2.1 on page 20. All CPMG experiments shown here were performed with the proton carrier on resonance for the H^{N} signals of interest. As we will demonstrate for a carbon-13 system in section 2.3, it is also possible to obtain unmodulated decays when the *rf* carrier is positioned *off resonance*. This could allow one to measure the rates R_2 of different protons in a single experiment and lead to savings in experimental time.

We have shown that a combination of multiple refocusing using moderate *rf* field-strengths and HSQC allows one to measure the apparent transverse relaxation rates R_2 of any proton that can be resolved in a 2D spectrum. This technique opens the way to measuring transverse relaxation rates of non-exchangeable protons such as H^{α}, H^{β}, etc., in ^{13}C-enriched proteins.

2.3 Scalar-coupled carbon-13 nuclei [41]

In his PhD thesis [33], Nicolas Aeby studied in detail scalar-coupled carbon-13 systems to extract their transverse relaxation rates R_2 by the moderate-amplitude CPMG technique. While he was able to measure R_2 in the two-spin system of ^{13}C-enriched glycine [32], the three-spin system of ^{13}C-enriched alanine created (in his words) "spin cacophony" and an unmodulated decay could not be observed, due to the lack of "flat regions" in his hybrid experiments. This was part of the discussion during his thesis exam, where Jens Dittmer was present as an examiner and led to the below-mentioned experiments, where the *carrier frequency* was introduced as a new tunable parameter, besides the pulse interval and the *rf* amplitude.

2.3.1 Off-resonance experiment in a three-spin system

Measurements have been carried out with a sample of ^{13}C- and ^{15}N-enriched L-alanine (Cambridge Isotope Laboratories, U-$^{13}C_3$, 98%; ^{15}N, 98%), 0.5 M in D_2O using a Bruker Avance spectrometer with a field of B_0 = 11.74 T (500 MHz for ^{1}H). The starting point is Figure 2.10 showing experimental echo amplitudes of C_x^α (blue) and simulated expectation values $\langle C_x^\alpha \rangle$ (red) in alanine, on resonance with $\Omega^\alpha = 0$ and an *rf* amplitude $\omega_1/(2\pi)$ = 20 kHz, as a function of the delay τ, in a hybrid experiment with $2n = 20$. Simulations were performed with a MATLAB® [71] program considering the full Hamiltonian without relaxation effects, written by Aeby [33].

Comparing Figure 2.10 with Figure 2.4 A on page 16, which shows the result of a similar hybrid experiment of an H^α proton in cyclosporin A, the differences are obvious. Where in Figure 2.4 A, most values for τ do *not* lead to any modulation and one could even think of trying random τ values to skip the hybrid experiment, in Figure 2.10, "flat regions" with high intensity values around 1 are scarce. The case shown here is a ^{13}C three-spin system, each spin having a different chemical shift. The range of chemical shifts in carbon-13 is about one order of magnitude larger than in protons. As it was shown in Equation 2.4 on page 12, the interval between two neighboring recoupling conditions is inversely proportional to the offset of the off-resonance spins. Therefore, we must expect up to ten times more frequent recoupling conditions. But this is not the only difference. We can recognize in Figure 2.10 two distinct recoupling patters: *narrow* dips, separated by *small* intervals, overlapped by *broad* dips separated by *large* intervals. The former pattern stems from the $J(C^\alpha C')$ coupling to the spectrally remote C' spin with a chemical shift of $\Omega'/(2\pi)$ = 15.77 kHz, while the broad dips are due to the $J(C^\alpha C^\beta)$ coupling to the C^β spin which has a chemical shift that is closer to C^α with $\Omega^\beta/(2\pi) = -4.32$ kHz. The recoupling dips from C^β are broadened due to the heteronuclear $J(C^\beta H^\beta)$ coupling. One could think of heteronuclear decoupling during the CPMG sequence on the proton channel to narrow these recoupling dips. It turns out that this will lead to complicated interferences between the CPMG cycle τ_{CPMG} and the cycle (or supercycle) of a (composite pulse) decoupling sequence [32]. This is even true for a continuous-wave (CW) irradiation. A safe way to circumvent these complications is to avoid heteronuclear decoupling

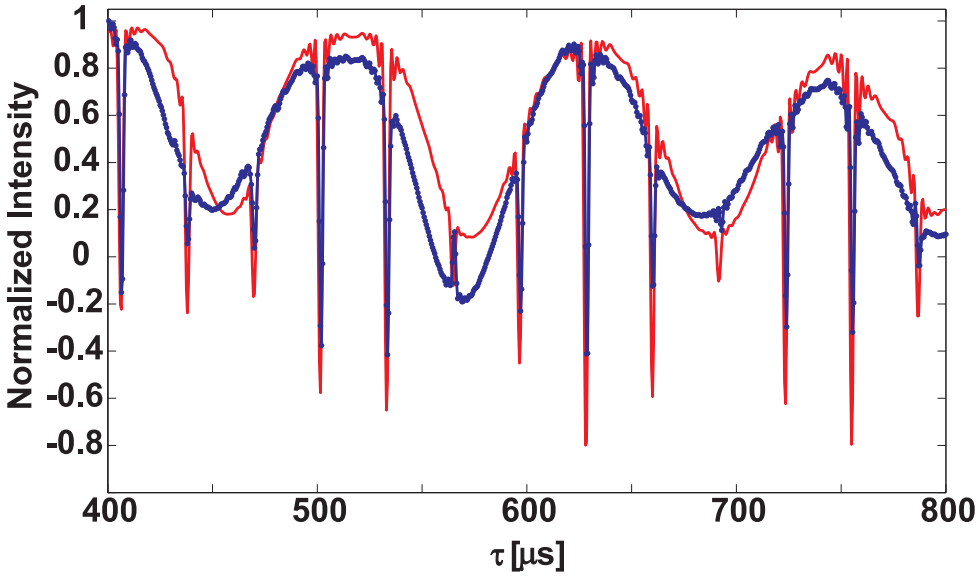

Figure 2.10: Amplitudes of $\langle C_x^{\alpha} \rangle$ of the 20$^{\text{th}}$ echo ($2n = 20$) in ^{13}C- and ^{15}N-enriched alanine, as a function of the delay τ. Experimental results are shown in blue, whereas simulated data are plotted in red. The ^{13}C *rf* amplitude was $\omega_1/(2\pi) = 20$ kHz, hence $\tau_\pi = 25$ µs. The τ delay has been varied between 400 and 800 µs in steps of 0.5 µs. The chemical shifts are $\delta(C^{\alpha}) = 50.37$, $\delta(C^{\beta}) = 16.02$, and $\delta(C') = 175.76$ ppm. At $B_0 = 11.74$ T, C^{β} and C' appear at offsets of -4.32 and 15.77 kHz with respect to C^{α}. The scalar coupling constants are $J(C^{\alpha}C^{\beta}) = 35.0$, $J(C^{\alpha}C') = 54.2$, $J(C^{\beta}C') = 1.2$, $J(C^{\alpha}H^{\alpha}) = 145.0$, $J(C^{\beta}H^{\alpha}) = 4.4$, $J(C'H^{\alpha}) = 4.2$, $J(C^{\beta}H^{\beta}) = 129.7$, $J(C^{\alpha}H^{\beta}) = 4.6$, and $J(C^{\alpha}N) = 5.7$ Hz. This figure was published in Aeby's thesis [33] and in Ref. [41].

altogether during the multiple refocusing sequence, so that the decoupler is activated only during signal acquisition, i.e., during the second half of the $2n^{\text{th}}$ echo.

To access modulation-free régimes, we decided to shift the carrier frequency away from the resonance of the spin of interest C^{α}. Since we would have to run a hybrid experiment for every carrier frequency, we decided to simulate the amplitude of modulation A_{mod}

$$A_{mod} = \frac{max(\langle I_x \rangle) - min(\langle I_x \rangle)}{2} \tag{2.15}$$

varying the interval τ and the carrier frequency. For each point $\langle I_x \rangle$ is calculated for increasing number of echoes $2n$. If all these values are identical, there is no modulation present and A_{mod} = 0. In contrast, if $\langle I_x \rangle$ oscillates between 1 and −1, A_{mod} = 1. Figure 2.11 shows the simulated 2D plot of the amplitude A_{mod} as a function of the delay τ against the offset Ω, separating the carrier frequency ω_{rf} from the chemical shift of the C^{α} carbon. The carrier frequency was stepped over a range of 6 kHz from the C^{α} towards the C' resonance. The *rf* amplitude was $\omega_1/(2\pi)$ = 20 kHz. Dark blue areas correspond to regions where modulations are weak ($A_{mod} \approx 0$), whereas yellow stripes indicate strong modulations ($A_{mod} \approx 1$). The thin stripes with positive slopes correspond to C^{α}C' recoupling, the broader stripes with negative slopes to the $C^{\alpha}C^{\beta}$ interactions. In the simulations, all three carbons (C^{α}, C^{β}, and C') and four protons (one H^{α} and three H^{β}, but none of the H^{N} protons which were replaced by deuterium) were taken into consideration. The protons in the simulation leave the general pattern in Figure 2.11 unchanged, but broaden the stripes stemming from $J(C^{\alpha}C^{\beta})$. Since this plot correlates a time axis with a frequency axis, it can be seen as a "pseudo-2D" spectrum.

To verify the simulations, echoes were recorded at two points on the map featuring extreme values for the amplitude of the modulations A_{mod}: at a crossing of two recoupling stripes (with an offset of +1 kHz from the C^{α} chemical shift and a delay of τ = 366.5 µs) and in the center of a "blue field" (with an offset of +1.275 kHz from the C^{α} chemical shift and a delay of τ = 391.25 µs). The resulting decays are shown in Figure 2.12. In agreement with the simulations, the echo decay of Figure 2.12 A, recorded at a crossing of yellow stripes in Figure 2.11, shows strong modulations leading to a fast decay of the echoes. On the other hand, the echo decay of Figure 2.12 B is free of any modulations and can be perfectly fitted with a monoexponential function, leading to a transverse relaxation rate R_2 = 0.48 s^{-1}. Transverse relaxation rates measured in other "blue fields" in the map of Fig. 2.11 are listed in Table 2.3, in order of increasing simulated amplitudes of the modulations A_{mod}.

To verify that the resulting $R_2(C^{\alpha})$ rates are reliable, 1 M natural abundance alanine, where no echo modulations are present, and 0.01 M uniformly enriched ^{15}N–^{13}C-alanine were mixed to guarantee the same pH and chemical exchange rates. The offset with respect to the C^{α}-resonance was +1.275 kHz and τ was 391.25 µs. The relaxation rate of the natural abundance sample was $R_2^{n.a.}$ = 0.389 ± 0.004 s^{-1}, and the relaxation rate in the isotopically enriched sample was $R_2^{i.e.}$ = 0.43 ± 0.01 s^{-1}. The difference $R_2^{i.e.}$ - $R_2^{n.a.}$ = 0.04 ± 0.01 s^{-1} is slightly too

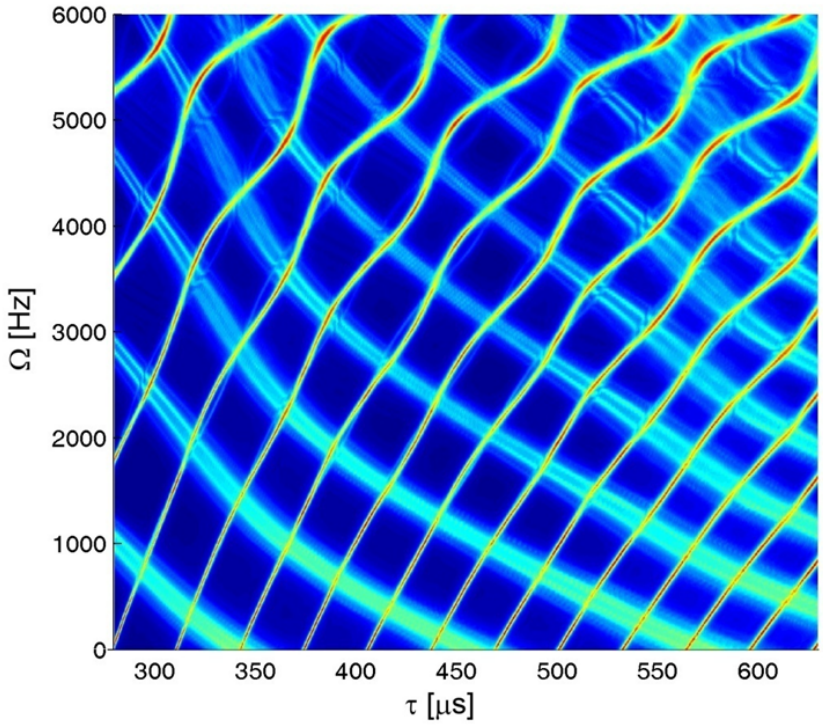

Figure 2.11: Simulations of the amplitude of the modulations A_{mod} of C^{α} in alanine, with respect to the echo delay τ and the offset Ω separating the carrier frequency ω_{rf} from the chemical shift of the C^{α} carbon. The thin stripes with positive slopes correspond to $C^{\alpha}C'$ recoupling, the broader stripes with negative slopes to the $C^{\alpha}C^{\beta}$ interactions. In the simulation, all three carbons (C^{α}, C^{β}, and C') and four protons (H^{α} and 3 H^{β}) were taken into account. The *rf* amplitude was $\omega_1/(2\pi)$ = 20 kHz. Dark blue areas correspond to regions without modulations, whereas yellow ridges indicate strong modulations.

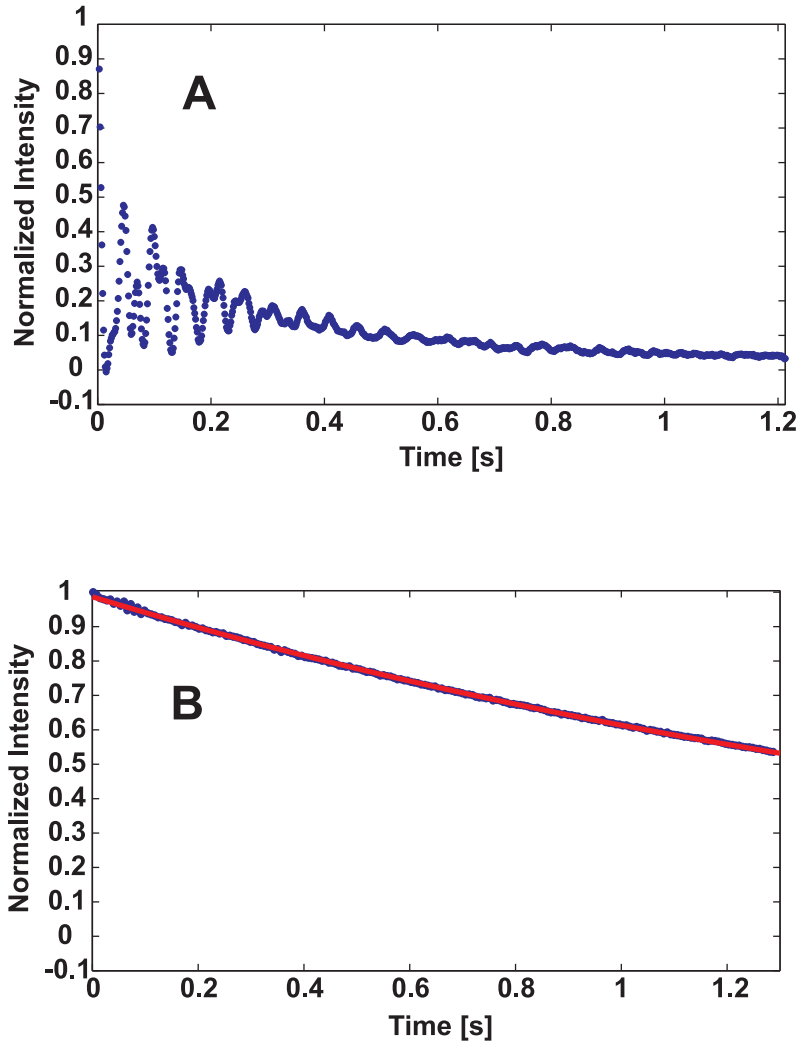

Figure 2.12: Decays of C^{α} echoes under a multiple refocusing sequence $90°_y - [\tau - 180°_x - \tau]_{2n}$, incrementing n from 1 to 800 in steps of 4. The *rf* amplitude was $\omega_1/(2\pi) = 20$ kHz, corresponding to a 180° pulse length $\tau_\pi = 25$ µs. A) Decay observed at a crossing of two yellow stripes in Fig. 2.11 with the carrier frequency +1 kHz from the chemical shift of C^{α} and $\tau = 366.5$ µs. B) Decay observed in a "blue field" of Fig. 2.11 with the carrier frequency +1.275 kHz from the chemical shift of C^{α} and $\tau = 391.25$ µs. Blue dots represent experimental data and red lines monoexponential fits $I(t) = \exp(-R_2\, t)$ with $t = n(4\tau + 2\tau_\pi)$. The transverse relaxation rate was determined to be $R_2 = 0.48\ \mathrm{s}^{-1}$.

Simulated A_{mod}	R_2/s^{-1}	τ/µs	Ω/Hz
0.024	**0.47**	467.50	1525
0.034	**0.48**	391.25	1275
0.035	**0.50**	492.50	1225
0.040	**0.47**	416.50	1125
0.042	**0.48**	366.75	375
0.046	**0.51**	467.50	475
0.052	**0.52**	517.00	975
0.057	**0.57**	491.00	200
0.073	**0.52**	541.50	725
0.091	**0.51**	566.50	500
0.102	**0.52**	590.50	275

Table 2.3: Transverse relaxation rates of C^{α} in ^{13}C- and ^{15}N-enriched alanine, measured in regions where the amplitude of the modulations A_{mod} are small, according to the simulated map of Fig. 2.11.

large to be explained by the additional dipolar relaxation to the neighboring carbon-13 nuclei C' and C^{β} in the enriched sample that should contribute only about 0.01 s^{-1}. It is possible that, in spite of our efforts, the modulations are still not completely suppressed, so that some unresolved residual couplings still contribute to broaden the lines and accelerate the echo decays. Nevertheless, our experimental relaxation rates seem to have errors smaller than 10%.

Could this off-resonance method open ways to make moderate-amplitude CPMG measurements *multi-selective*, i.e., can we find conditions, where unmodulated decays for several coupling pairs could be obtained? To answer this question, we have to overlay maps of modulations as in Figure 2.11, and search for "dark blue" zones that are free of modulations. If we look at Figure 2.11 and imagine to overlay it with another map having a similar density of recoupling conditions, this could become difficult. But keeping in mind that this map represents modulations of a *three-spin system* of *carbon-13*, we can be more optimistic. First, in a two-spin system (or more generally speaking: in a J-coupled system with only two chemical shifts), there will be only one type of recoupling and half of the lines in Figure 2.11 would disappear. And second, we know that the spacings of the recoupling conditions parallel to the τ axis will be much larger in a proton system with its small distribution of chemical shifts, due to the relation stated in Equation 2.4 on page 12.

2.4 Trains of 360° pulses [72]

In this section, we will present results observed for a proton in cyclosporin A, where a train of 360° pulses (in stead of the conventional 180° pulses) with moderate *rf* amplitude was able to generate a modulation-free decay, i.e., to decouple a homonuclear spin pair. We decided to publish these results despite the lack of simulations or theory that were able to explain this surprising outcome.

2.4.1 Measurements on an amide proton in cyclosporin A

We generalize the moderate-amplitude CPMG sequence used in this entire chapter to $90°_y - [\tau - m(180°_x) - \tau]_{2n}$. For $m = 1$ we have the standard refocusing scheme with an on-resonance 180° pulse, while $m = 2$ is the new scheme with an on-resonance 360° pulse that *fails* to refocus linear product operator terms like the chemical shift, heteronuclear couplings or the inhomogeneity of the main magnetic field B_0. Experiments are also performed for $m = 3$ with refocusing 540° pulses and for $m = 4$ with non-refocusing 720° pulses to exclude spin locking effects due to pulses of longer duration that are not directly related to the nutation angle. As in the subsection 2.2.1 we look at protons in cyclosporin A (CsA) and focus our

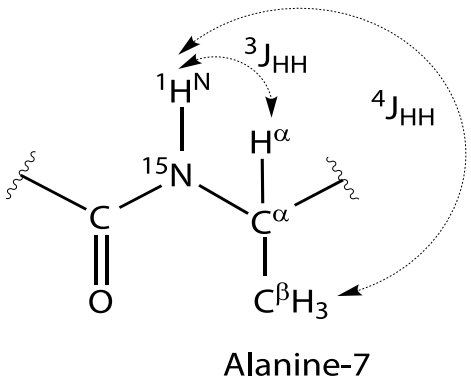

Figure 2.13: Fragment of cyclosporin A (see Fig. 2.3 on p. 15) containing the proton $I = H^N$ of Ala7. The only resolved coupling is ${}^3J(H^NH^\alpha) = 7.4$ Hz that leads to a doublet of the $I = H^N$ signal in the proton NMR spectrum. The long-range coupling ${}^4J(H^NH^\beta)$ contributes to line broadening.

attention on the doublet of proton $I = H^N$ of the amino acid residue Ala7 (Figure 2.13). The only resolved coupling is ${}^3J(H^NH^\alpha) = 7.4$ Hz; the long-range couplings ${}^4J(H^NH^\beta)$ to the three methyl protons merely contribute to broaden the lines. The *rf* carrier was was placed on the chemical shift (7.68 ppm) of proton $I = H^N$, hence $\Omega_I = 0$. In a field $B_0 = 11.74$ T (500 MHz for protons), the offset of the coupling partner $S = H^\alpha$ is $\Omega_S/(2\pi) = 1.578$ kHz. The *rf* amplitude was set at $\omega_1/(2\pi) = 5.5$ kHz. Signals were recorded with "hybrid" schemes using m =1, 2, 3, or 4 with $n = 50$, i.e., the amplitudes of the $2n^{\text{th}} = 100^{\text{th}}$ "echoes" were observed as a function of the interval τ in each case.

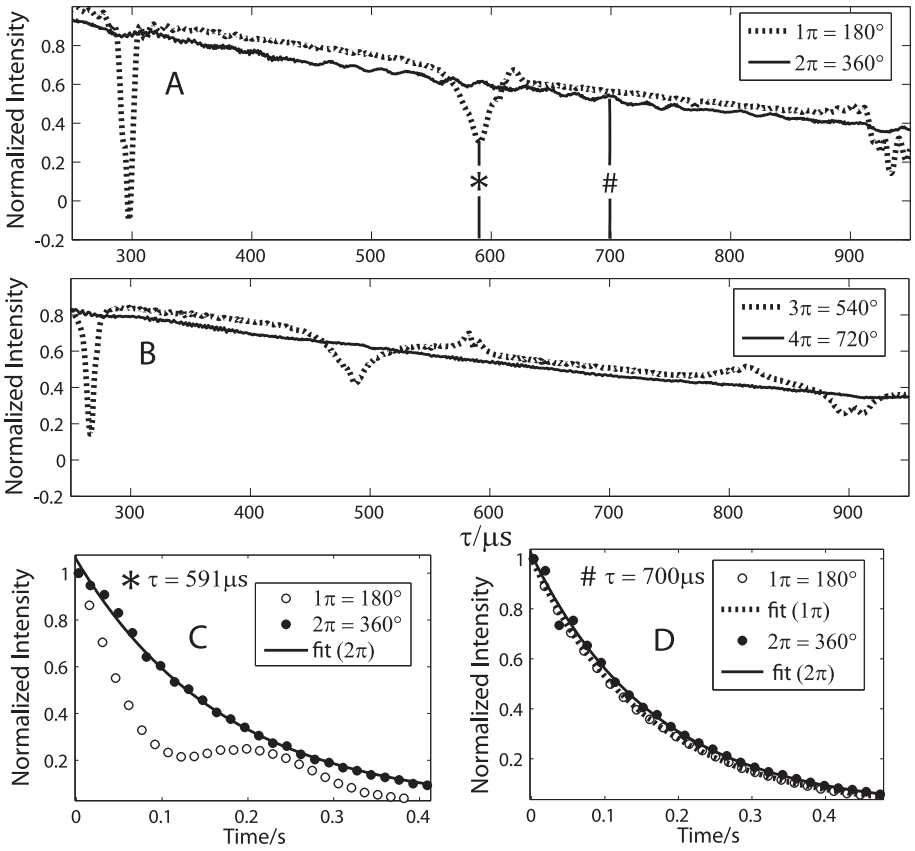

Figure 2.14: A) Amplitude of the H^N proton doublet of Ala7 in CsA recorded with the hybrid scheme $90°_y - [\tau - m(180°_x) - \tau]_{2n}$ for $n = 50$ (100^{th} echo) as a function of $280 < \tau < 950$ µs (in steps of 0.5 µs). The dashed and the solid lines correspond to echoes with $m = 1$ ($\pi = 180°$), and to rotations of $m = 2$ ($2\pi = 360°$), respectively. The curves are normalized by the initial amplitude of the decay for $m = 1$. The vertical lines at $\tau = 591$ µs ($*$) and $\tau = 700$ µs (#) indicate the conditions chosen for the CPMG sequence and its $2\pi = 360°$ equivalent in C) and D). B) The dashed and the solid lines correspond to echoes with $m = 3$ ($3\pi = 540°$) and to rotations of m = 4 ($4\pi = 720°$), respectively. Their amplitudes are normalized by the signals for $m = 1$ in A). C) Decays of the H^N proton doublet of Ala7 recorded with the sequence $90°_y - [\tau - m(180°_x) - \tau]_{2n}$ for $\tau = 591$ µs as a function of the number of cycles n. Empty circles ($m = 1$): n = 1, 10, 20, ..., 200, so that the time axis $T = n(4\tau + 2m\tau_\pi)$ extends over $0 < T < 381$ ms. No R_2 rate could be extracted from the modulated decay. Filled circles ($m = 2$): the fit of the unmodulated decay leads to $R_2 = 5.78\ s^{-1}$. D) Decays of the H^N proton doublet of Ala7 recorded with the sequence $90°_y - [\tau - m(180°_x) - \tau]_{2n}$ for $\tau = 700$ µs as a function of the number of cycles n. Empty circles: echoes with $m = 1$. Fitting the unmodulated decay leads to $R_2 = 6.43\ s^{-1}$. Filled circles: $m = 2$ and $0 < T < 474$ ms. The decay rate is $R_2 = 5.98\ s^{-1}$.

In Figure 2.14 A, we compare signal amplitudes observed using this hybrid scheme with traditional refocusing pulses with $m = 1$ (π or 180° pulses, dashed line) and with a sequence with $m = 2$ (2π or 360° pulses, solid line). Figure 2.14 B shows a comparison between $m = 3$ (3π or 540° pulses, dashed line) and $m = 4$ (4π or 720° pulses, solid line). The sequences with $m = 1$ and 3 lead to nearly flat responses when the modulations are quenched, but to fairly sharp "dips" at the recoupling conditions. The dips observed with 540° pulses are shifted compared to those seen with 180° pulses because the *rf* pulse lengths are different and the recoupling depends on the cycle $\tau_{\mathrm{CPMG}} = (\tau + m\tau_\pi + \tau)$. Remarkably, sequences with $m = 2$ and 4 (solid line in Figure 2.14 A for 360° pulses, and solid line in Figure 2.14 B for 720° pulses) did *not* lead to any recoupling effects. Yet, the overall decay rates are very similar. Since the dips have disappeared, there would be no longer any need to run the time-consuming hybrid experiments.

With reference to Figure 2.14 A, a conventional refocusing sequence with 180° pulses ($m = 1$) leads to recoupling when using $\tau = 591$ µs ($*$) and to quenching at $\tau = 700$ µs (#). In the former case, one observes modulated echoes (empty circles in Fig. 2.14 C). By contrast, the use of a sequence with 360° pulses ($m = 2$) with the same interval $\tau = 591$ µs (filled circles in Fig. 2.14 C) leads to a clean monoexponential decay with $R_2 = 5.78\ \mathrm{s}^{-1}$. For $\tau = 700$ µs, both schemes with $m = 1$ and 2 show monoexponential decays (Fig. 2.14 D) with $R_2(m = 1) = 6.43\ \mathrm{s}^{-1}$ and $R_2(m = 2) = 5.98\ \mathrm{s}^{-1}$ (empty and filled circles). We were expecting that $R_2(m = 2)$ will be affected by the inhomogeneity of the static field, since no refocusing pulses were used. But surprisingly, the rate obtained with the sequence $R_2(m = 2)$ is slightly *smaller* than the $R_2(m = 1)$ obtained with conventional refocusing, i.e., the lifetime of the transverse magnetization appears actually prolonged by using trains of 360° rather than 180° pulses.

Thus, quenching *with* and *without* recoupling are characteristic of sequences of *odd* and *even* multiples of 180° pulses. For $m = 2$ the quenching effect cannot be attributed to a simple spin locking effect arising from to the fact that 360° pulses ($2\tau_\pi = 182$ µs) last twice as long as 180° pulses ($\tau_\pi = 91$ µs). Indeed, for $m = 3$ recoupling effects re-appear. Clearly, the quenching mechanism depends on whether m is odd or even.

2.4.2 Discussion

There are three questions which arise from the experiments with 360° pulses. Why does a train of 360° pulses with moderate *rf* amplitude *not* lead to modulations, but generates an oscillation-free decay? Why do *no* recoupling conditions appear? And why are the decays $R_2(m = 2)$ obtained from 360° pulse trains not *faster* than those from CPMG sequences with 180° pulses $R_2(m = 1)$, where the inhomogeneous broadening should be only present for even m?

Nicolas Aeby performed similar experiments using our CPMG sequence, where the on-resonance pulse for spin I was set to $\beta = 180°$, but the off-resonance pulse for spin S had an effective flip angle of $\beta_{eff} = 360°$ [33]. The effective flip angle for a given *rf* amplitude ω_1 and

and offset Ω_S is

$$\beta_{eff} = \omega_{eff} \cdot \tau_\pi = \sqrt{\omega_1^2 + \Omega_S^2} \cdot \tau_\pi \tag{2.16}$$

The effective *rf* field is tilted away from the z-axis by

$$\theta = \arctan\left(\frac{\omega_1}{\Omega_S}\right) \tag{2.17}$$

using the definition of Ref. [15] such that $\theta = \pi/2$ for the on-resonance case $\Omega_S = 0$.

Aeby first considered the ^{13}C two-spin system of doubly enriched glycine and set the *rf* amplitude to a value $\omega_1 \approx 0.577\ \Omega_S$ that corresponds to an effective off-resonance rotation of $\beta_{eff} = 360°$. The hybrid experiment with these parameters showed clearly *no* recoupling conditions (Figure 7.3 in Ref. [33]). He continued with the fully ^{13}C-enriched alanine (discussed in section 2.3), on resonance with C^α and again applied an effective $\beta_{eff} = 360°$ rotation on the C' resonance. This removed all narrow recoupling dips stemming from $J(C^\alpha C')$ and left the $J(C^\alpha C^\beta)$ recouplings, which no longer appeared as broad dips, but as a binomial triplet of intensities 1:3:3:1 (see Figure 2.15 and compare with Figure 2.10 on page 30). This is the "signature" of the three H^β protons that cause four different effective offsets with respect to the C^α carbon [41].

One does not often encounter 360° pulses in NMR. The most common usage is probably for pulse calibration, when either a 180° or a 360° pulse is optimized, by searching for the zero-crossing of the signal. In 1969 Freeman and Wittekoek used a CPMG with soft 360° pulses to measure T_1 in a selective manner [73]. After an initial inversion pulse, they followed the magnetization by acquiring the signal during the 360° pulses of this "CPMG sequence", while in between the pulses, the magnetization was along the z-axis and relaxed with T_1.

A full rotation, at least for ideal pulses without relaxation, is an identity operation. It should be equivalent to *not* applying any *rf* field. Aeby's experiments therefore achieve a "selective" refocusing in a smart way: Spin I was rotated by 180° and spin S by 360°, i.e., remained unaffected, at least for the picture of an ideal pulse. This experiment did not rely on the accumulation of pulse errors; a fact that would agree with the lack of recoupling conditions.

In our experiments with the adapted CPMG sequence for $m = 2$, the on-resonance rotation was 360° and should ideally had no influence on spin I. The off-resonance rotations for the experiments in CsA mentioned above were $\beta_{eff} = 375°$ and therefore overshot a full rotation by $\epsilon = 15°$. It is known already from Hahn's first echo experiments with 90° pulses that the refocusing property is not restricted to a 180° rotation. Hennig described that arbitrary but identical pulses in multi-echo sequences are able to refocus [74]. For uncoupled spin-1/2 nuclei, refocusing with pulse trains of $\beta = 15°$ are possible, but one has to keep in mind that

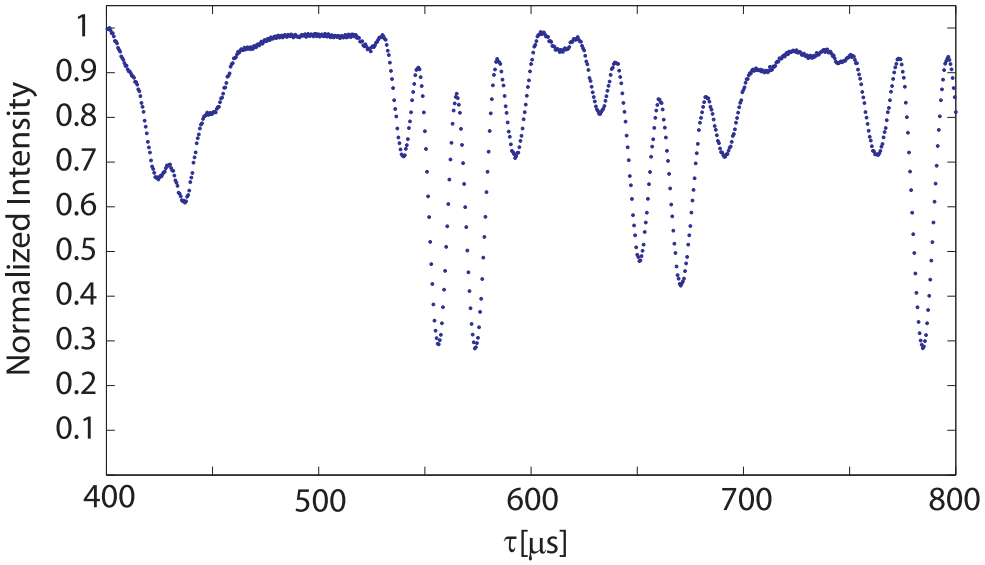

Figure 2.15: Experimental echo amplitudes C_x^α in ^{13}C- and ^{15}N-enriched alanine, observed with a hybrid experiment $[\tau - 180°_x - \tau]_{20}$ comprising $2n = 20$ 180° pulses. The ^{13}C *rf* amplitude corresponds to a 180° pulse length $\omega_1/(2\pi) = 54.92$ µs. This leads to a rotation about the tilted effective field ($\theta = 30°$) through $\beta_{eff} = 360°$ for the off-resonance C' magnetization which has an offset $\Omega_S/(2\pi) = 15.77$ kHz. The τ delay has been varied between 400 and 800 µs in steps of 0.5 µs. This figure was published in Aeby's thesis [33] and in Ref. [41].

besides T_2, also T_1 and the flip angle itself will have an influence on the echo amplitudes. So, the off-resonance pulses could guarantee in our case refocusing and the on-resonance pulses would not affect the spins. This would be, again as in Aeby's example but with exchanged roles of the spins I and S, a new way for selective decoupling.

Computer simulations of pulse sequences including 360° rotations can become tricky. If a 360° rotation appears in a propagator to solve the Liouville-von Neumann equation (the equation of motion for the density operator [14]), the rotation axis becomes undefined and discontinuities appear. This was illustrated for example in the work of Emsley and Bodenhausen to optimize shaped selective pulses [75], where quaternions were used to circumvent this problem. Quaternions have four components and can be represented by a sum of a scalar and a vector. Siminovitch wrote a review about quaternions in the context of rotations in NMR [76, 77].

Our first simulations of trains of moderate 360° pulses in a two-spin system indeed suffered from these singularities. We switched to SpinDynamica [34], where Prof. Levitt confirmed that the ambiguities of the Euler angles are not an issue. When simulating trains of 360° pulses in a two-spin system, under the experimental conditions described above, the signal was fully modulated.

So far, we were not able to simulate our observations of trains of moderate 360° pulses that lead to a modulation-free decay. Our simulations did not include relaxation, since we do expect a coherent mechanism behind this form of decoupling.

There is still the third question open, why we measured slower decays with trains of 360° pulses, than with 180° pulses. With our moderate amplitude CPMG method, we optimize the delay τ to avoid a recoupling with spins at a defined offset Ω_S. Now it can happen that long-range couplings are too small to show dips in a hybrid experiment for the number of echoes $2n$. This would lead to an unresolved modulation in the CPMG experiment varying $2n$ and slightly accelerate its decay. If we use 360° pulses with a moderate amplitude, there will be for each offset Ω another effective nutation angle β_{eff} along with an overshoot ϵ. Multiple pulses of any angle (except 360°) can refocus magnetization and therefore decouple, if applied selectively on one pulse. So, the moderate multiple 360° pulses could have the advantage of quenching couplings, stemming from spins at *any* offset Ω. This is an attempt to explain the slower decaying magnetization under multiple 360° pulses. The only "recoupling" one could imagine would appear for an on- *and* off-resonance identity rotation, e.g., at β = 360° and β_{eff} = 720°. As defined in Equation 2.16, the off-resonance flip angle is of course independent of the free evolution delay τ. As mentioned before, the hybrid experiment as a function of τ becomes obsolete. Recoupling would appear only on the chemical shift axis (corresponding to the y-axis in the 2D simulation of Figure 2.11 on page 32) and would be at $\Omega/(2\pi) \approx 9.5$ kHz for the *rf* amplitude $\omega/(2\pi)$ = 5.5 kHz, used in the experiments above. Such an offset is too large for protons at a Larmor frequency of 500 MHz.

It is evident that this topic needs more time for experimental and theoretical investigations, until a fully satisfying explanation can be presented.

2.5 A comparison of different methods

In this whole chapter, we continuously used our in-house method, the moderate-amplitude CPMG sequence, to measure transverse relaxation of homonuclear coupled spins. In the final part of this chapter, we will compare several pulse sequences, to measure the transverse relaxation of protons without echo modulations. A part of this work was presented at the EUROMAR conference 2012 in Dublin.[5]

2.5.1 Introduction of different methods [20]

There are two ways to prevent evolution under chemical shifts: spin-locking, and refocusing. Spin-locking gives the chemical shift no chance to evolve, while refocusing leaves it to evolve freely, before changing its sign to achieve a "time reversal". By analogy, these two strategies can also be applied to homonuclear J-evolution. Using moderate-amplitude CPMG sequences that benefit from the SITCOM effect (see subsection 2.1.2), we can in effect "lock" I_x and suppress its conversion into $2I_yS_z$. As can be seen in Figure 2.2 C (on p. 11), the evolution due to the coupling is successfully inhibited. So what pulse sequence could be used to refocus homonuclear J-evolution? This task can be fulfilled by the insertion of a hard 90° pulse, with a phase orthogonal to the excitation pulse, at the top of an echo (i.e., half-way between two 180° pulses of a conventional CPMG sequence), as proposed by Takegoshi et al. [78] and van Zijl et al. [79]. This idea can take the form of a sequence

$$90^\circ_y - [\tau - 180^\circ_x - \tau - 90^\circ_x - \tau - 180^\circ_x - \tau]_n \tag{2.18}$$

Since the central 90°_x pulse coincides with an echo, with the refocused magnetizations aligned along the pulse axis, only evolution due to homonuclear J-couplings need to be considered. In a two-spin system IS, the product operators before and after the central 90°_x pulse are:

$$(I_x + S_x)\cos\theta_J + (2I_yS_z + 2S_zI_y)\sin\theta_J \xrightarrow{90^\circ_x} (I_x + S_x)\cos\theta_J - (2I_zS_y + 2S_yI_z)\sin\theta_J \tag{2.19}$$

where $\theta_J = \pi J 2\tau$. The 90°_x pulse leaves the in-phase terms unchanged, since they lie parallel to the x-axis, but swaps the two antiphase terms while changing their signs. A simulation of the evolution of the product operators of this "perfect echo" is shown in Figure 2.2 D on page 11 for $n = 1$. For arbitrary values of 2τ, the signal will be purely in-phase *at the end* of each block. This type of refocusing is well known for homonuclear dipolar interactions in solids [80] and for first-order quadrupolar interactions [81]. The resulting echoes are known as solid echoes, dipolar echoes or quadrupolar echoes, all of which involve spin operators that are bilinear or quadratic [11] (the 180° pulses are usually dropped if the carrier is on resonance

[5] T.F. Segawa, D. Carnevale, and G. Bodenhausen, *How to Measure Transverse Relaxation of Protons*, EUROMAR 2012, Dublin.

so that the offset or chemical shift can be neglected). The combined refocusing of chemical shifts and dipolar couplings with "perfect echo" sequences in the solid state was dubbed "Hahn-solid-Hahn echo" by Schmidt-Rohr [82].

All pulses are "hard" or non-selective and therefore the sequence is broadband, i.e., works over a wide range of offsets. The drawback is that the J-refocusing only works perfectly for a two-spin system. With more spins, the oscillations are not completely suppressed. The decoupling, however, becomes successful for any spin system if the inter-pulse delays are short enough to fulfill the condition $\theta_J = \pi J 2\tau \ll 1$ (a corollary is that the number of echo blocks n can become quite large) [83]. This condition is however much less strict than for spin-locking, where τ should be small compared to the inverse $2\pi/\Omega_S$ of the chemical shift, i.e., $\Omega_s\tau \ll 1$. The sequence was named PROJECT (periodic refocusing of J-evolution by coherence transfer), since the interconversion of the antiphase terms in Equation 2.19 is achieved by a symmetrical homonuclear coherence transfer. It is a very useful building block for various intervals t in homonuclear coupled systems, since the amplitude is attenuated by $\exp(-t/T_2)$, for example for T_2-weighted diffusion-ordered spectroscopy (DOSY) [84]. Since the refocusing effect relies on the symmetric exchange of coherence between coupling partners, their initial magnetizations must be equal.

For the actual measurement of R_2's in homonuclear coupled systems, as discussed in subsection 2.2.1 (p. 18), the in-phase magnetization I_x and the antiphase term $2I_yS_z$ generally do not relax with the same rate. While moderate-amplitude CPMG benefits from the SITCOM effect (Figure 2.2 C) or spin-locking and can yield a "pure" in-phase rate $R_2(I_x)$, J-refocusing will lead to an "apparent transverse relaxation rate", i.e., a mixture of $R_2(I_x)$, and $R_2(2I_yS_z)$, (Figure 2.2 D). This mixture is a function of τ; if τ is very short, the contribution of $R_2(2I_yS_z)$ is small and the apparent transverse relaxation rate should be close to $R_2(I_x)$. Since in most practical cases $R_2(I_x) < R_2(2I_yS_z)$, the former might therefore be overestimated, especially for longer τ. Another point is related to the interconversion of the antiphase terms in Equation 2.19. Since these two antiphase terms are interchanged by the $90°_x$ pulse, their relaxation rates *cannot* be determined separately, but only their average. This is not the case for the relaxation rates of the in-phase terms I_x and S_x, since these are not interconverted. These details are of secondary relevance when the determination of an *apparent* T_2 is sufficient, as it is the case in T_2-weighted experiments.

Barrère et al. have described an experiment similar to J-refocusing, in which the sum of the signals that can pass a zero-quantum filter (ZQF) and a double-quantum filter (DQF) is not modulated by the J-coupling [85]. This sequence was designed to measure relaxation, in contrast to the J-refocusing sequences reviewed above. As for Takegoshi's perfect echo, this sequence is broadband and works perfectly only for AX-systems. Barrère's sequence looks rather similar to Takegoshi's sequence in Equation 2.18:

$$90^\circ_y - \tau - 180^\circ_x - \tau - 90^\circ_y 90^\circ_\phi - \tau - 180^\circ_x - \tau \tag{2.20}$$

There are now two 90° pulses at the time of the echo in the middle of the sequence. The first $90°_y$ fails to refocus the J-coupling (due to its phase), but creates double-quantum coherences (DQC) from the antiphase terms. The phase of the $90°_\phi$ pulse and the receiver phase are cycled to achieve multiple-quantum (MQ-)filtration. Since the method is based on a summation of two experiments, it cannot be run in the fashion of PROJECT sequences with short values for τ to decouple general homonuclear spin systems. The transverse relaxation rate is again a mixture of decay rates of in- and antiphase magnetization, but the interconversion of the antiphase terms does *not* occur, in contrast to the sequence of Equation 2.19.

Both sequences, the perfect echo and the summation of ZQF- and DQF-signals (called from now on "MQF sequence") were independently designed earlier to generate "planar mixing". In contrast to "isotropic mixing" with $I \cdot S = I_x S_x + I_y S_y + I_z S_z$, this is an effective Hamiltonian that contains equal contributions of x and y components, such as a ZQ- (e.g., $I_x S_x + I_y S_y$) or a DQ-Hamiltonian (e.g., $I_x S_x - I_y S_y$) [86]. They were applied to reduce multiplet complexity in COSY experiments [86] and to observe spin waves by NMR [87]. Schulte-Herbrüggen et al. [86] started with a ZQ planar sequence like Barrère and simplified this sequence to the "perfect echo".

Therefore, while "decoupling" with these sequences is based on an effective Hamiltonian that is *planar*, our CPMG under SITCOM achieves decoupling with an *isotropic* Hamiltonian (except at recoupling conditions, where it has the weak coupling form $I_z S_z$, as shown in Equation 2.5 on page 12). Schulte-Herbrüggen et al. [86] explain that these two effective Hamiltonians are equivalent for a two-spin system, but only the isotropic one can be realized for arbitrarily complex and strongly coupled spin system, in contrast to the planar one. All these considerations do not include relaxation, but they confirm that both classes of sequences will show no effective evolution under homonuclear J-couplings.

2.5.2 Experimental comparison

For an experimental comparison of the different methods to measure the transverse relaxation, we decided to choose simple proton spin systems. Relaxation measurements were performed on a proton AX and an AX_2-system to investigate the limitations of some sequences. Spectra were recorded at a ^{1}H Larmor frequency of 500 MHz (B_0 = 11.74 T) and a temperature of T = 300 K. The AX-system were the two protons in 2,3-dibromothiophene, dissolved in CD_2Cl_2, with a chemical shift difference of $\Delta\Omega$ = 188 Hz and a J-coupling of 5.8 Hz. 3,5-dichlorophenol in $CDCl_3$ was chosen as an AX_2-system with a chemical shift difference of $\Delta\Omega$ = 99.3 Hz and a J-coupling of 1.75 Hz. Of course, the fastest method to obtain a good value for T_2 in such a small molecule would be simply to measure T_1, where no modulations occur. But here our goal was an experimental study of the methods.

Decays for the magnetization of the H^4 proton of 2,3-dibromothiophene (AX-system) are shown in Figure 2.16. The experimental conditions are summarized in Table 2.4. As expected, all decays were free of echo modulations. By looking at the decays in Figure 2.16 and the rates

in Table 2.4, we can group them into three categories. The first category with the slowest decays consists of the moderate-amplitude CPMG (red circles) and the spin lock sequence (blue squares). The experimental points lie on the exponential curve and the two decays were nearly identical with $R_2 = 0.114\ s^{-1}$ for the CPMG and $R_2 = 0.119\ s^{-1}$ for spin-locking. These were closely followed by the PROJECT sequence (brown triangles), again with an excellent fit, but a faster decay of $R_2 = 0.130\ s^{-1}$. The two remaining ones, the perfect echo (green diamonds) and the multiple-quantum filtration (MQF) sequence (black stars) did not only lead to a much faster decay, but also showed a similar zigzag pattern and a deviation from an exponential decay. But both rates were very close with $R_2 = 0.42\ s^{-1}$ for the perfect echo and $R_2 = 0.39\ s^{-1}$ for the MQF sequence.

The superposition of the decays from our CPMG and the spin-locking sequence, a standard technique to measure R_2 (or rather $R_{1\rho}$) in homonuclear systems, confirms that the decays measured with the moderate-amplitude CPMG sequence are equivalent to $R_{1\rho}$. This underlines, as seen by simulations in Figure 2.2, that the moderate-amplitude CPMG sequence effectively *locks* the in-phase coherence I_x. PROJECT signals were free of modulations, but not anymore relaxing with a "pure" R_2, since a small conversion into faster relaxing antiphase coherences cannot be inhibited. The remaining two decays from the perfect echo and the MQF sequence were 3-4 times faster than the others. As it can be seen from Table 2.4, both methods do not vary the number of blocks n, but increment the inter-pulse delays up to values $\tau \gg 1/J$, where in- and antiphase coherences are freely interconverted. We expect an average of $R_2(I_x)$ and $R_2(2I_yS_z)$ (see Equation 2.12 on page 19) and therefore, these decays should give us the same rate as obtained from a *single refocusing* experiment, shown in Figure 2.4 C on page 16 for a ^{1}H two-spin system in cyclosporin A. Using Equation 2.14 on page 20, we can estimate the antiphase relaxation rate to $R_2(2I_yS_z) \approx 0.7\ s^{-1}$, around six times faster than $R_2(I_x)$. But why were the exponential fits in Figure 2.16 unsatisfactory and why did both decays, from the perfect echo and the MQF sequence, show the same zigzag structure? We must remember that perfect echo and PROJECT are the same sequences, but the first one is run as a function of the delay τ (in the manner of Carr and Purcell's method "A", see subsection 2.1.1) and the second one is run as a multiple-echo sequence (in the style of Carr and Purcell's method "B"), incrementing the number of blocks n, while keeping τ constant. In their original paper, Takegoshi et al. [78] applied both methods to their sequence. When τ is varied, the mixture of I_x and $2I_yS_z$ is a function of this delay and therefore varies for each data point. The minima in the zigzag must be points with the highest amount of $2I_yS_z$ in the mixture. To avoid this, the delays should be synchronized by multiples of $1/J$. The MQF sequence was tried with incrementing the number of blocks n, which did not work. The small differences between the rates obtained from the MQF ($0.39\ s^{-1}$) and the perfect echo sequence ($0.42\ s^{-1}$), could stem from the property that the latter exchanges the antiphase components, while the former should not (see discussion in the subsection 2.5.1). This hypothesis could be verified, if the individual antiphase relaxation rates could be experimentally determined.

As discussed above, the experiments confirm that all sequences work off resonance, except the moderate-amplitude CPMG.

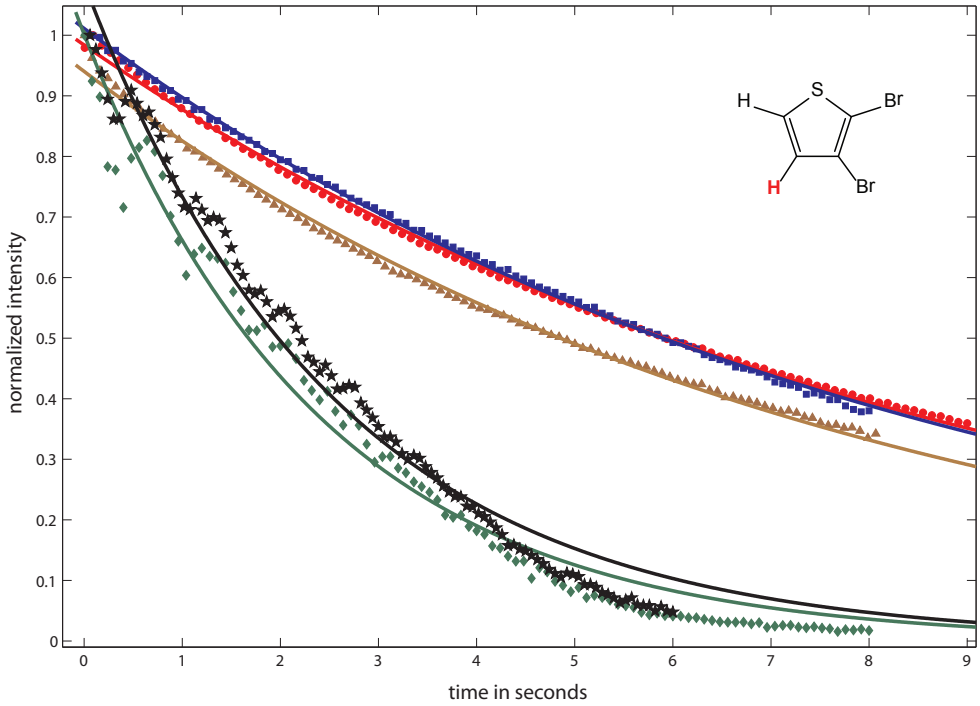

Figure 2.16: Transverse decays in the ^{1}H AX-system 2,3-dibromothiophene (shown as inset) of the H^4 proton (in red) at 500 MHz (B_0 = 11.74 T) and T = 300 K. The solvent was CD_2Cl_2, the protons had a chemical shift difference $\Delta\Omega$ = 188 Hz and a J-coupling of 5.8 Hz. Red circles were obtained by the moderate-amplitude CPMG sequence, blue squares with spin-locking, brown triangles with the PROJECT sequence, green diamonds with a perfect echo and black stars with the multiple-quantum filtration (MQF) sequence. Since all decays were free of modulations, they were fitted with an exponential decay; the lines are plotted with the same color coding. The slowest decays were obtained by CPMG and spin-locking, closely followed by PROJECT. The perfect echo and the MQF sequence did not only lead to a clearly faster decay, but also showed a characteristic zigzag pattern and a deviation from an exponential decay. Detailed experimental parameters and the fitted transverse relaxation rates are listed in Table 2.4.

Method	R_2 from fit	τ in ms	n	*rf* carrier	others
CPMG	**0.114 s^{-1}** (red)	1	1;15:15:1500	on-resonance	ω_1 = 500 Hz τ_π = 1 ms
Spin-locking	**0.119 s^{-1}** (blue)	80:80:8000		half-way between the two ^{1}H's	ω_{SL} = 2 kHz
PROJECT	**0.130 s^{-1}** (brown)	1	1;20:20:2000	off-resonance	
MQF	**0.39 s^{-1}** (black)	15:15:1500	1	off-resonance	8-step phase cycle
Perfect echo	**0.42 s^{-1}** (green)	1;20:20:2000	1	off-resonance	

Table 2.4: Experimental parameters and fitted transverse relaxation rates for the H^4 proton in the AX-system 2,3-dibromothiophene, corresponding to the decays in Figure 2.16. τ are the delays in the individual pulse sequences, and the total duration for spin-locking, respectively. n is the number of basic blocks applied. All pulses are "hard", except when the *rf* amplitude is mentioned in the table.

Decays for the AX_2-system in 3,5-dichlorophenol, looking at the triplet of the H^4 proton (para to the phenol group) are shown in Figure 2.17 and the experimental conditions are summarized in Table 2.5. The color coding for the different methods were the same as for the AX-system in Figure 2.16. The order of the decays remained the same as for the AX-system. In this system, the decays measured by the MQF (black stars) and the perfect echo sequence (green diamonds) were strongly modulated; some of the intensities became negative. Note that the y-axis (intensity) varies from -0.5 to 1 in Figure 2.17, but only from 0 to 1 in Figure 2.16. As expected and discussed above, these sequences are limited to an AX-system. Such partially suppressed modulations in AX_n-systems were discussed by van Zijl et al. [79]. Once again, this result proves the close relationship between the sequences MQF and perfect echo. The short τ value in the PROJECT sequence (brown triangles) generated an oscillation-free decay, again with a slightly faster relaxation rate of 0.208 s^{-1}. And finally, the slowest and almost identical rates were found by the moderate-amplitude CPMG (0.149 s^{-1}) and the spin-locking sequence (0.158 s^{-1}). It is interesting to note that for both investigated spin systems the rate measured by CPMG was slightly smaller than the one from spin-locking. $R_{1\rho}$ can depend on the amplitude of the *rf* locking field ω_{SL}. For both systems, we have chosen a value of $\omega_{SL} \approx 10\Delta\Omega$. This condition could be only fulfilled for small differences of chemical shifts, otherwise the risk of heating cannot be excluded. An estimation of the antiphase relaxation rate $R_2(2I_yS_z)$ becomes difficult in this AX_2 system, since the modulated decays are not straight forward to fit. The only source containing $R_2(2I_yS_z)$ would be the rate from the PROJECT sequence. But for a reliable calibration, an independent and direct measurement of the antiphase decay $R_2(2I_yS_z)$ would be desirable.

To conclude the results of this experimental comparison, in-phase decays of $R_2(I_x)$ in homonuclear systems can be obtained by either *spin-locking* or *the moderate-amplitude CPMG sequence*. Spin-locking has the broadband advantage, but may cause heating for large *rf* locking

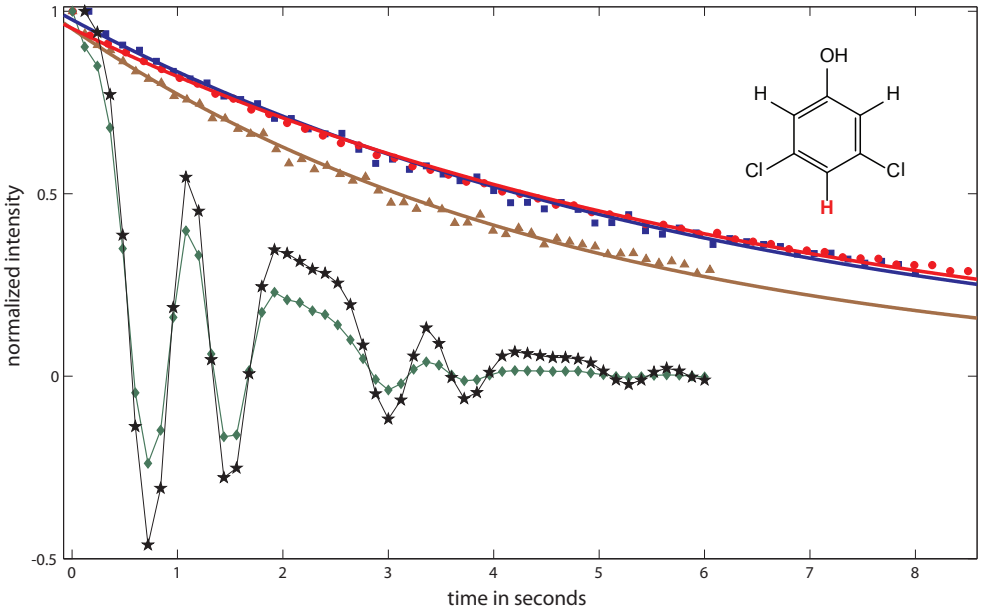

Figure 2.17: Transverse decays in the ^{1}H AX$_2$-system 3,5-dichlorophenol (shown as inset) of the triplet of the H^4 proton, para to the phenol group, (in red) at 500 MHz (B_0 = 11.74 T) and T = 300 K. The solvent was $CDCl_3$, the protons had a chemical shift difference $\Delta\Omega$ = 99.3 Hz and a J-coupling of 1.75 Hz. Red circles were obtained by the moderate-amplitude CPMG sequence, blue squares with spin-locking, brown triangles with the PROJECT sequence, green diamonds with a perfect echo and black stars with the multiple-quantum filtration (MQF) sequence. The first three unmodulated decays were fitted with exponential decays; the modulated decays from perfect echo and MQF were *not* fitted, but the data points were joined with lines to guide the eye. The slowest decays were, as for the AX-system, obtained by CPMG and spin-locking, closely followed by PROJECT. The perfect echo and the MQF sequence led both to a fast and modulated decay, again showing a similar pattern. Note that the y-axis (intensity) varies here from -0.5 to 1, but only from 0 to 1 in Figure 2.16. Detailed experimental parameters and the fitted transverse relaxation rates can be found in Table 2.5.

Method	R_2 from fit	τ in ms	n	*rf* carrier	others
CPMG	**0.149 s^{-1}** (red)	1	1;30:30:1500	on-resonance	ω_1 = 300 Hz τ_π = 1 ms
Spin-locking	**0.158 s^{-1}** (blue)	160:160:8000		half-way between the two ^{1}H's	ω_{SL} = 1 kHz
PROJECT	**0.208 s^{-1}** (brown)	1	1;30:30:1500	off-resonance	
MQF	**no fit** (black)	30:30:1500	1	off-resonance	8-step phase cycle
Perfect echo	**no fit** (green)	1;30:30:1500	1	off-resonance	

Table 2.5: Experimental parameters and fitted transverse relaxation rates for the triplet proton in the AX_2-system 3,5-dichlorophenol, corresponding to the decays in Figure 2.17. τ are the delays in the individual pulse sequences, and the total duration for spin-locking, respectively. n is the number of basic blocks applied. All pulses are "hard", except when the *rf* amplitude is mentioned in the table.

amplitudes ω_{SL}. Moderate-amplitude CPMG is a selective technique and may need some preliminary "hybrid" experiments or simulations to avoid recoupling condition, but there is no risk of heating. A *selective* spin-lock applied on resonance could be a possible alternative (see also discussion in chapter 4). As mentioned before PROJECT is an ideal solution for T_2-weighted experiments: it guarantees for all homonuclear spin systems in a broadband manner an exponential decay. But since the generation of small amount of antiphase magnetization cannot be avoided, the first two methods should be preferred for the exact measurements of $R_2(I_x)$. And finally, there are the perfect echo and the MQF sequence, which are limited to an AX-system and measure a mixture of $R_2(I_x)$ and $R_2(2I_yS_z)$. Additionally, the resulting decays depend on τ and the MQF sequence needs an 8-step phase cycle to be completed. Therefore, these two sequences are practically not of interest.

2.5.3 Direct measurements of the antiphase relaxation

The comparison of methods to measure R_2 in protons raised our interest in the relaxation of the antiphase magnetization $2I_yS_z$. The measurement of $R_2(2I_yS_z)$ is a well-known problem in the *heteronuclear* case: a locking *rf* field on spin I in y-direction is sufficient, as proposed by Peng et al. in 1991 [88]. This strategy was adapted by Meersmann and Bodenhausen in 1995 for the homonuclear case of protons [47], where the transverse component was *selectively* locked. They studied the antiphase decays of H^α and H^N protons in cyclosporin A (CsA), as well as of an aromatic proton in a DNA dodecamer. To our knowledge, there were no further attempts to measure antiphase decay rates in protons.

We went back to the proton AX_2-system in 3,5-dichlorophenol, applied a "hard" $90_y°$ pulse, waited for a delay $1/(2J)$ to obtain pure antiphase components $2I_yS_z$ and then applied a spin-

locking field on the y-axis. To our surprise, both doublets were evolving under the J-coupling during the locking period. We realized that the carrier was set in the middle between the two protons, as for the spin-locking experiments in the subsection 2.5.2. Therefore, a chemical shift evolution took place for both spins in the first delay, what led to a Hartmann-Hahn [89] or TOCSY [28] effect under the subsequent spin lock. While a spin lock suppresses chemical shifts and J-evolution for two spins lying parallel in the xy-plane

$$[(I_x + S_x), I \cdot S] = 0 \tag{2.21}$$

in the case of two antiparallel spins, a J-evolution takes place

$$[(I_x - S_x), I \cdot S] = i(-2I_y S_z + 2I_z S_y) \tag{2.22}$$

where the rate of evolution is $2\pi J$ and not πJ, as in free evolution [14]. The commutation of Equation 2.22 is also used for the generation of the recently discovered *long-lived coherences* (LLC's) [90, 91], a method for narrowing the *homogeneous* linewidth. There, the chemical shifts of the spins need to be suppressed, to generate a slow decaying coherence that oscillates with $2J$. This is in contrast to our decoupling efforts, where we want to suppress the scalar evolution.

We then adopted the scheme of Meersmann and applied a selective spin lock of ω_{SL} = 30 Hz on the triplet proton in 3,5-dichlorophenol. The decay showed some modulations at the beginning and could not be properly fitted with a monoexponential decay. A biexponential fit worked better and led to a faster rate of 1.29 s^{-1} and a slower of 0.18 s^{-1}. Meersmann had obtained monoexponential decays in CsA. The difference between the two systems are chemical shift difference of $\Delta\Omega$ = 99.3 Hz and a J-coupling of 1.75 Hz in our case versus of $\Delta\Omega \approx$ 1.6 kHz and $J \approx$ 7 Hz for an amide proton in CsA at both 500 MHz. It is evident that $\Delta\Omega$ is much larger in Meersmann's system. ω_{SL} must be chosen that it is large enough to suppress the evolution of the J-coupling, when irradiated on resonance, but also weak enough to avoid affecting the S spin. Our system fails to satisfy both conditions. The locking field along the y-axis of 30 Hz affects the "S_z" part of $2I_yS_z$ and generates, "S_x", leading to the multiple-quantum coherence $2I_yS_x$. On the other hand, if we go too low with ω_{SL}, the J-evolution could not anymore be suppressed. For this system with relatively close chemical shifts, we were not able to find an optimal condition to obtain a monoexponential decay of the antiphase signal.

Other attempts were made with echo sequences. Of course, ideal pulses should cause modulations and therefore, moderate-amplitude CPMG sequences were tested. The first question was when measuring $2I_yS_z$, along which axis, x or y, the 180° pulse should be applied. In any case, the refocusing for the "I_y" part is combined with an inversion of the "S_z" part. We decided to apply the pulse along the x-axis, as done for the corresponding I_x magnetization. The results

were similar to the ones with spin-locking: a proper monoexponential decay could not be obtained.

Why is a stabilization of the antiphase term $2I_yS_z$ so difficult? In contrary to the in-phase term I_x, the antiphase product operator is bilinear and the two axes are perpendicular. As seen above, in a homonuclear experiment, there is always the risk to perturb the S spin along the z-axis, while trying to stabilize the I spin on the y-axis. The solution to this problem might have certain parallels with sequences to preserve heteronuclear multiple-quantum coherences (MQC) and probe their relaxation dispersion [54, 55]. A simple locking fails, since all four coherences in the MQC subspace, i.e., $2I_xS_x$, $2I_xS_y$, $2I_yS_x$, and $2I_yS_y$, should be simultaneously preserved. Their solution is based on the broadband decoupling schemes MLEV and WALTZ [1, 92]. So, the question arises, if a composite-pulse sequence exists that would preserve antiphase terms. In a discussion with Prof. Burkhard Luy, he mentioned DIPSI [93] as a potential candidate sequence. This broadband heteronuclear decoupling sequence was designed to decouple protons from carbon-13, when scalar couplings among protons are present. He also noted that an interconversion of the antiphase terms, similar to the perfect echo sequence (Equations 2.18 and 2.19 on page 41) could take place. To investigate in this direction, further simulations and experiments will be needed.

Measuring directly the relaxation of homonuclear antiphase terms remains a challenging task.

3 Fourier Double Resonance

Double resonance is one of the oldest class of NMR experiments and dates back to 1954, when Virginia Royden from Varian Associates in Palo Alto, California, performed the first heteronuclear decoupling experiment, by irradiating the ^{13}C frequency while observing the signals of the coupled protons [94]. As apparent from the name, double resonance includes two *rf* fields, where the first one B_1 is *observing* and the second one B_2 is *perturbing* the NMR frequencies [95].

In this chapter we present two complementary types of double resonances experiments: *decoupling* and *tickling*. While the former is probably known to any NMR user, the latter does not play a significant role anymore in today's NMR spectroscopy. Spin "tickling" was the preferred method to study connectivities before the advent of Fourier transform (FT) NMR [2] and two-dimensional correlation spectroscopy [96]. If a weak second resonance $\omega_2/(2\pi) < J$ is irradiated at the frequency of an *individual* transition, all connected resonances will *split* by $\omega_2/(2\pi)$. So, tickling will increase the number of lines in the spectrum, while decoupling does the opposite.

There are numerous double resonance experiments. An irradiation of a second frequency in continuous-wave (CW) NMR may cause at the same time a nuclear Overhauser enhancement *and* a coherent effect such as tickling or decoupling. These effects can be separated in a clean way by performing Fourier transform (FT) double resonance, as discussed in detail by Ernst et al. in the paper "Equivalence of Fourier spectroscopy and slow passage in NMR" in 1974 [97]. If the irradiation is applied *before* the 90° excitation pulse, only the nuclear Overhauser enhancement will be seen. If the irradiation is applied *after* the 90°, so during acquisition in a simple 1D, depending on the B_2 field strength, coherent effect such as tickling or decoupling will occur. This is a clear advantage of FT double resonance over CW double resonance. As we know from heteronuclear decoupling in FT NMR spectroscopy, it is sufficient for example to irradiate the protons, while acquiring the signal of the carbon-13 spins, which are *not* irradiated. The "homonuclear challenge" arises, when protons should be decoupled from other protons. An *rf*-pulsing during acquisition is not possible in FT mode, since the receiver will be damaged; a problem that does not exist in CW mode. It was Jesson et al. in 1973 that

proposed an elegant solution for this problem, where they *shared* the dwell time, between the *rf*-irradiation and the acquisition [10]. They used this method for homonuclear decoupling and for selective saturation, but also mentioned spin tickling. Such a scheme is also known as *windowed acquisition*, a term that stems from a homonuclear decoupling experiment in the *solid* state by Mehring and Waugh in 1972 [98]. This strategy is still popular today in solid-state NMR, but not often used in liquid-state experiments. An exception is a single-scan sequence for the calibration of the pulse length by Wu and Otting from 2005 [99]. They performed a nutation experiment and included windows for acquisition. This nice example illustrates, how a windowed acquisition can allow to reduce a (pseudo) 2D to a 1D experiment and save a lot of time.

In this chapter, we first present a modified homonuclear decoupling sequence that can selectively decouple at multiple frequencies. In the second section, we use the same sequence to promote *Fourier spin tickling*, a versatile tool for NMR spectroscopy that seems to be forgotten.

3.1 Polychromatic homonuclear decoupling [36]

3.1.1 Introduction

The idea of studying decoupling not only in the *time*, but also in the *frequency* domain, occurred while working on the pulse trains of 360° (discussed in section 2.4). If we could decouple homonuclear couplings, while keeping the chemical shift evolution, this would be perfect for homonuclear decoupling of NMR spectra. Here, it is essential to keep the chemical shift information and therefore *not* to use an echo, in contrast to our time domain experiments in chapter 2. It turned out that 360° pulses were not an ideal solution for this purpose, but thanks to Diego Carnevale's idea of replacing the moderate 180° pulses in our CPMG sequence with very short pulses of $\beta \approx 1°$, we were ready to start decoupling in the frequency domain.

Decoupling is a well-known tool to simplify NMR spectra, gain resolution, and identify chemical shifts and J-couplings in solution. Although heteronuclear decoupling (e.g., irradiating ^{1}H while observing ^{13}C) is a routine operation, homonuclear decoupling (e.g., acquiring a ^{1}H decoupled ^{1}H spectrum) remains a challenge, because the Larmor frequencies of coupled spins can be very close. First attempts to achieve homonuclear decoupling are older than Fourier transform (FT) NMR spectroscopy and employ continuous-wave (CW) double resonance proposed by Anderson and Freeman in 1962 [9]. In 1976, Aue et al. proposed J-resolved 2D spectroscopy, in which a skew projection generates a broadband homonuclear decoupled spectrum [100]. By introducing a constant-time period, Bax and Freeman designed a 2D, where the projection on the indirect axis shows a broadband homonuclear decoupled spectrum [101]. Pines and co-workers introduced the *bilinear rotation decoupling* (BIRD) method in 1982, which is based on discrimination of protons coupled to carbon-12 or carbon-13 and works broadband too. Shaka et al. focused their attention on the *processing* of 2D J-spectra to circumvent the problem of "phase-twist" lineshapes that make a 45° projection vanish [102]. In 1997, Zangger and Sterk presented an original solution of the "homonuclear problem" by combining selective pulses and magnetic field gradients [103]. These methods have the "broadband advantage", but may suffer from low sensitivity. Additionally, a time-intensive 2D experiment must be run to obtain a decoupled 1D. An alternative is the band-selective homonuclear decoupling approach, inspired from broadband *heteronuclear* decoupling sequences using shaped inversion pulses, that was designed for carbon-13 by McCoy and Mueller [104] and for protons by Kupče and Freeman [105]. This scheme uses the time-shared acquisition mode in the style of Jesson et al. [10]. Multiple regions can be irradiated simultaneously with several interleaved sequences in the manner of "delays alternating with nutation for tailored excitation" (DANTE) [38, 39]. It is possible to acquire a signal in real time while one or several homonuclear scalar interactions are removed selectively. A review about *Homonuclear Decoupling in Proteins* was written by Kupče et al. in 1998 [106].

This list of methods for homonuclear decoupling is not complete and there are many examples of improved pulse sequences. But it shows that the question asked by Prof. Hans Primas to his PhD student Richard Ernst, more than half a century ago, is still valid today: *Can one decouple*

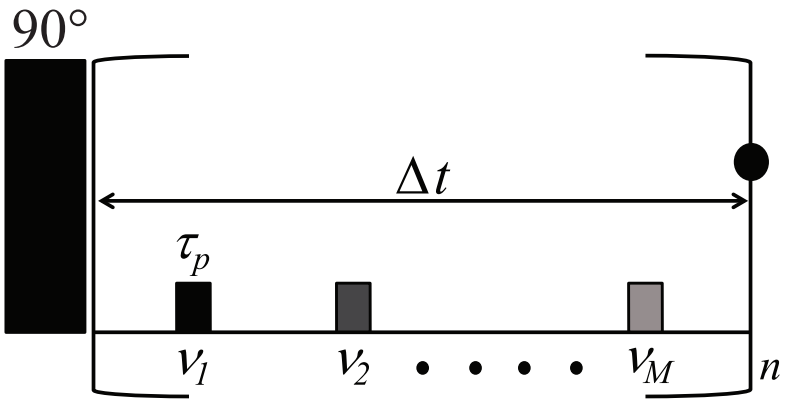

Figure 3.1: Scheme for polychromatic decoupling. The tall rectangle represents the initial $90°_y$ excitation pulse with an *rf* amplitude $\omega_1/(2\pi)$, whereas the small rectangles represent decoupling pulses of duration τ_p and *rf* amplitude $\omega_2/(2\pi)$ applied initially along the x axis at effective frequencies ν_m, which can be shifted at will by incrementing the *rf* phase from one pulse to the next within each comb $m = 1, 2, ..., M$. The black dot represents the acquisition of a single data-point averaged over the time interval during which the receiver is activated. The signal $s(t)$ is built up by acquiring n data points through an n-fold repetition of the loop.

all homonuclear interactions in a high-resolution spectrum, so as to observe only chemical shifts?

3.1.2 Theory

Our method is based on the early technique known as homonuclear decoupling (HD) that is still in use, and in which the dwell time is shared between gated CW irradiation and the recording of the signal [10]. In these methods, the irradiated signal disappears, and all couplings to the spin that is saturated by the *rf* irradiation are cancelled. The method proposed by Jesson et al. [10] uses an initial excitation pulse followed by bursts of CW irradiation, all with the same phase. In our experiment, as shown in Figure 3.1, only brief *rf* pulses with a flip angle $\beta \leq 1°$ are applied in each dwell time. By setting the phases to be initially *perpendicular*, analogous to the modification of Meiboom and Gill for spin–echo trains [7], the on-resonance spin is in effect selectively spin locked and hence decoupled, and a narrow singlet is observed at the irradiation frequency.

Diego Carnevale showed that the decoupling effect can be rationalized in terms of average Hamiltonian theory (AHT) [40]. For the case of the pulse sequence in Figure 3.1 with one pulse per dwell time, simulations performed with Mathematica [35] showed that the decoupling effect is already observed when only the zeroth-order term of the Magnus expansion is considered. By setting to zero the differences between the frequencies of the two parallel single-quantum (SQ) transitions associated with each spin, the following “decoupling

condition" was found:

$$\langle\omega_2\rangle/(2\pi) = (\tau_p/\Delta t)\cdot\omega_2/(2\pi) = |J|/2 \tag{3.1}$$

where $\omega_2/(2\pi)$ is the *rf* amplitude of the brief pulses in the dwell time with a duration τ_p and Δt is the dwell time. The ratio $\tau_p/\Delta t$ is the duty cycle (a dimensionless percentage) and determines the average *rf* frequency $\langle\omega_2\rangle/(2\pi)$ that corresponds to our average Hamiltonian. The observation is stroboscopic and occurs at multiples of the dwell time Δt. If the assumptions to fulfill such an average Hamiltonian are met, a HD experiment is equivalent, no matter if we irradiate during the whole dwell time with a very weak field (ignoring for the moment the problem of detection) or with a single brief pulse *anywhere* during the dwell time. It also means that our brief pulses in the dwell time can have the same effect as selective homonuclear decoupling with a very weak *rf* irradiation. We propose to keep the duty cycle $\tau_p/\Delta t$ as small as possible, so that several pulses $m = 1,2,...,M$ can be accommodated in each dwell time Δt with different effective frequencies ν_m. This makes our HD sequence *polychromatic*.

When looking at the evolution of the involved product operators, the decoupling effect has striking similarities with the "stabilization by interconversion within a triad of coherences under multiple refocusing" (SITCOM) effect [8], which was discussed in detail in subsection 2.1.1 of this thesis and is illustrated in Figure 2.2 on page 11. In a two-spin system without irradiation, the J-coupling normally converts an initial in-phase term I_x into an antiphase term $2I_yS_z$ during free evolution. But if decoupling pulses are inserted, a third operator, the longitudinal two-spin order $2I_zS_z$, comes into play to complete this new triad. The partial conversion of $2I_yS_z$ into $2I_zS_z$ hinders the buildup of the former and thus stabilizes the initial I_x term. Figure 3.2 shows a simulation of the time dependence of these three product operators and of their norm. Because the norm is constant, coherence transfer must be confined to the subspace spanned by the triad of noncommuting operators. In the original SITCOM effect, a Carr–Purcell–Meiboom–Gill (CPMG) sequence with moderate *rf* amplitudes generated $2I_yS_y$ as a third term of the triad, leading likewise to the stabilization of I_x. Strictly speaking, we cannot consider this decoupling as an alternative case of the "SITCOM" effect, since $2I_zS_z$ is *not* a coherence and it is *selective locking* and not anymore *multiple refocusing* that creates the stabilization of I_x. This equivalence of the moderate-amplitude CPMG and the selective spin-lock sequences are in agreement with the results obtained from transverse decays in the study presented in section 2.5.

The simulations of Figure 3.2 were performed with short decoupling pulses. Assuming a continuous *rf* irradiation with the same average field $\langle\omega_2\rangle/(2\pi) = \omega_2/(2\pi)$ the identical evolution of the product operators were obtained. This is a confirmation for the validity of our average Hamiltonian approach. The average *rf* amplitude used for decoupling for the simulation in Figure is *higher* than the condition $\langle\omega_2\rangle/(2\pi) = |J|/2$ stated in Equation 3.1. The reason is the residual oscillation of the in-phase coherence I_x, which causes symmetrical decoupling sidebands. Although we have a decoupled signal at the offset when irradiating with $\langle\omega_2\rangle/(2\pi) = |J|/2$, the sidebands are very intense. The amplitude of the modulation can be

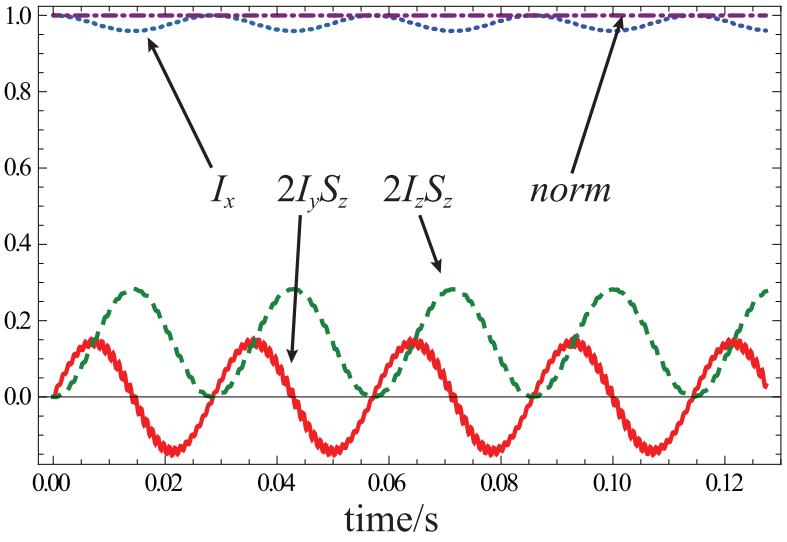

Figure 3.2: Simulation of three product operators belonging to the subspace I_x, $2I_yS_z$, $2I_zS_z$ (blue/dotted, red/continuous, and green/dashed lines, respectively) starting with the initial operator $(I_x + S_x)$ in a two-spin system subjected to the experiment of Figure 3.1 with $\Omega_I = 0$, $\Omega_S/(2\pi) = 1$ kHz, $J_{IS} = 10$ Hz, $\tau_p = 1$ µs, $\Delta t = 100$ µs, i.e., a duty cycle of 1% with $\omega_2/(2\pi) = 3.5$ kHz and $\langle\omega_2\rangle/(2\pi) = 35$ Hz. The norm of the three operators $N = \left(\langle I_x\rangle^2 + \langle 2I_yS_z\rangle^2 + \langle 2I_zS_z\rangle^2\right)^{1/2}$ (purple/dashed–dotted line) is conserved. Upon Fourier transformation, the shallow amplitude modulation of the expectation value $\langle I_x\rangle$ gives rise to weak sidebands. The evolution of the product operators are identical when simulating a CW *rf* irradiation of $\langle\omega_2\rangle/(2\pi) = \omega_2/(2\pi) = 35$ Hz, confirming the average Hamiltonian approach. By comparing with Figure 2.2 on page 11 in the subsection 2.1.2, the similarities with the SITCOM effect under the moderate-amplitude CPMG sequence become evident. The only difference to Figure 2.2 C is the presence of the longitudinal two-spin order $2I_zS_z$ under the selective spin-lock here, compared to the $2I_yS_y$ in the echo sequence. The simulations were performed with mPackages/SpinDynamica [34] on Mathematica.

attenuated by higher *rf* amplitudes and shifts simultaneously the sidebands away. A similar process in the SITCOM of moderate-amplitude CPMG can be observed in the simulations of Figure 3.2 A-C on page 11.

Interestingly, the condition in Equation 3.1 coincides with an optimal *single field polarization transfer* (SFPT), as introduced by Rey Castellanos et al. [107]. By irradiating a J-coupled line with $\omega_2/(2\pi) = |J|/2$, the original SQ coherence I_x is fully converted into longitudinal two-spin order $2I_zS_z$ after a time of $\tau_p = 1/(\sqrt{2}J)$. As highlighted by the name of this polarization transfer sequence, only one field/frequency must be irradiated. A synchronization, e.g., as in Hartmann-Hahn transfers, or pulses on both frequencies, as in the INEPT sequence, are not needed.

A side effect of the time-shared or window-acquired method is a manifestation of the Bloch-Siegert effect [108]. The apparent chemical shift becomes a function the average *rf* amplitude $\langle\omega_2\rangle$ (in rad/s):

$$\Omega^{app} = \sqrt{\Omega^2 + \langle\omega_2\rangle^2} = \Omega\sqrt{1 + \frac{\langle\omega_2\rangle^2}{\Omega^2}} \tag{3.2}$$

This equation is reminiscent of the effective *rf* field ω_{eff} for the off-resonance effect of pulses, as used for example in Equation 2.16 on page 38 in section 2.4, where the same norm of the chemical shift and the *rf* amplitude appears. Taking the first two terms of a series expansion around $\langle\omega_2\rangle/\Omega$, for $0 < \langle\omega_2\rangle \ll \Omega$, we can write Equation 3.2 in the form [109]

$$\Omega^{app} \approx \Omega\left(1 + \frac{1}{2}\frac{\langle\omega_2\rangle^2}{\Omega^2}\right) = \Omega + \frac{\langle\omega_2\rangle^2}{2\Omega} \tag{3.3}$$

where the ratio $\langle\omega_2\rangle^2/(2\Omega)$ gives the systematic "error" to the unperturbed chemical shift Ω in units of rad/s. In our HD experiments, we assume an *rf* duty cycle $\tau_p/\Delta t = 0.01 = 1$ % with $\tau_p = 1$ µs and $\Delta t = 100$ µs for a corresponding spectral width of 10 kHz. If we consider an *rf* peak amplitude $\omega_2/(2\pi) = 1$ kHz, which leads to an average *rf* amplitude $\langle\omega_2\rangle/(2\pi) = 10$ Hz, resonances within an offset of $\Omega/(2\pi) > 500$ Hz (i.e., above 1 ppm at 500 MHz) will have systematic errors within

$$0 < \frac{\langle\omega_2\rangle^2}{(2\Omega)\cdot(2\pi)} < 0.1 \text{ Hz} \tag{3.4}$$

In other words, the resonances in the spectrum are barely perturbed. If nevertheless a correction of the error to the offset caused by the Bloch-Siegert shift is desired, the following formula can be applied:

$$\Omega \approx \Omega^{app}/\left[1 + \langle\omega_2\rangle/\left(2\Omega^2\right)\right] \approx \Omega^{app}/\left[1 + \langle\omega_2\rangle/\left(2(\Omega^{app})^2\right)\right] \tag{3.5}$$

where we have simply replaced Ω by Ω^{app} on the right-hand side. If $\omega_2 \gg \Omega$, we are in the (broadband) spin-locking régime and only a single unmodulated signal at the carrier

frequency should appear. This is obviously not an option for us, since all the information about the chemical shifts of the spin system are lost. It is the Bloch-Siegert shift that would make decoupling by 360° pulses in the frequency domain unpractical.

3.1.3 Experimental results

All the experiments were carried out in a static field B_0 = 11.7 T (500 MHz for protons). At this field, the two protons of 2,3-dibromothiophene in DMSO-d_6 are weakly coupled with $(\Omega_A - \Omega_X)/(2\pi) = 305$ Hz and $J_{AX} = 5.8$ Hz. In Figure 3.3, the unperturbed spectrum of this AX system is compared with the best decoupling spectrum. The carrier frequency was set on the left-hand resonance, as indicated by a wavy arrow. Good decoupling and minimal interference of decoupling sidebands is obtained with a *rf* field strength that was empirically optimized to $\omega_2/(2\pi) \approx 900$ Hz, corresponding to an average *rf* amplitude $\langle\omega_2\rangle/(2\pi) \approx 18$ Hz using a duty cycle of 2 %. In this case, the average *rf* amplitude is therefore ca. 3 times larger than the coupling constant J. Looking at Figure 3.3 b, it is striking that the decoupled singlet at the carrier frequency is clearly higher and narrower than the decoupled off-resonance peak. The on-resonance peak is only broadened by the homogeneous linewidth $(T_2\pi)^{-1} = R_2/\pi$, since a spin-lock field has the same property as an echo and removes the inhomogeneous contribution to line broadening. Since this locking field is highly selective, the linewidth of the off-resonance peak $(T_2^*\pi)^{-1} = R_2^*/\pi$ remains unaffected. This is an interesting observation, when thinking of methods to measure transverse relaxation in homonuclear coupled systems (see for example section 2.5).

Figure 3.4 shows spectra of the strongly-coupled AB system of 2,3,6-trichlorophenol superimposed with the solvent peak of $CDCl_3$ marked with an asterisk. In contrast to the AX system of Figure 3.3, some decoupling sidebands are clearly visible in the strongly-coupled AB system of Figure 3.4. This is due to lower average *rf* field that must be chosen for close chemical shifts. Nevertheless, a reasonable decoupling efficiency is achieved. The difference between the two chemical shifts is $(\Omega_A - \Omega_B)/(2\pi) = 98$ Hz and the coupling constant $J_{AB} = 8.7$ Hz. As for the AX system in Figure 3.3, the decoupling pulse length was τ_p = 1 µs for a dwell time Δt = 50 µs, leading to a duty cycle of 2 %. The decoupling field-strength was $\omega_2/(2\pi) \approx 240$ Hz, corresponding to an average *rf* amplitude $\langle\omega_2\rangle/(2\pi) \approx 4.8$ Hz. In this case, the irradiated average *rf* amplitude is close to the condition of of Equation 3.1 with $\langle\omega_2\rangle/(2\pi) \approx J/2$.

Decoupling experiments with one pulse per dwell time, at a single effective frequency ν_1 were applied to the $A_2M_2X_3$ system of propan-1-ol ($HOCH_2CH_2CH_3$). The conventional spectrum and three decoupled spectra with carrier frequencies set on one of the three multiplets are shown in Figure 3.5. The decoupling pulse length was τ_p = 1 µs for a dwell time Δt = 100 µs in a duty cycle of 1%. The peak field strength was $\omega_2/(2\pi) \approx 1.6$ kHz in all cases, corresponding to a flip angle of $\beta = \omega_2\tau_p \approx 0.6°$. If the carrier frequency is set on the chemical shift $\Omega(A_2)$, the multiplicity of the coupling partner M_2 is simplified by decoupling $^3J_{AM}$, whereas the fine structure due to $^3J_{MX}$ is not affected, as shown in the inset of Figure 3.5 b. If the carrier

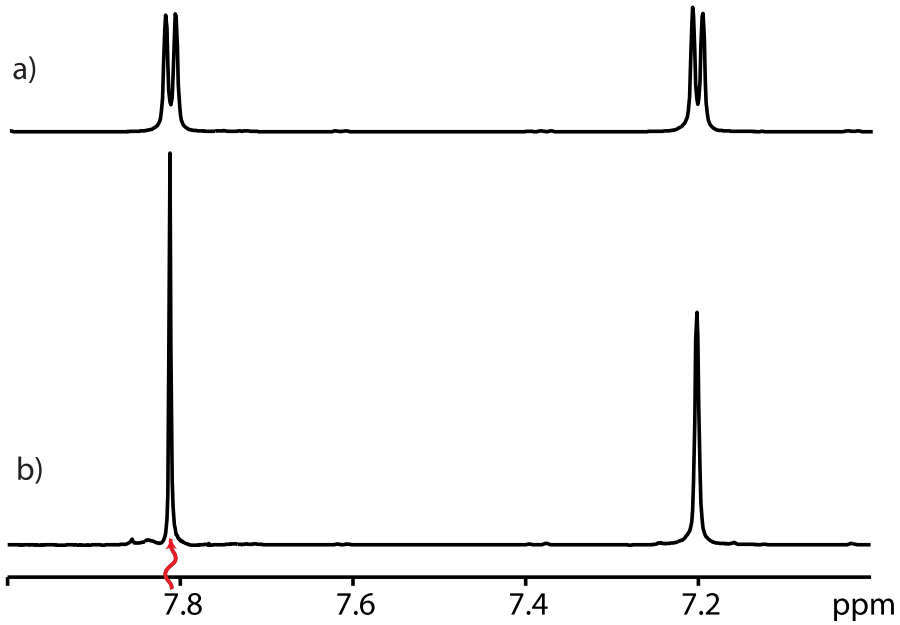

Figure 3.3: a) Conventional NMR spectrum of 2,3-dibromothiophene in DMSO-d_6 at 500 MHz. b) Decoupled spectrum of the same sample with the carrier frequency set on the left-hand doublet indicated by the red wavy arrow. The difference between the two chemical shifts is 305 Hz and the coupling constant J_{AX} = 5.8 Hz. The pulse length was τ_p = 1 µs for a dwell time Δt = 50 µs (duty cycle 2 %). The decoupling field-strength was $\omega_2/(2\pi) \approx 900$ Hz, corresponding to an average *rf* amplitude $\langle\omega_2\rangle/(2\pi) \approx 18$ Hz. Both spectra were processed with 1 Hz line broadening.

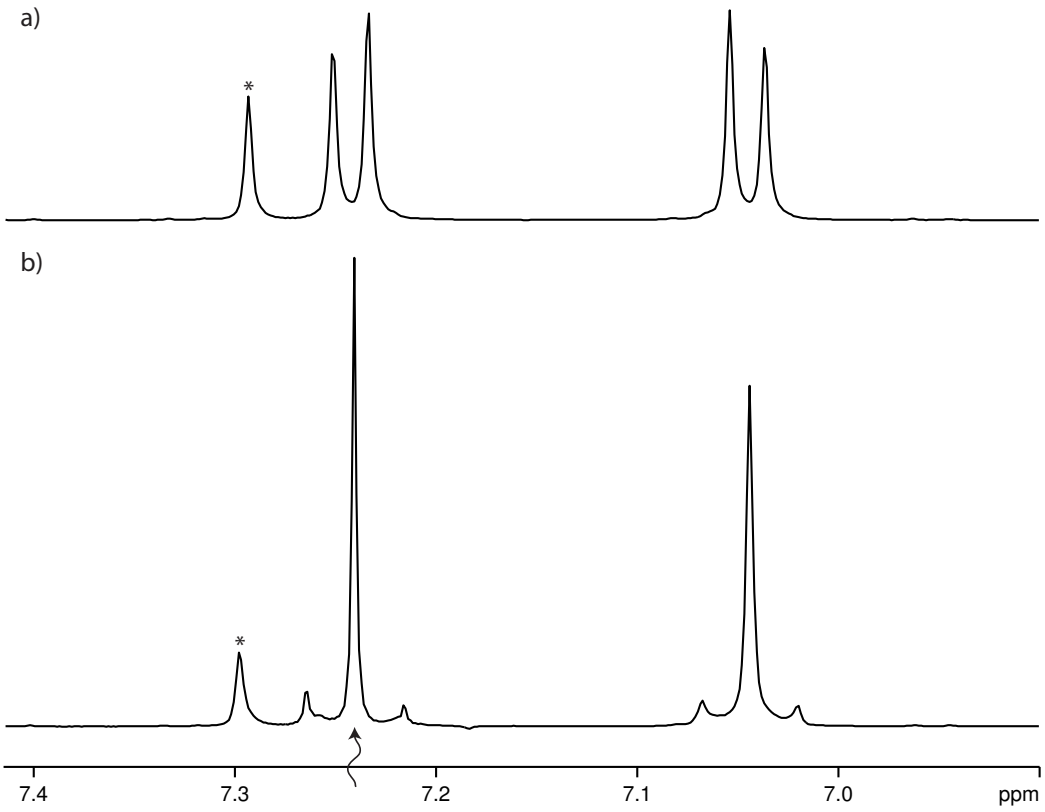

Figure 3.4: a) Conventional NMR spectrum of 2,3,6-trichlorophenol in $CDCl_3$ at 500 MHz. b) Decoupled spectrum of the same sample with the carrier frequency set on the resonance indicated by a wavy arrow. The difference between the two chemical shifts is 98 Hz and the coupling constant $J_{AB} = 8.7$ Hz. The decoupling pulse length was $\tau_p = 1$ µs for a dwell time $\Delta t = 50$ µs (duty cycle 2 %). The decoupling field-strength was $\omega_2/(2\pi) \approx 240$ Hz, corresponding to an average *rf* amplitude $\langle\omega_2\rangle/(2\pi) \approx 4.8$ Hz. Both spectra were processed with 1 Hz line broadening. The singlet at ~ 7.3 ppm, indicated by an asterisk, stems from the residual $CHCl_3$ of the solvent.

frequency is set on $\Omega(X_3)$, the multiplicity of the coupling partner M_2 is simplified by decoupling $^3J_{MX}$, but the triplet due to $^3J_{AM}$ remains (inset Figure 3.5 c). Clearly, our sequence can decouple all interactions between the irradiated spin and its J-coupled partners, but does not affect couplings between spins that are not irradiated. In Figure 3.5 d, the carrier frequency was set on the central M_2 resonance of the $A_2M_2X_3$ system. Because the M_2 spins are coupled to both A_2 and X_3 when $^4J_{AX} = 0$, all three resonances are decoupled in this case. These experiments show that, as expected, decoupling works also for magnetically equivalent spins. Furthermore, in all three samples considered, we did not observe any anomalies of the integrals in the decoupled spectra.

To make our sequence polychromatic, i.e., to decouple simultaneously resonances at several frequencies, we will interleave several pulses in one dwell time, as shown in Figure 3.1. The *rf* amplitudes of this individual decoupling pulses can be varied. It is known that the effective frequency ν_m (in Hz) of a comb C_m of pulses can be shifted at will from the common carrier frequency ν_{rf} by a frequency shift

$$\Delta\nu_m = \nu_m - \nu_{rf} = \Delta\phi_m/(2\pi\Delta t) \tag{3.6}$$

by shifting the phase of the k^{th} pulse of comb C_m through $k\Delta\phi_m$. Such phase modulation schemes have been used with the DANTE sequence [38, 39, 110, 111]. Because the position within the dwell time Δt of the pulses belonging to any one comb C_m is immaterial, one can readily interleave several combs with $m = 1,2,...,M$. This allows in effect to irradiate simultaneously at a manifold of frequencies ν_m with $m = 1,2,...,M$.

An example is shown in Figure 3.6 for ethylpropionate which contains two distinct spin subsystems labeled A_2X_3 and $A_2'X_3'$. The conventional spectrum is shown in Figure 3.6 a whereas the spectrum obtained with two combs of decoupling pulses ($M = 2$, $m = 1$ and 2) is shown in Figure 3.6 b. A wavy arrow indicates the transmitter frequency, which is set in the middle between the two spins A_2 and A_2'. The phases of the decoupling pulses in each comb have been independently incremented so that the two effective frequencies match the two offsets that must be irradiated to achieve a two-fold or "bichromatic" decoupling. The desired shift from the carrier frequency to the spins A_2 and A_2' is $\Delta\nu_m = \pm 454.5$ Hz, respectively. Using Equation 3.6, we find that the phase increment in every dwell time is

$$\Delta\phi_m = 2\pi\Delta\nu_m\Delta t \tag{3.7}$$

and therefore $\Delta\phi_{m=1} = -\Delta\phi_{m=2} = +8.2°$ for $\Delta t = 50$ µs in this symmetric case. As explained by Kupče et al. [106], the sidebands in Figure 3.6 b are *not* decoupling sidebands, as we have seen them for example in Figure 3.4 b. These are *modulation sidebands*, which were introduced by the modulated *rf* field. These modulation sidebands have different signs, while the decoupling sidebands appear with the same sign.

Polychromatic decoupling can be a valuable tool to identify and measure J-couplings that are hidden by other signals. An example is given by the ^{1}H spectra of the cyclic peptide cyclosporin

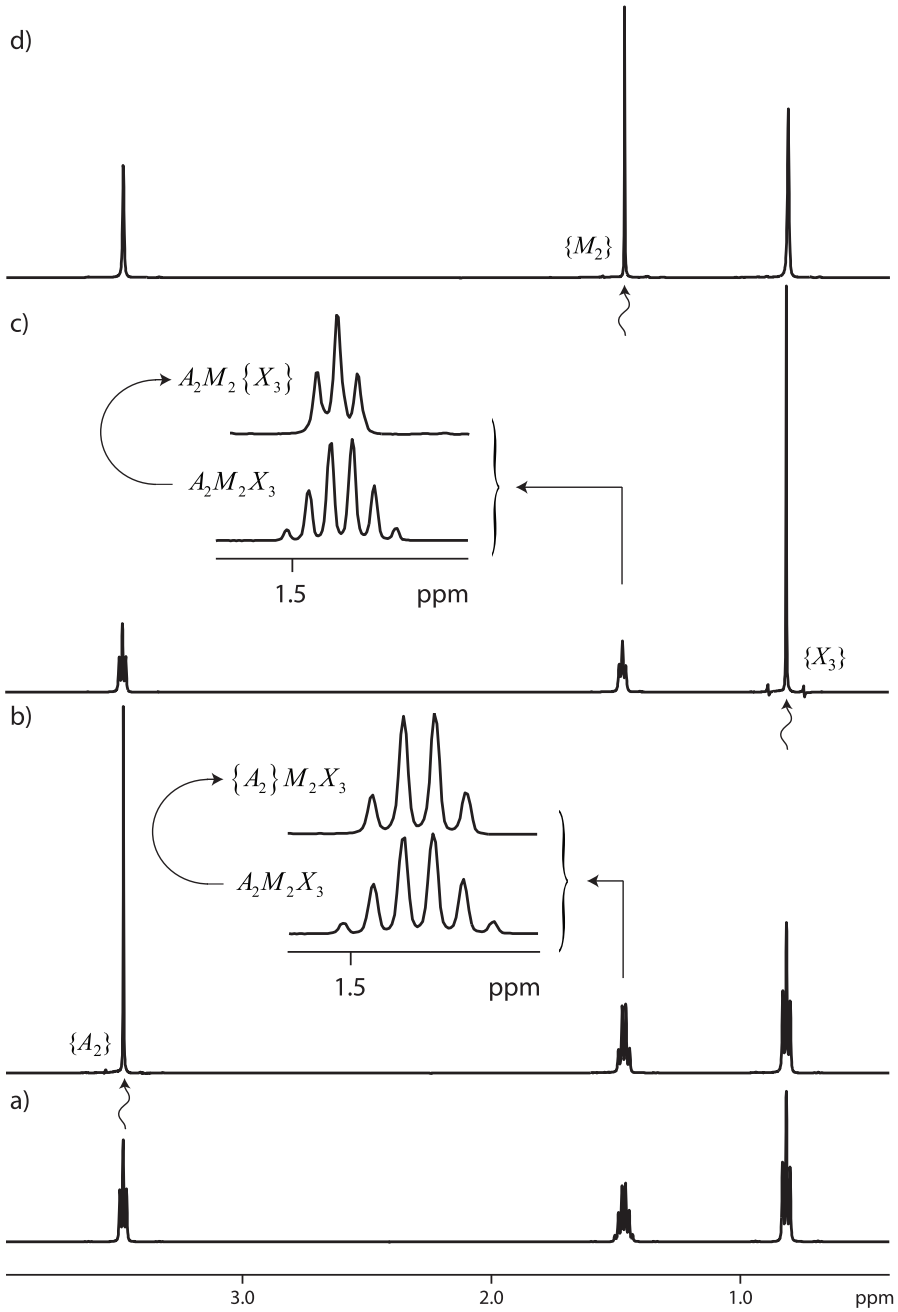

Figure 3.5: a) Conventional NMR spectrum of the $A_2M_2X_3$ system of propan-1-ol in D_2O at 500 MHz. b) Decoupled spectrum obtained with the carrier frequency (wavy arrow) set on the A_2 resonance. The inset shows the simplification of the multiplet of the coupling partner M_2, which has become a simple quadruplet. c) Decoupled spectrum with the carrier frequency (wavy arrow) set on the X_3 resonance. The inset shows the simplification of the multiplet of the coupling partner M_2, which now appears as a simple triplet. d) Decoupled spectrum with the carrier frequency (wavy arrow) set on the central multiplet of M_2, leaving three fully decoupled singlets. The pulse length was $\tau_p = 1$ µs for a dwell time $\Delta t = 100$ µs (duty cycle 1%). The peak *rf* field strength was $\omega_2/(2\pi) \approx 1.6$ kHz in all cases. All spectra were processed with 1 Hz line broadening except for the expansions shown in the insets, for which no line broadening was used.

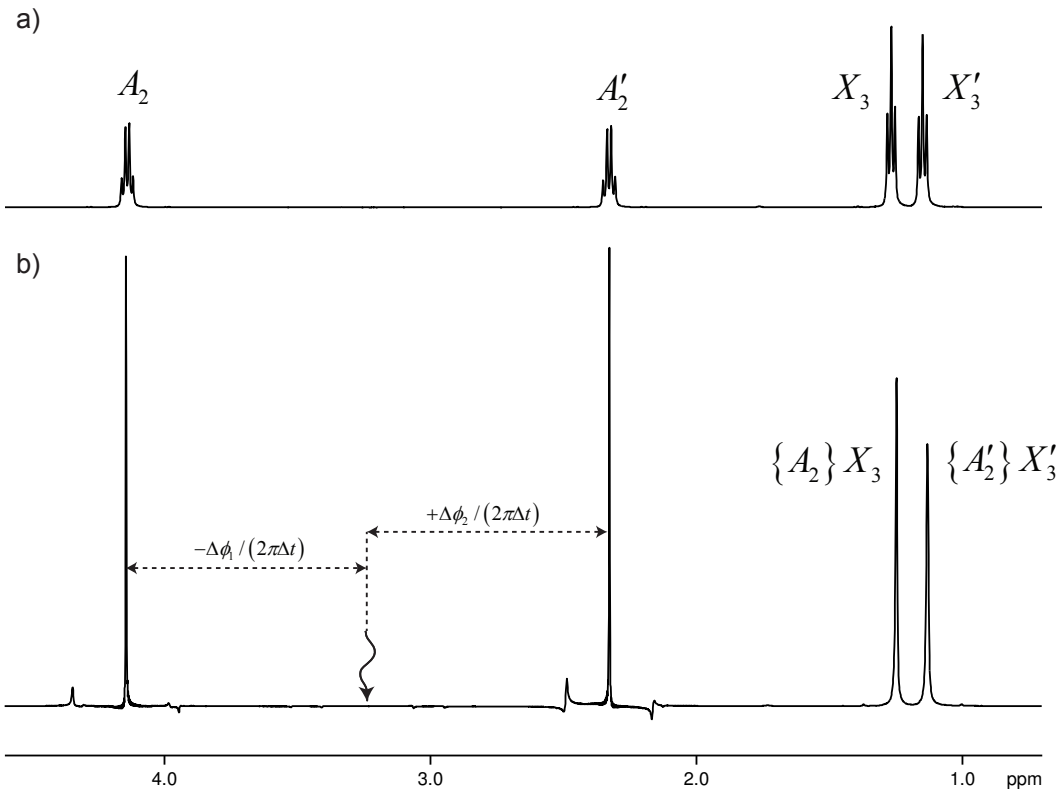

Figure 3.6: a) Conventional NMR spectrum of ethylpropionate ($CH_3CH_2COOCH_2CH_3$) at 500 MHz, showing quartets and triplets belonging to the two independent A_2X_3 and $A_2'X_3'$ systems. b) Decoupled spectrum obtained with "bichromatic" decoupling, where the carrier frequency (wavy arrow) was positioned half-way between the chemical shifts of the A_2 and A_2' spins. A fully decoupled spectrum is obtained by superimposing two combs (m = 1, 2) of pulses and incrementing the phases of the *rf* pulses belonging to each comb to match the chemical shifts of the A_2 and A_2' spins, which are at ±454.5 Hz with respect to the carrier. Since the dwell time was Δt = 50 µs, the phase shifts were chosen to be $\Delta\phi_{m=1}$ = +8.2° and $\Delta\phi_{m=2} = -\Delta\phi_{m=1}$ = –8.2°. As a result, the triplets of the X_3 and X_3' groups collapsed to singlets. The *rf* field strength was $\omega_2/(2\pi) \approx 5.7$ kHz for both combs, all pulse lengths were τ_p = 1 µs, and the total duty cycle was 4%. All spectra were processed with 1 Hz line broadening.

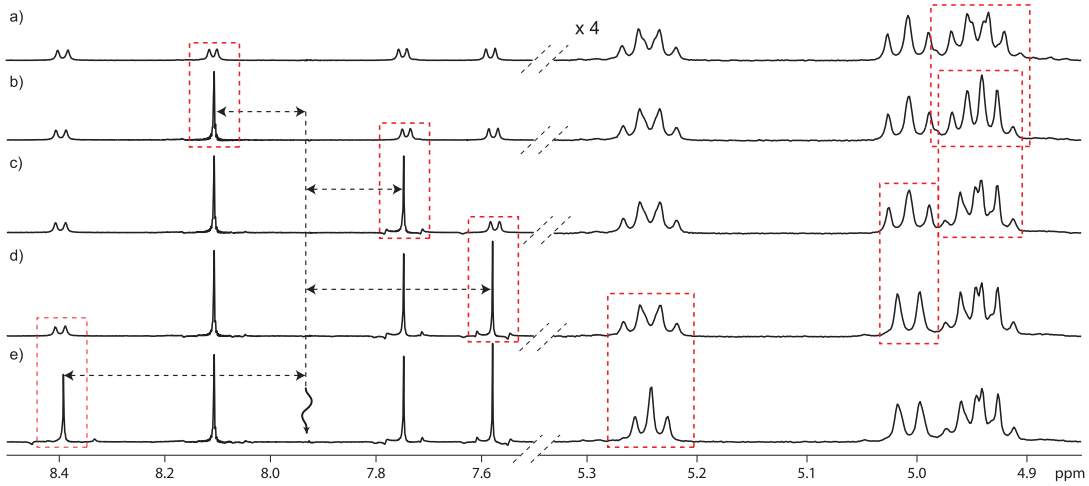

Figure 3.7: a) Part of a conventional ^{1}H spectrum of the cyclic peptide cyclosporin A (CsA) in C_6D_6 at 500 MHz (the chemical structure is displayed in Fig. 2.3 on p. 15). On the left-hand side, the H^N region is expanded, whereas the H^α region is shown on the right-hand side, with a fourfold amplification of the vertical scale. b)–e) Spectra with polychromatic decoupling obtained with up to $M = 4$ interleaved combs of decoupling pulses, so as to irradiate and decouple up to four H^N resonances simultaneously. A black wavy arrow indicates the common carrier frequency. The different effective irradiation frequencies are $\Delta\nu_{m=1} = -89.7$ Hz, $\Delta\nu_{m=2} = +89.7$ Hz, $\Delta\nu_{m=3} = +174.3$ Hz, and $\Delta\nu_{m=4} = -232.3$ Hz with respect to the carrier. Since the dwell time was $\Delta t = 100$ µs, the phase increments of the four interleaved combs of decoupling pulses were chosen to be $\Delta\phi_{m=1} = -1.6°$, $\Delta\phi_{m=2} = +1.6°$, $\Delta\phi_{m=3} = +3.1°$, and $\Delta\phi_{m=4} = -4.2°$. The effect of decoupling $J(H^\alpha,H^N)$ is highlighted in the H^α region by dashed red rectangles. The remaining multiplet structures can be ascribed to $J(H^\alpha,H^\beta)$ couplings, which would be hard to determine in a). The group of signals at about 4.95 ppm corresponds to two overlapping multiplets. The individual decoupling pulse lengths were $\tau_p = 1$ µs, with a total duty cycle of $4 \cdot 2\% = 8\%$ for the sum of the four combs. The decoupling field strengths were optimized empirically ($0.9 \leq \omega_2/(2\pi) \leq 2.3$ kHz).

A (CsA) in Figure 3.7. From a) to e), up to four H^N multiplets are decoupled simultaneously by means of $M = 0,1,2,3$, or 4 interleaved combs of decoupling pulses, the phases of which are incremented to match the desired offsets (dashed arrows). On the right-hand side of Figure 3.7, the coupling partners H^α show multiplicities that are simplified, because up to four $J(H^\alpha,H^N)$ interactions are decoupled simultaneously. The stepwise simplifications are highlighted by dashed red rectangles. The residual multiplets that are caused by $J(H^\alpha,H^\beta)$ couplings can be easily determined, thus, revealing previously hidden information.

The number M of effective frequencies is limited by the total duty cycle. In theory, we could think of filling up 100 pulses of length $\tau_p = 1$ µs in the dwell time of $\Delta t = 100$ µs, leading to a maximal duty cycle of 100%. Even with one hundred effective decoupling frequencies, our sequence could not become truly broadband, since the decoupling on every frequency remains highly selective. Of course we have to keep in mind that, not only the sensitivity goes

down with a smaller acquisition window, but also the Bloch-Siegert shifts are cumulative for every additional effective irradiation frequency. So far, we have not taken into account the apparent chemical shift Ω^{app} due to the Bloch-Siegert effect (Equations 3.2 and 3.3 on page 57), when calculating the phase increment $\Delta\phi_m$ for our polychromatic scheme (Equation 3.7 on page 61). This correction could lead to a better quality of decoupling, guaranteeing an on-resonance field for every effective frequency ν_m, and should be considered when the number of effective irradiation frequencies M is further increased.

In the spirit of self-deprecating acronyms such as INEPT and INADEQUATE, we like to refer to our method as "window-acquired spin-tailoring experiment" (WASTE). Since WASTE is not broadband, we have to know the chemical shifts of the spins we want to decouple. Therefore, besides the identification of the coupling partner, the practical relevance of WASTE is primarily the simplification of complex multiplets that allow to extract a value for the remaining J-splittings. Nevertheless, it would be possible to generate a fully decoupled spectrum using WASTE, where the number of the effective carrier frequencies ν_m will be always lower than the number of the singlets obtained (e.g., an irradiation on a single carrier frequency is sufficient to generate the three fully decoupled singlets in Figure 3.5). Here, we used WASTE as a 1D experiment, but it can be implemented in the detection or evolution periods of any multidimensional experiment to selectively decouple multiple interactions. We believe that WASTE can contribute to the characterization of complex systems, including biological macromolecules.

We started a collaboration with Dr. Aitor Moreno from Bruker Biospin Switzerland in Fällanden, to develop a more user-friendly version of our WASTE sequence. He suggested to implement WASTE in an existing time-shared HD program, using a shaped pulse. The shape of the pulse is defined over the whole acquisition time $n \cdot \Delta t$ (compare Figure 3.1), containing the oscillations of all desired irradiation frequencies. With this sequence, Moreno decoupled successfully $M = 7$ frequencies at once. A similar shape approach was proposed by Espindola et al. [112]. The strategy is based on the fundamental paper of Tomlinson and Hill from 1973 entitled "Fourier synthesized excitation of nuclear magnetic resonance with application to homonuclear decoupling and solvent line suppression" [113]. Moreno's and our approach is close, but not fully identical. The shaped pulse showed good results for larger duty cycles than in our experiments, but the full shape will not be used, since windows for detection must be left. Without a doubt, polychromatic decoupling using a shaped HD pulse is fast and easy to implement.

3.2 Fourier spin tickling [114]

3.2.1 Introduction

In the long bygone days of continuous-wave NMR, a selected transition within a multiplet of a high-resolution spectrum could be irradiated by a highly selective continuous-wave (CW) radio-frequency (*rf*) field with a very weak amplitude $\omega_2/(2\pi) \leq J$. This causes splittings of connected transitions, allowing one to map the connectivities of all transitions within the energy-level diagram of the spin system. Such "tickling" experiments stimulated the invention of two-dimensional spectroscopy, but seem to have been forgotten for many years. We show that tickling can readily be achieved in homonuclear systems with Fourier transform spectrometers by applying short pulses in the intervals between the sampling points. Extensions to heteronuclear systems are even more straightforward since they can be carried out using very weak CW *rf* fields.

It is now half a century ago that Wes Anderson and Ray Freeman, then both at Varian Associates in Palo Alto, California, published two seminal papers about theoretical and experimental aspects of double resonance in high-resolution NMR [9, 12]. This was before the advent of Fourier transform (FT) NMR [2], when the signal was measured by continuously sweeping the carrier and receiver frequencies (or the main magnetic field) in the manner of "slow passage". In double resonance[1] experiments, a second *rf* field is applied to characterize the energy levels of the spin systems. If the amplitude $\gamma B_2/(2\pi) = \omega_2/(2\pi)$ of the second *rf* field is equal or greater than the spin coupling constant J, a collapse of the multiplets onto the underlying chemical shifts can be observed, a phenomenon that has come to be known as decoupling [9]. If the *rf* amplitude $\omega_2/(2\pi)$ is smaller than the spin coupling constant J but larger than the linewidth [19], all transitions that have an energy level in common with the irradiated transition will be split into doublets. If the irradiation coincides exactly with the frequency of a single transition, and if all couplings are smaller than the chemical shift differences, all connected transitions split into symmetrical doublets with equal intensities, with a splitting equal to the amplitude of the second *rf* field. This phenomenon has later come to be known as "spin tickling"[2] [12, 115]. The increased complexity, which appears to achieve the opposite effect as decoupling, offers a means to study connectivities of transitions in a spin system.

A tickling spectrum helps to discriminate between two possible types of connected transitions [1]. If the energy levels that are not shared differ by $\Delta m = \pm 2$ as shown in Figure 3.8, i.e., if they span a double-quantum (DQ) transition, the connected transitions are called progressive (see the red transitions in energy-level diagram of Figure 3.8 a). On the other hand, if these energy levels differ by $\Delta m = 0$, they span a zero-quantum (ZQ) transition and are called regressive (blue transitions in energy-level diagram of Figure 3.8 a). In the latter case, the splitting induced by tickling is usually well resolved, but in the case of progressively connected

[1] In modern experiments, the term double resonance is often used when *rf* pulses are applied to two different nuclei.

[2] The inventors of spin tickling in 1962 [12], Ray Freeman and Weston A. Anderson, received the 2012 Russell Varian Prize.

transitions, the lines are broader and the splitting is often hard to resolve, so that the two types can easily be distinguished. Freeman and Anderson explained the splitting of the lines by a partial admixture of allowed single-quantum (SQ) transitions and forbidden (ZQ or DQ) transitions. Both become equally allowed at exact resonance [95, 116, 117]. The broadening in the progressive case can be attributed to the fact that DQ transitions are more sensitive than ZQ transitions to the inhomogeneity of the static magnetic field B_0.

To illustrate this effect, a J-coupled two-spin system IS was investigated by numerical simulations using the SIMPSON program [118]. The chemical shifts were set at $\Omega_I/(2\pi) = 5$ Hz and $\Omega_S/(2\pi) = 405$ Hz, respectively, with a scalar coupling $J = 10$ Hz. The lowest-frequency line of the I spin doublet at $\Omega_I/(2\pi) - J/2 = 0$ Hz was irradiated with an average *rf* field strength $\langle\omega_2\rangle/(2\pi) = 1$ Hz. To simulate the inhomogeneity of the B_0 field, both *rf* carrier and receiver frequencies were shifted in 21 steps of 0.1 Hz from –1 to +1 Hz around the resonance condition. Relaxation was not taken into account. Figure 3.9 shows the spectral lines of the off-resonance spin S. A few selected spectra with offsets –1.0, –0.5, 0.0, 0.5, 1.0 Hz are shown in Figures 3.9 a-e. The intensities are always symmetrical with respect to the chemical shift of spin S. The 1 Hz splittings in the on-resonance spectrum in Fig. 3.9 c are equal to the average amplitude of the tickling field. The sum of all 21 spectra is plotted in Figure 3.9 f. This reproduces the experimental pattern of the broad progressively connected peaks and narrow regressively connected peaks. The differential broadening originates from the distinct slopes of the individual peaks across Figures 3.9 a-e.

Spin tickling is a convenient method to assign spectral transitions to the energy levels, and thus to reconstruct the entire energy-level diagram. The approach is not limited to magnetic resonance spectroscopy. A similar splitting of lines in vibrational spectroscopy was explained by Fermi already in 1931 [119] and is known today as Fermi resonance in infra-red and Raman spectroscopy [95, 117]. In modern NMR, continuous-wave (CW) "slow-passage" experiments have been almost fully replaced by pulsed experiments. To study connectivities, two-dimensional correlation spectroscopy (COSY) [96] has become popular. If the second pulse has a small flip angle (e.g., in "COSY-45") one can readily determine the relative signs of J-couplings from inspection of the multiplet structures [96, 101]. The combination of FT NMR and tickling was discussed (in German) by F. Günther in 1971[3] [120] but this was largely overlooked. In his calculations, Günther showed that tickling not only broadens the inhomogeneous linewidths in a manner that depends on the connectivity, but the *natural homogeneous* linewidths are also broadened in a differential manner. Such relaxation effects are reminiscent of the recently discovered long-lived coherences (LLC's) [90, 91]. Wokaun and Ernst described a two-dimensional (2D) experiment where tickling is applied to multiple-quantum coherences in the evolution interval t_1 while the signal is observed in Fourier mode in the detection interval t_2 [121].

[3] The volume numbering of the Annalen der Physik was modified in 2010. The original reference of Günther's publication (as cited by Ernst et al.) is: Annalen der Physik, 7. Folge, Band 27, Heft 4, 1971, S. 396-408. Note that the year of publication has changed from 1971 to 1972!

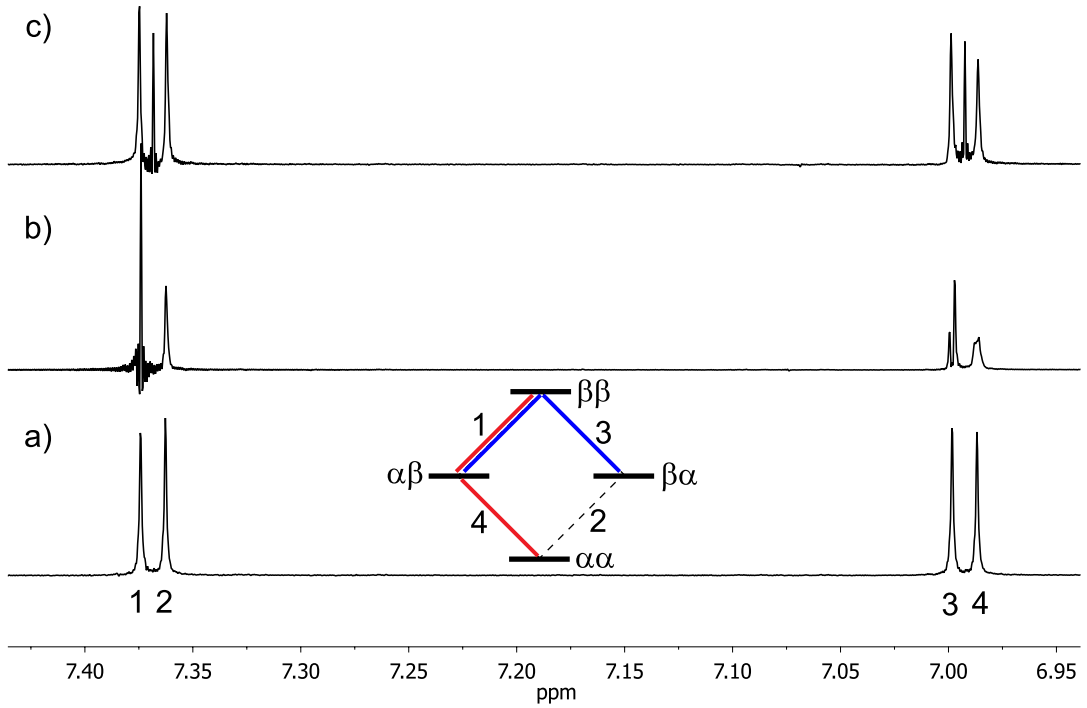

Figure 3.8: a) Normal proton spectrum at 500 MHz of the *AX* system 2,3-dibromothiophene with the corresponding energy-level diagram, where the transitions are numbered from "1" to "4". The red transitions "1" and "4" are connected progressively, the blue transitions "1" and "3" regressively. b) Tickling spectrum obtained by irradiating resonance "1" with an average amplitude $\langle\omega_2\rangle/(2\pi) = 1$ Hz (see text). Peak "2" is not affected, since this transition is parallel to the irradiated one and is therefore not connected. The lines "3" and "4" of the coupling partner are both split by tickling. The regressively connected resonance "3" splits into two narrow lines, while the progressively connected resonance "4" splits into a broadened doublet. c) Similar experiment with the same average rf amplitude $\langle\omega_2\rangle/(2\pi) = 1$ Hz as in b), but with the carrier frequency shifted to the middle of the left-hand doublet, half-way between transitions "1" and "2". This brings about "incipient decoupling", leading to two additional lines coinciding with the chemical shifts. However, the *rf* amplitude is too weak to achieve complete decoupling. As usual, all spectra were processed by Fourier transform. No line-broadening was used.

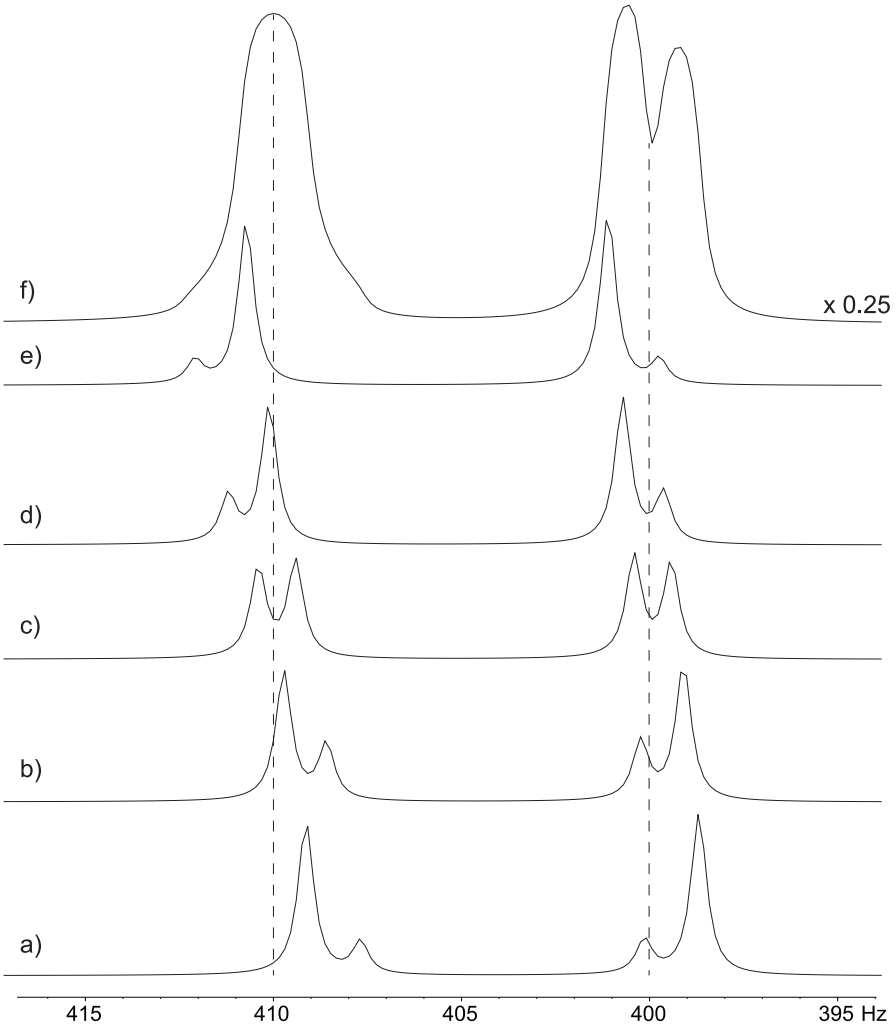

Figure 3.9: Series of spectra simulated with SIMPSON [118] to mimic the effect of the inhomogeneity of the B_0 field in spin-tickling experiments. A two-spin system IS was considered, with $\Omega_I/(2\pi) = 5$ Hz, $\Omega_S/(2\pi) = 405$ Hz, and $J = 10$ Hz. The frequency of both carrier and receiver was varied from –1.0 to 1.0 Hz in 21 steps of 0.1 Hz across the I spin transition at 0 Hz. Only the multiplet of the off-resonance spin S is shown. a)-e) Five spectra with offsets –1.0, –0.5, 0.0, 0.5 and 1.0 Hz. f) Sum of all 21 spectra. A 1 µs pulse was applied in each dwell time of 100 µs duration (1% duty cycle), with an *rf* field strength $\omega_2/(2\pi) = 100$ Hz, resulting in an average tickling field strength of $\langle\omega_2\rangle/(2\pi) = 1$ Hz. A line broadening of 0.5 Hz was applied. Relaxation was not considered. The vertical dashed lines at $\Omega_S/(2\pi) \pm J/2$ are given to guide the eye and highlight the different displacements of the signals as a function of the carrier and receiver offsets.

Today, tickling does not play a significant role in NMR spectroscopy, but there appear to be no obstacles to its renaissance. In the previous section 3.1, we developed a method dubbed "window-acquired spin-tailoring experiment" (WASTE) that allows one to eliminate the effects of a manifold of homonuclear scalar couplings by alternating the sampling of the free induction decay with brief *rf* pulses. This is closely related to the time-shared method suggested by Jesson et al., who also mentioned spin tickling [10]. If *rf* pulses and signal acquisition alternate, the effect of the second *rf* field can be described by an average Hamiltonian [40]. By using a similar time-shared sequence, but with a weaker *rf* field and setting the carrier on a single transition, tickling experiments can be readily carried out. Thus double resonance tickling *and* decoupling experiments can be transferred from CW to FT NMR [19, 97].

3.2.2 Experiments

For the sake of illustration, consider the pair of weakly coupled protons in 2,3-dibromothiophene dissolved in DMSO-d_6. We have already used this simple two-spin system to test our WASTE decoupling sequence, shown in Figure 3.3 on page 59. This AX system has a homonuclear scalar coupling $J_{AX} = 5.8$ Hz and a chemical shift difference $(\Omega_A - \Omega_X)/(2\pi) = 305$ Hz at 500 MHz (see Figure 3.8 a). Figure 3.8 b shows the tickling spectrum obtained when an *rf* field with an average amplitude $\langle\omega_2\rangle/(2\pi) = 1$ Hz is set on the left-most resonance "1", as evidenced by the interference pattern. The neighbouring line "2" remains unperturbed. This confirms that these two transitions do *not* share any common energy level, as expected for "parallel" transitions. The left-hand peak "3" of the other doublet splits into two narrow lines, while the right-hand peak "4" is broadened. The transition "3" is regressively connected (blue lines in energy-level diagram), while "4" is progressively connected to transition "1" (red lines in energy-level diagram). All of this is consistent with the energy-level diagram in Figure 3.8. If we irradiate half way between transitions "1" and "2", as we do for decoupling, but with the same very weak *rf* amplitude, all four transitions remain visible and no tickling effects are observed. Two new lines appear at the chemical shifts of the two nuclei, indicating the onset of decoupling, but the *rf* amplitude is too weak to obtain only two singlets, as shown in Figure 3.8 c.

In a three-spin system, an unambiguous assignment of transitions to the energy-level diagram by simple inspection of the multiplets is no longer possible. We consider 2,3-dibromopropionic acid, the same molecule as Freeman and Anderson [12] chose to "tickle". This molecule gave rise to a strongly coupled ABC-system in the 60 MHz spectrometer used for their original paper, but now appears as an ABX-system at 500 MHz. Figure 3.10 a shows a normal one-dimensional (1D) spectrum. For simplicity, we kept the same numbering of the spectral lines. In a three-spin system, the energy-level diagram can be represented by a cube where the 12 transitions correspond to the 12 edges, with four parallel transitions for each spin, which correspond to the doublet-of-doublets of each spin. Figure 3.10 b shows a tickling spectrum obtained by irradiating the left-most resonance C4 with an average amplitude $\langle\omega_2\rangle/(2\pi) = 1.5$ Hz, showing the usual beat pattern. It can be seen that none of the three other C transitions

are affected, since they are all parallel to C4. There are two pairs of connected transitions: A1 and B1 are both split into broad doublets since they are progressively connected, while A2 and one of the overlapping lines B2 or B3 are split into narrow doublets because of their regressive connectivities. The remaining lines A3, A4, B2 or B3 and B4 are not affected since they are not connected to C4. A single experiment is not sufficient to determine all connectivities. For a full analysis, we refer to the original work of Freeman and Anderson [12], where they also determine the relative signs of the J-couplings.

As in our homonuclear decoupling experiments discussed in section 3.1, the tickling field was generated by a sequence of n short pulses, each with a typical duration of $\tau_p = 1$ µs, inserted in the n dwell times. If the latter have a duration of $\Delta t = 50$ µs as required for a spectral width of $1/\Delta t = 20$ kHz, this corresponds to a duty cycle of 2%. The peak *rf* amplitude of each tickling pulse was $\omega_2/(2\pi) = 50$ Hz, resulting in an average amplitude $\langle\omega_2\rangle/(2\pi) = 1$ Hz that satisfies the tickling condition $\langle\omega_2\rangle/(2\pi) \leq J$. Therefore the pulse scheme is identical to the one shown in Figure 3.1 on page 54, using only one effective irradiation frequency ($M = 1$) for the time being. For the calibration of the tickling field B_2, short pulses with a higher *rf* amplitude are more convenient.

Since homonuclear tickling and decoupling can be achieved with the same pulse sequence, there is no need to introduce yet another acronym, and we prefer to stick to WASTE and replace the original "T" for "Tailoring" by "T" for "Tickling". We are not aware of any experimental demonstration of homonuclear spin tickling since the advent of Fourier spectroscopy.

In *heteronuclear* spin systems, tickling can be readily carried out on Fourier transform spectrometers, since one can apply a weak CW field to one nucleus while observing the other in Fourier mode. Thus one can observe a splitting of ^{13}C lines in a phosphine when some connected ^{31}P transitions are irradiated as it was shown by Colquhoun and McFarlance in 1978 [122]. The heteronuclear version of tickling is actually quite easy to implement, since it is sufficient to apply a weak CW field to one of the transitions of the "heteronucleus" during acquisition (but not before the *rf* pulse to avoid inducing nuclear Overhauser effects). For illustration, we tickled the heteronuclear ^{1}H-^{13}C two-spin system in ^{13}C-enriched formate in D_2O. A standard pulse sequence for CW heteronuclear "decoupling" was applied with a weak CW irradiation with $\omega_2/(2\pi) = 1$ Hz and the *rf* carrier set on the left line of the proton doublet, while the carbon-13 signal was acquired. Figure 3.11 a shows the normal carbon-13 doublet, split by the heteronuclear J-coupling of 195 Hz. Figure 3.11 b shows a ^{13}C{^{1}H}-tickling spectrum. Both carbon lines are split by 1 Hz. Note the differential broadening, with narrow lines to the left and broad lines to the right. Figure 3.11 c and d show similar experiments with stronger tickling fields with $\omega_2/(2\pi) = 5$ and 33 Hz. In such heteronuclear systems, higher *rf* amplitudes can be employed than in homonuclear proton systems, since the tickling condition $\omega_2/(2\pi) \leq J = 195$ Hz is less restrictive. Nevertheless, the differential line broadening is most visible when the tickling fields are weak, which facilitates the identification of different types of connectivities, as can be seen in Figure 3.11 b. The variation of the tickling field amplitude in Figures 3.11 b-d demonstrates that tickling could also be used to calibrate weak *rf* fields.

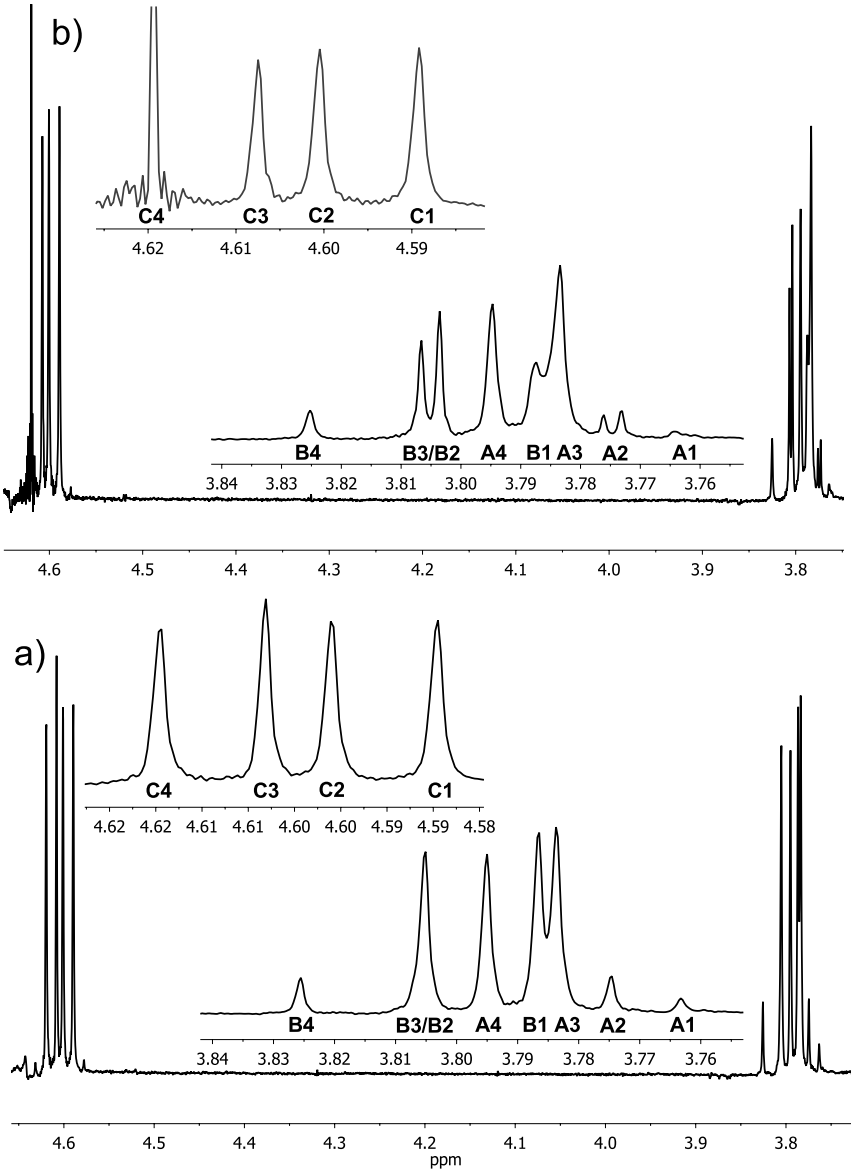

Figure 3.10: a) Normal 500 MHz proton spectrum of the three-spin ABC system of 2,3-dibromopropionic acid, with expanded multiplets showing the 12 transitions of spins A, B and C, using the numbering of Freeman and Anderson [12]. b) Tickling spectrum obtained by irradiating line C4 with an *rf* field with an average amplitude $\langle\omega_2\rangle/(2\pi) = 1.5$ Hz, as evidenced by the typical beat pattern. None of the other C lines are affected since they all correspond to transitions that are parallel to C4. In a three-spin system, the energy-level diagram can be represented by a cube where the twelve transitions correspond to the twelve edges. Changes to the spectrum are visible in the A and B regions in the top figure: The A1 line is hardly visible due to broadening, B1 is also broadened, while A2 is split, and one of the overlapping lines B2 or B3 is also split. Lines A3, A4, B4 and one of the overlapping lines B2 or B3 are unaffected and must therefore correspond to transitions that are not connected to C4.

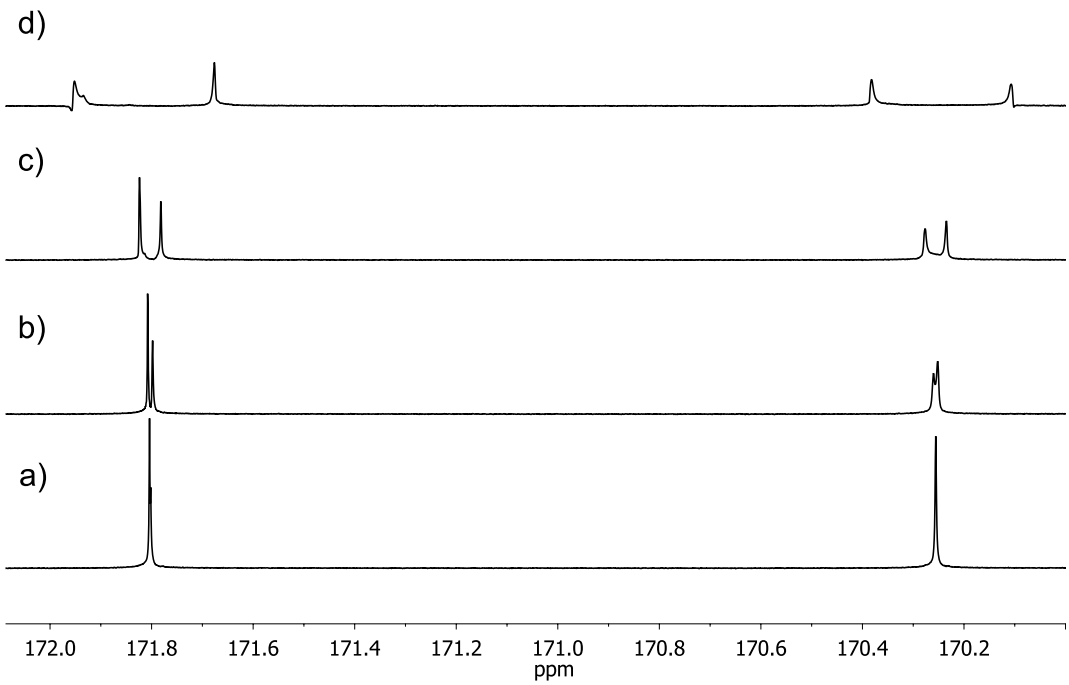

Figure 3.11: a) Normal carbon-13 spectrum at 11.7 T (500 MHz for protons) of ^{13}C-enriched formate showing the carbon-13 doublet J_{CH} = 195 Hz. b) Tickling spectrum obtained with CW irradiation on the left proton peak with $\omega_2/(2\pi)$ = 1 Hz during ^{13}C signal acquisition. Both ^{13}C peaks are split by 1 Hz; the right signal being clearly broadened. c) and d) Same experiments as in b) but with tickling amplitudes $\omega_2/(2\pi)$ = 5 and 33 Hz.

In our case, we knew the correct carrier frequency from the proton spectrum of ^{13}C-enriched formate. Freeman and Anderson showed, that with the help of heteronuclear tickling experiments, they were able to indirectly detect weak or hidden resonances [123]. Observing the proton signal, while shifting the carrier in the range of carbon-13 frequencies, they were able to measure the carbon-13 resonances with a high precision, by observing the splitting of the coupled proton lines. This experiment can be seen as a distant predecessor of INEPT [25].

Can Fourier tickling be useful in modern NMR? Since it requires only one-dimensional experiments, tickling is a quick approach to characterize the progressive or regressive connectivity of particular resonances, comparable to a selective or "soft" COSY [124]. Another application might be the elimination of degeneracies in NMR spectra. Currently, we are not aware of any other techniques that are able to *split* lines in an NMR spectrum. In 1976, Courtieu et al. separated singlet and triplet lines in an AX_2-system by combining tickling with a partially oriented medium [125]. The unperturbed signal of A is a binomial triplet with the intensities 1:2:1. This is the sum of the symmetric triplets (1:1:1) and an antisymmetric singlet (0:1:0). If a tickling field would irradiate one of the two *doubly* degenerate X_2 transitions, all connected

transitions will split *twice*, making again a "triplet", out of every one of the three triplet lines. The antisymmetric singlet is *not* connected to X_2, and will consequently not split. The new center line therefore consists of the full singlet line and one half of an initial triplet line, where a proper separation is not possible. This experiment was successful in a partially oriented media with residual dipolar couplings, since the degeneracies of the X_2 lines are lifted and an isolated singlet line can be obtained. Courtieu et al. performed inversion recovery experiments on these isolated lines and found a clearly slower relaxation of the singlet compared to the triplet. Although this is an indirect experiment, parallels to singlet-state NMR spectroscopy are evident [126, 127].

Besides, we like dusting off the spider webs that have covered spin tickling over the last half century to expose this brilliant idea to the bright light of Fourier NMR.

4 Conclusions and Outlook

A starting point of this thesis was the "stabilization by interconversion within a triad of coherences under multiple refocusing" (SITCOM) (see subsection 2.1.2 on page 9). SITCOM is the effect that can transform the *moderate-amplitude CPMG* into a decoupling sequence, so that echo modulations can be quenched [8]. When working on selective decoupling in section 3.1, we observed an identical interplay of three product operators. Both *triads* are shown in Figure 4.1. On the left is the original SITCOM of the *moderate-amplitude CPMG* with the *multiple-quantum coherence* $2I_yS_y$ as the third product operator. On the right we see the case for a *selective spin-locking field*, where the third product operator is the *longitudinal two-spin order* $2I_zS_z$. The two schemes of interconversions, in the style of Dittmer and Bodenhausen [8], are shown below the corresponding simulations in Figure 4.1. As for our situation, if we start with the in-phase magnetization I_x (blue), it is the J-coupling that makes a partial conversion to the antiphase magnetization $2I_yS_z$ (red). On the left-hand side, for the case of our CPMG, the $180°_x$ pulses have a *moderate rf* amplitude $\omega_1 \geq \Omega_S$. This leads to a *ideal refocusing* of the "I_y" component of the antiphase $2I_yS_z$, but an *imperfect inversion* of the "S_z" component, generating the multiple-quantum coherence $2I_yS_y$ (green). On the right-hand side, for the selective continuous-wave (CW) irradiation, the J-evolution is *not* fully suppressed. It is the on-resonance "I_y'" component of the antiphase term $2I_yS_z$ that will be nutated to "I_z" by the weak *rf* field along the x-axis. Since the off-resonance spin S is unaffected by the selective irradiation, we obtain the longitudinal two-spin order $2I_zS_z$ (yellow). It is interesting to note that in the first case of CPMG, it is an *off*-resonance effect that stops the anti-phase buildup, while in the second case of the selective spin-lock, it is an *on*-resonance effect.

Once again we would like to stress that SITCOM is *selective*, but the 180° pulses applied are of *moderate* (and not selective) strength. Such a CPMG sequence has the interesting property that while the *chemical shifts* are *refocused*, the *J-evolution* is *locked*. Therefore, both spins, on- and off-resonance are decoupled and have a *homogeneous* linewidth/decay. For the *selective spin-lock* however, the off-resonance signal is decoupled, but its linewidth remains *inhomogeneous* (see for example the different linewidths in Figure 3.3 b on page 59).

The first report of SITCOM by Dittmer and Bodenhausen is from 2004 [37] and describes a

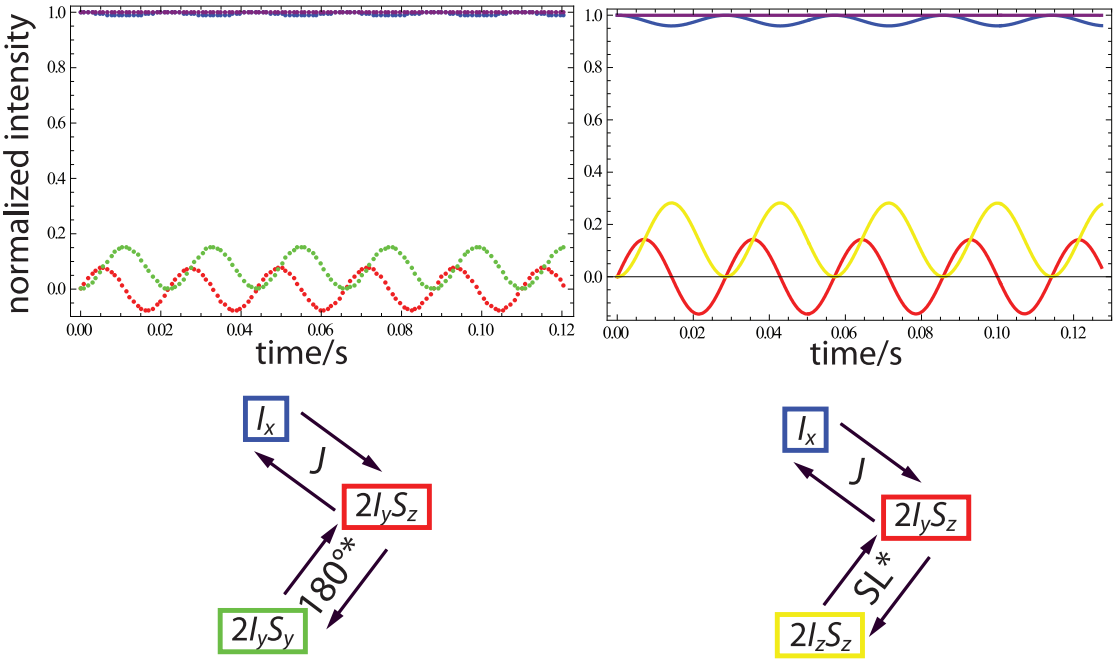

Figure 4.1: Simulations of product operators for a moderate-amplitude CPMG sequence (left) and a selective spin locking (right) applied on resonance to a J-coupled two-spin system IS. Both achieve decoupling and stabilization of an unmodulated in-phase term I_x (blue). The three respective product operators involved show the same interplay (see text). The two graphics below sketch the interactions of the triad, as it was done in Ref. [8], where the colors of the boxes corresponds to the color-coding of the expectation values in the simulations. "180°*" stands for a *moderate* amplitude refocusing pulse, "SL*" for a *selective* spin lock. The in-phase magnetization I_x is blue, the antiphase magnetization $2I_yS_z$ is red, the multiple-quantum coherence (MQC) $2I_yS_y$ is green, and the longitudinal two-spin order $2I_zS_z$ is yellow. Shown in purple are the norms of the two sorts of triads that are constant (compare also Fig. 2.2 on p. 11 and Fig. 3.2 on p. 56). The left simulation was generated by a CPMG sequence of $n = 127$ blocks, with a moderate *rf* amplitude of the refocusing pulse $\omega_1/(2\pi) = 10.4$ kHz and a free evolution delay $2\tau = 900$ µs, applied to a IS system, coupled by $J = 7$ Hz and an off-resonance chemical shift of $\Omega_S/(2\pi) = 1.5$ kHz. The right simulation was generated by $n = 1261$ short pulses of $\omega_2/(2\pi) = 3.5$ kHz, with a duration of $\tau_p = 1$ µs during the dwell time of $\Delta t = 100$ µs, corresponding to an average *rf* field of $\langle\omega_2\rangle/(2\pi) = 35$ Hz. The IS system had a coupling $J = 10$ Hz and an off-resonance chemical shift $\Omega_S/(2\pi) = 1$ kHz. Simulations were performed with the mPackages code (now superseded by SpinDynamica [34]) for Mathematica developed by Malcolm H. Levitt.

heteronuclear system of a proton and a nitrogen-15 nucleus. Their goal is to study relaxation of the multiple-quantum coherence $2I_yS_y$ under a CPMG sequence. Imperfections by pulsing on the two channels are compensated by the J-coupling and stabilizes $2I_yS_y$, inhibiting the buildup of $2I_yS_z$. This example shows that SITCOM is neither limited to the homonuclear case nor restricted to a starting operator of I_x. In analogy, by starting at the bottom of the triad on the right-hand side of Figure 4.1, we could think of a stabilization of longitudinal two-spin order $2I_zS_z$, under a selective CW irradiation.

Single field polarization transfer (SFPT) by Rey Castellanos et al. [107] is another application inside the triad on the right-hand side of Figure 4.1, created by a spin-locking field, as mentioned in section 3.1. They optimize the *rf* field in such a way ($\langle\omega_2\rangle/(2\pi) = |J|/2$), that the amplitude of $2I_zS_z$ becomes maximal and use this for a polarization transfer. Again, this was demonstrated for the *heteronuclear* case. Inspired by the SFPT experiments, we could see in our moderate-amplitude CPMG sequence a way to create the multiple-quantum coherence (MQC) $2I_yS_y$. SFPT might be of more practical relevance, since a simple CW irradiation suffices for its purpose.

The question remains open, if there could be other *triads of product operators* that share a similar interplay as seen in Figure 4.1. One could search for similar mechanisms in systems containing a *dipolar* coupling instead of the J-coupling.

As experimentally tested, both sequences *moderate-amplitude CPMG* and *selective spin locking* work for magnetically equivalent spins, e.g., an AX_2 system. This is a clear advantage compared to the J-refocusing of the "perfect echo" [78, 79] or the multiple-quantum filtration sequence [85], restricted to two-spin systems, as it was illustrated in the section 2.5. Even for AX systems, only the SITCOM based methods can measure a pure in-phase relaxation rate $R_2(I_x)$, where the others decay by a mixture of in-phase $R_2(I_x)$ and the (in practice) faster antiphase relaxation rates $R_2(2I_yS_z)$. The short inter-pulse delays in the PROJECT sequence [83] open J-refocusing to equivalent spins. The unmodulated decay remains slightly faster than $R_2(I_x)$, due to minor contributions of $R_2(2I_yS_z)$.

In contrast to spin locking, CPMG shows *recoupling conditions*, where the J-modulation is reintroduced. They occur at the same resonance conditions between the chemical shift Ω_S and the pulse repetition rate ν_{rep}, known from sidebands in the DANTE sequence [38, 39]: $\Omega_S = 2k\pi\nu_{rep}$. We are trying to avoid recoupling conditions and therefore scan first possible delays τ in the "hybrid" experiments (discussed in subsection 2.1.2). Recently, Smith et al. [128] inverted this perspective, used hard pulses for full modulation in the CPMG and performed a constant-time version of the "hybrid" experiment. This generates not only recoupling dips, spaced by $\Delta\tau = \pi/\Omega_S$, but a full oscillation with Ω_S as a function of τ. Smith et al. used this sequence to read out chemical shifts that were not resolved in a strongly inhomogeneous field.

We have used SITCOM in the moderate-amplitude CPMG to suppress echo modulations and measure transverse relaxation. We cannot use it as a decoupling sequence for a spectrum, because the echoes refocus the chemical shift and nothing but a single peak at the origin

would be left. Therefore, we switched to selective spin locking to collapse multiplets in a spectrum. Could we use conversely this sequence to measure R_2's in protons? The demands of a decoupling sequence in time or frequency domain are different. In the spectrum, our main goal is to generate a collapsed singlet. We do not have to worry about the spectral linewidths, which are proportional to the transverse relaxation rates R_2. When measuring relaxation, of course we want the extract rate R_2, with a minimum of echo modulations. Fortunately, this condition is identical to a minimum of decoupling sidebands, so, selective spin-locking is an excellent candidate to measure R_2's of homonuclear coupled systems.

Can we further reduce the experimental time and read out the homogeneous linewidth directly from a window-acquired homonuclear decoupling spectrum (WASTE)? This would be a reduction of the pseudo 2D to a single-scan 1D. The different linewidths in the example of the decoupled *AX* system in Figure 3.3 on page 59 are promising. One thing we observed is that depending on the strength of the locking field, the (not anymore free) induction decay does *not* go to zero, even for a long duration. This is due to a steady-state between relaxation and *rf* pulsing [18]. Such a direct current (DC) signal gives a signal at zero frequency after Fourier transformation. A simple phase cycle can avoid this issue.

In our polychromatic decoupling sequence baptized "window-acquired spin-tailoring experiment" (WASTE), we profit from the fact that a selective decoupling field can be generated by a short pulse in the dwell time, fulfilling the average Hamiltonian condition [40]. This opens the way for *polychromatic* irradiation, by filling in several short pulses with different effective frequencies. An effective frequency can be generated by constantly shifting the phase of the short pulses in every dwell time. Additionally, the 90° phase shift between the non-selective excitation pulse and the decoupling pulses allow to observe (and not destroy) the irradiated signal.

Even though selective spin locking as an NMR sequence is very old, we think that our "SITCOM" perspective is new. *Multiple echoes* and *spin locking* are two very elementary and complementary techniques in NMR spectroscopy and seem to be once again the best solution, if transverse relaxation should be measured despite the presence of echo modulations.

The very last part of this thesis, section 3.2 about *Fourier spin tickling*, is the exception in that it does *not* speak about decoupling. It is as well an elementary NMR method [12] but not anymore used and certainly forgotten among the younger generation of NMR spectroscopists. We want to advertise that spin tickling is straightforward to implement on a standard Fourier transform NMR spectrometer. To our knowledge, it is the only technique that can split (in contrary to decoupling that collapses multiplets) single resonances in a coupled system. The experiment of Courtieu et al. [125], briefly discussed at the end of section 3.2, gives an idea of how fascinating experiments could be performed using spin tickling. Having the WASTE sequence, everything is ready to perform *polychromatic tickling*.

Abbreviations and Acronyms

COSY	correlation spectroscopy
CPMG	Carr-Purcell-Meiboom-Gill multiple spin echo sequence
CsA	cyclosporin A
CW	continuous-wave
DANTE	delays alternating with nutation for tailored excitation
DIPSI	decoupling in the presence of scalar interactions
DQC	double-quantum coherence
FID	free induction decay
FT	Fourier transform
HD	homonuclear decoupling
HSQC	heteronuclear single-quantum correlation spectroscopy
INADEQUTE	incredible natural-abundance double-quantum transfer experiment
INEPT	insensitive nuclei enhanced by polarization transfer
MLEV	Malcolm Levitt's decoupling cycle
MQC	multiple-quantum coherence
MQF	multiple-quantum filter
NMR	nuclear magnetic resonance
NOESY	nuclear Overhauser effect spectroscopy
ppm	parts per million
PROJECT	periodic refocusing of J-evolution by coherence transfer
rf	radio-frequency
ROESY	rotating frame nuclear Overhauser effect spectroscopy
SITCOM	stabilization by interconversion within a triad of coherences under multiple refocusing
SQC	single-quantum coherence
TOCSY	total correlation spectroscopy
WALTZ	decoupling sequence: $\{1\bar{2}3\,1\bar{2}3\,\bar{1}2\bar{3}\,\bar{1}2\bar{3}\}$
WASTE	window-acquired spin tailoring/tickling experiment
ZQC	zero-quantum coherence

Bibliography

[1] R. Freeman. *Spin Choreography: Basic Steps in High Resolution NMR*. Spektrum, 1997.

[2] R.R. Ernst and W.A. Anderson. Application of Fourier transform spectroscopy to magnetic resonance. *Rev. Sci. Instrum.*, 37(1):93–102, 1966.

[3] E.L. Hahn. Spin echoes. *Phys. Rev.*, 80:580–594, 1950.

[4] A.G. Redfield. Nuclear magnetic resonance saturation and rotary saturation in solids. *Phys. Rev.*, 98:1787–1809, 1955.

[5] I. Solomon. Etude de la relaxation en résonance mangétique par la méthode de "précession forcée transitoire". *C. R. Acad. Sci. Paris*, 248:92–94, 1959.

[6] H.Y. Carr and E.M. Purcell. Effects of diffusion on free precession in nuclear magnetic resonance experiments. *Phys. Rev.*, 94:630–638, 1954.

[7] S. Meiboom and D. Gill. Modified spin-echo method for measuring nuclear relaxation times. *Rev. Sci. Instrum.*, 29(8):688–691, 1958.

[8] J. Dittmer and G. Bodenhausen. Quenching echo modulations in NMR spectroscopy. *ChemPhysChem*, 7(4):831–836, 2006.

[9] W.A. Anderson and R. Freeman. Influence of a second radiofrequency field on high-resolution nuclear magnetic resonance spectra. *J. Chem. Phys.*, 37(1):85–103, 1962.

[10] J.P. Jesson, P. Meakin, and G. Kneissel. Homonuclear decoupling and peak elimination in Fourier transform nuclear magnetic resonance. *J. Am. Chem. Soc.*, 95(2):618–620, 1973.

[11] O.W. Sørensen, G.W. Eich, M.H. Levitt, G. Bodenhausen, and R.R. Ernst. Product operator formalism for the description of NMR pulse experiments. *Prog. Nucl. Magn. Reson. Spectrosc.*, 16:163–192, 1983.

[12] R. Freeman and W.A. Anderson. Use of weak perturbing radio-frequency fields in nuclear magnetic double resonance. *J. Chem. Phys.*, 37(9):2053–2073, 1962.

[13] J. Keeler. *Understanding NMR Spectroscopy*. John Wiley & Sons, 2nd edition, 2011.

[14] P.J. Hore, J.A. Jones, and S. Wimperis. *NMR: The Toolkit*. Oxford Chemistry Primers. Oxford University Press, USA, 2000.

[15] M.H. Levitt. *Spin Dynamics: Basics of Nuclear Magnetic Resonance*. Wiley, 2nd edition, 2008.

[16] J. Cavanagh, W.J. Fairbrother, A.G. Palmer III, M. Rance, and N.J. Skelton. *Protein NMR Spectroscopy: Principles And Practice*. Academic Press, 2nd edition, 2007.

[17] A. Abragam. *Principles of Nuclear Magnetism*. International Series of Monographs on Physics. Oxford University Press, USA, 1983.

[18] C.P. Slichter. *Principles of Magnetic Resonance*. Springer, 3rd edition, 1996.

[19] R.R. Ernst, G. Bodenhausen, and A. Wokaun. *Principles of Nuclear Magnetic Resonance in One and Two Dimensions*. International Series of Monographs on Chemistry. Clarendon Press, Oxford, 1987.

[20] T.F. Segawa and G. Bodenhausen. Modulations of spin echoes in liquids. In R. K. Harris and R. E. Wasylishen, editors, *Encyclopedia of Magnetic Resonance*. John Wiley & Sons, Ltd, Chichester. accepted.

[21] E.L. Hahn and D.E. Maxwell. Spin echo measurements of nuclear spin coupling in molecules. *Phys. Rev.*, 88:1070–1084, 1952.

[22] R. Freeman and H.D.W. Hill. Determination of spin-spin relaxation times in high-resolution NMR. In L.M. Jackmann and F.A. Cotton, editors, *Dynamic Nuclear Magnetic Resonance Spectroscopy*, pages 131–162. Academic Press, 1975.

[23] A. Kumar and R.R. Ernst. Influence of nonresonant nuclei on NMR spin echoes in liquids and in solids. *J. Magn. Reson.*, 24(3):425–447, 1976.

[24] D.E. Kaplan and E.L. Hahn. Expériences de double irradiation en résonance magnétique par la méthode d'impulsions. *J. Phys. Radium*, 19(11):821–825, 1958.

[25] G.A. Morris and R. Freeman. Enhancement of nuclear magnetic resonance signals by polarization transfer. *J. Am. Chem. Soc.*, 101(3):760–762, 1979.

[26] H.S. Gutowsky, R.L. Vold, and E.J. Wells. Theory of chemical exchange effects in magnetic resonance. *J. Chem. Phys.*, 43(11):4107–4125, 1965.

[27] A. Allerhand. Analysis of Carr-Purcell spin-echo NMR experiments on multiple-spin systems. I. The effect of homonuclear coupling. *J. Chem. Phys.*, 44(1):1–9, 1966.

[28] L. Braunschweiler and R.R. Ernst. Coherence transfer by isotropic mixing: Application to proton correlation spectroscopy. *J. Magn. Reson.*, 53(3):521–528, 1983.

[29] A. Bax and D.G. Davis. Practical aspects of two-dimensional transverse NOE spectroscopy. *J. Magn. Reson.*, 63(1):207–213, 1985.

[30] Z. Tošner, A. Škoch, and J. Kowalewski. Behavior of two almost identical spins during the CPMG pulse sequence. *ChemPhysChem*, 11(3):638–645, 2010.

[31] K. Gopalakrishnan, N. Aeby, and G. Bodenhausen. Quenching and recoupling of echo modulations in NMR spectroscopy. *ChemPhysChem*, 8(12):1791–1802, 2007.

[32] N. Aeby and G. Bodenhausen. Determination of transverse relaxation rates of individual spins while quenching echo modulations due to homonuclear scalar couplings. *Chem. Phys. Lett.*, 463:418–421, 2008.

[33] N. Aeby. *Effects of homonuclear scalar couplings during multiple refocusing sequences in nuclear magnetic resonance*. PhD thesis, EPFL, Lausanne, 2008.

[34] SpinDynamica code for Mathematica, programmed by Malcolm H. Levitt, available at www.SpinDynamica.soton.ac.uk.

[35] Mathematica. *Version 7.0*. Wolfram Research, Inc., Champaign, Illinois, 1988-2008.

[36] D. Carnevale, T.F. Segawa, and G. Bodenhausen. Polychromatic decoupling of a manifold of homonuclear scalar interactions in solution-state NMR. *Chem. Eur. J.*, 18(37):11573–11576, 2012.

[37] J. Dittmer and G. Bodenhausen. Multiple refocusing in NMR spectroscopy: Compensation of pulse imperfections by scalar couplings. *ChemPhysChem*, 5(11):1750–1754, 2004.

[38] G. Bodenhausen, R. Freeman, and G.A. Morris. A simple pulse sequence for selective excitation in Fourier transform NMR. *J. Magn. Reson.*, 23(1):171–175, 1976.

[39] G.A. Morris and R. Freeman. Selective excitation in Fourier transform nuclear magnetic resonance. *J. Magn. Reson.*, 29(3):433–462, 1978.

[40] U. Haeberlen and J.S. Waugh. Coherent averaging effects in magnetic resonance. *Phys. Rev.*, 175:453–467, 1968.

[41] T.F. Segawa, N. Aeby, and G. Bodenhausen. Apparent transverse relaxation rates in systems with coupled carbon-13 spins. *Phys. Chem. Chem. Phys.*, 12:9772–9776, 2010.

[42] B. Baishya, T.F. Segawa, and G. Bodenhausen. Apparent transverse relaxation rates in systems with scalar-coupled protons. *J. Am. Chem. Soc.*, 131(48):17538–17539, 2009.

[43] T.F. Segawa, B. Baishya, and G. Bodenhausen. Transverse relaxation of scalar-coupled protons. *ChemPhysChem*, 11(15):3343–3354, 2010.

[44] A. Rüegger, M. Kuhn, H. Lichti, H.-R. Loosli, R. Huguenin, C. Quiquerez, and A. von Wartburg. Cyclosporin A, ein immunsuppressiv wirksamer Peptidmetabolit aus Trichoderma polysporum (Link ex Pers.) Rifai. *Helv. Chim. Acta*, 59(4):1075–1092, 1976.

[45] H. Kessler, H.-R. Loosli, and H. Oschkinat. Peptide conformations. Part 30. Assignment of the 1H-, 13C-, and 15N-NMR spectra of cyclosporin A in CDCl3 and C6D6 by a combination of homo- and heteronuclear two-dimensional techniques. *Helv. Chim. Acta*, 68(3):661–681, 1985.

[46] H.-R. Loosli, H. Kessler, H. Oschkinat, H.-P. Weber, T.J. Petcher, and A. Widmer. Peptide conformations. Part 31. The conformation of cyclosporin A in the crystal and in solution. *Helv. Chim. Acta*, 68(3):682–704, 1985.

[47] T. Meersmann and G. Bodenhausen. Transverse relaxation in proton NMR. Separate measurement of decay rates of in-phase and antiphase coherences. *J. Magn. Reson. A*, 115(2):277–282, 1995.

[48] J. Kowalewski and L. Mäler. *Nuclear Spin Relaxation in Liquids: Theory, Experiments, And Applications*. Series in Chemical Physics Series. Taylor & Francis Group, 2006.

[49] D.P. Burum and R.R. Ernst. Net polarization transfer via a J-ordered state for signal enhancement of low-sensitivity nuclei. *J. Magn. Reson.*, 39(1):163–168, 1980.

[50] G. Bodenhausen and D.J. Ruben. Natural abundance nitrogen-15 NMR by enhanced heteronuclear spectroscopy. *Chem. Phys. Lett.*, 69(1):185–189, 1980.

[51] T.F. Segawa, B.. Baishya, and G. Bodenhausen. Transverse relaxation of scalar coupled protons in magnetic resonance of non-deuterated proteins. *Appl. Magn. Reson.*, 42:353–361, 2012.

[52] M. Verde. *Chemical Exchange in Proteins - Relaxation of Multiple- and Single-Quantum Coherences Studied by NMR*. PhD thesis, EPFL, Lausanne, 2009.

[53] P. Pelupessy, F. Ferrage, and G. Bodenhausen. Accurate measurement of longitudinal cross-relaxation rates in nuclear magnetic resonance. *J. Chem. Phys.*, 126(13):134508, 2007.

[54] M. Verde, S. Ulzega, F. Ferrage, and G. Bodenhausen. Preservation of heteronuclear multiple-quantum coherences in NMR by double-resonance irradiation. *J. Chem. Phys.*, 130(7):074506, 2009.

[55] S. Ulzega, M. Verde, F. Ferrage, and G. Bodenhausen. Heteronuclear double resonance in nuclear magnetic resonance spectroscopy: Relaxation of multiple-quantum coherences. *J. Chem. Phys.*, 131(22):224503, 2009.

[56] B. Boulat and G. Bodenhausen. Measurement of proton relaxation rates in proteins. *J. Biomol. NMR*, 3(3):335–348, 1993.

[57] R. Ishima, P.T. Wingfield, S.J. Stahl, J.D. Kaufman, and D.A. Torchia. Using amide 1H and 15N transverse relaxation to detect millisecond time-scale motions in perdeuterated proteins: Application to HIV-1 protease. *J. Am. Chem. Soc.*, 120(40):10534–10542, 1998.

[58] P. Lundström and M. Akke. Off-resonance rotating-frame amide proton spin relaxation experiments measuring microsecond chemical exchange in proteins. *J. Biomol. NMR*, 32(2):163–173, 2005.

[59] R. Ishima and D.A. Torchia. Extending the range of amide proton relaxation dispersion experiments in proteins using a constant-time relaxation-compensated CPMG approach. *J. Biomol. NMR*, 25(3):243–248, 2003.

[60] C. Griesinger, G. Otting, K. Wüthrich, and R.R. Ernst. Clean TOCSY for proton spin system identification in macromolecules. *J. Am. Chem. Soc.*, 110(23):7870–7872, 1988.

[61] A.G. Palmer III, J. Cavanagh, P.E. Wright, and M. Rance. Sensitivity improvement in proton-detected two-dimensional heteronuclear correlation NMR spectroscopy. *J. Magn. Reson.*, 93(1):151–170, 1991.

[62] L. Kay, P. Keifer, and T. Saarinen. Pure absorption gradient enhanced heteronuclear single quantum correlation spectroscopy with improved sensitivity. *J. Am. Chem. Soc.*, 114(26):10663–10665, 1992.

[63] J. Schleucher, M. Schwendinger, M. Sattler, P. Schmidt, O. Schedletzky, S.J. Glaser, O.W. Sørensen, and C. Griesinger. A general enhancement scheme in heteronuclear multidimensional NMR employing pulsed field gradients. *J. Biomol. NMR*, 4(2):301–306, 1994.

[64] F. Delaglio, S. Grzesiek, G.W. Vuister, G. Zhu, J. Pfeifer, and A. Bax. NMRPipe: A multidimensional spectral processing system based on UNIX pipes. *J. Biomol. NMR*, 6(3):277–293, 1995.

[65] G. Cornilescu, J.L. Marquardt, M. Ottiger, and A. Bax. Validation of protein structure from anisotropic carbonyl chemical shifts in a dilute liquid crystalline phase. *J. Am. Chem. Soc.*, 120(27):6836–6837, 1998.

[66] P. Schanda. Fast-pulsing longitudinal relaxation optimized techniques: Enriching the toolbox of fast biomolecular NMR spectroscopy. *Prog. Nucl. Magn. Reson. Spectrosc.*, 55(3):238–265, 2009.

[67] D. Jeannerat. Computer optimized spectral aliasing in the indirect dimension of 1H-13C heteronuclear 2D NMR experiments. A new algorithm and examples of applications to small molecules. *J. Magn. Reson.*, 186(1):112–122, 2007.

[68] P. Schanda and B. Brutscher. Very fast two-dimensional NMR spectroscopy for real-time investigation of dynamic events in proteins on the time scale of seconds. *J. Am. Chem. Soc.*, 127(22):8014–8015, 2005.

[69] L. Frydman, T. Scherf, and A. Lupulescu. The acquisition of multidimensional NMR spectra within a single scan. *Proc. Natl. Acad. Sci. U. S. A.*, 99(25):15858–15862, 2002.

[70] P. Pelupessy. Adiabatic single scan two-dimensional NMR spectrocopy. *J. Am. Chem. Soc.*, 125(40):12345–12350, 2003.

[71] MATLAB. *R2009a*. The MathWorks Inc., Natick, Massachusetts, 1984-2009.

[72] B. Baishya, T.F. Segawa, and G. Bodenhausen. Quenching homonuclear couplings in magnetic resonance by trains of non-refocusing pulses. *J. Magn. Reson.*, 211(2):240–242, 2011.

[73] R. Freeman and S. Wittekoek. Selective determination of relaxation times in high resolution NMR. *J. Magn. Reson.*, 1(2):238–276, 1969.

[74] J. Hennig. Echoes - How to generate, recognize, use or avoid them in MR-imaging sequences. Part I: Fundamental and not so fundamental properties of spin echoes. *Concepts Magn. Reson.*, 3(3):125–143, 1991.

[75] L. Emsley and G. Bodenhausen. Optimization of shaped selective pulses for NMR using a quaternion description of their overall propagators. *J. Magn. Reson.*, 97(1):135–148, 1992.

[76] D.J. Siminovitch. Rotations in NMR: Part I. Euler-Rodrigues parameters and quaternions. *Concepts Magn. Reson.*, 9(3):149–171, 1997.

[77] D.J. Siminovitch. Rotations in NMR: Part II. Applications of the Euler-Rodrigues parameters. *Concepts Magn. Reson.*, 9(4):211–225, 1997.

[78] K. Takegoshi, K. Ogura, and K. Hikichi. A perfect spin echo in a weakly homonuclear J-coupled two spin-1/2 system. *J. Magn. Reson.*, 84(3):611–615, 1989.

[79] P.C.M. van Zijl, C.T.W. Moonen, and M. von Kienlin. Homonuclear J refocusing in echo spectroscopy. *J. Magn. Reson.*, 89(1):28–40, 1990.

[80] J.G. Powles and P. Mansfield. Double-pulse nuclear-resonance transients in solids. *Phys. Lett.*, 2(2):58–59, 1962.

[81] M. Bloom, E.L. Hahn, and B. Herzog. Free magnetic induction in nuclear quadrupole resonance. *Phys. Rev.*, 97:1699–1709, 1955.

[82] K. Schmidt-Rohr. Complete dipolar decoupling of 13C and its use in two-dimensional double-quantum solid-state NMR for determining polymer conformations. *J. Magn. Reson.*, 131(2):209–217, 1998.

[83] J.A. Aguilar, M. Nilsson, G. Bodenhausen, and G.A. Morris. Spin echo NMR spectra without J modulation. *Chem. Commun.*, 48:811–813, 2012.

[84] C.S. Johnson Jr. Diffusion ordered nuclear magnetic resonance spectroscopy: principles and applications. *Prog. Nucl. Magn. Reson. Spectrosc.*, 34(34):203–256, 1999.

[85] C. Barrère, P. Thureau, A. Thévand, and S. Viel. A convenient method for the measurements of transverse relaxation rates in homonuclear scalar coupled spin systems. *Chem. Commun.*, 47:9209–9211, 2011.

[86] T. Schulte-Herbrüggen, Z.L. Mádi, O.W. Sørensen, and R.R. Ernst. Reduction of multiplet complexity in COSY-type NMR spectra. The bilinear and planar COSY experiments. *Mol. Phys.*, 72(4):847–871, 1991.

[87] Z.L. Mádi, B. Brutscher, T. Schulte-Herbrüggen, R. Brüschweiler, and R.R. Ernst. Time-resolved observation of spin waves in a linear chain of nuclear spins. *Chem. Phys. Lett.*, 268(3-4):300 – 305, 1997.

[88] J.W. Peng, V. Thanabal, and G. Wagner. Improved accuracy of heteronuclear transverse relaxation time measurements in macromolecules. Elimination of antiphase contributions. *J. Magn. Reson.*, 95(2):421–427, 1991.

[89] S.R. Hartmann and E.L. Hahn. Nuclear double resonance in the rotating frame. *Phys. Rev.*, 128:2042–2053, 1962.

[90] G. Pileio, M. Carravetta, and M.H. Levitt. Extremely low-frequency spectroscopy in low-field nuclear magnetic resonance. *Phys. Rev. Lett.*, 103:083002, 2009.

[91] R. Sarkar, P. Ahuja, P.R. Vasos, and G. Bodenhausen. Long-lived coherences for homogeneous line narrowing in spectroscopy. *Phys. Rev. Lett.*, 104:053001, 2010.

[92] A.J. Shaka and J. Keeler. Broadband spin decoupling in isotropic-liquids. *Prog. Nucl. Magn. Reson. Spectrosc.*, 19(1):47–129, 1987.

[93] A.J. Shaka, C.J. Lee, and A. Pines. Iterative schemes for bilinear operators; application to spin decoupling. *J. Magn. Reson.*, 77(2):274–293, 1988.

[94] V. Royden. Measurement of the spin and gyromagnetic ratio of 13C by the collapse of spin-spin splitting. *Phys. Rev.*, 96:543–544, 1954.

[95] R. Freeman. Double resonance in liquids. In R.K. Harris and R.E. Wasylishen, editors, *Encyclopedia of Magnetic Resonance*. John Wiley & Sons, Ltd, Chichester, 2011. http://dx.doi.org/10.1002/9780470034590.emrstm0134.pub2.

[96] W.P. Aue, E. Bartholdi, and R.R. Ernst. Two-dimensional spectroscopy. Application to nuclear magnetic resonance. *J. Chem. Phys.*, 64(5):2229–2246, 1976.

[97] R.R. Ernst, W.P. Aue, E. Bartholdi, A. Höhener, and S. Schäublin. Equivalence of Fourier spectroscopy and slow passage in nuclear magnetic resonance. *Pure Appl. Chem.*, 37(1-2):47–60, 1974.

[98] M. Mehring and J.S. Waugh. Magic-angle NMR experiments in solids. *Phys. Rev. B*, 5:3459–3471, 1972.

[99] P.S.C. Wu and G. Otting. Rapid pulse length determination in high-resolution NMR. *J. Magn. Reson.*, 176(1):115–119, 2005.

[100] W. P. Aue, J. Karhan, and R. R. Ernst. Homonuclear broad band decoupling and two-dimensional J-resolved NMR spectroscopy. *J. Chem. Phys.*, 64(10):4226–4227, 1976.

[101] A. Bax and R. Freeman. Investigation of complex networks of spin-spin coupling by two-dimensional NMR. *J. Magn. Reson.*, 44(3):542–561, 1981.

[102] A.J. Shaka, J. Keeler, and R. Freeman. Separation of chemical shifts and spin coupling in proton NMR. Elimination of dispersion signals from two-dimensional spectra. *J. Magn. Reson.*, 56(2):294–313, 1984.

[103] K. Zangger and H. Sterk. Homonuclear broadband-decoupled NMR spectra. *J. Magn. Reson.*, 124(2):486–489, 1997.

[104] M.A. McCoy and L. Mueller. Selective shaped pulse decoupling in NMR: homonuclear [carbon-13]carbonyl decoupling. *J. Am. Chem. Soc.*, 114(6):2108–2112, 1992.

[105] Ē. Kupče and R. Freeman. Band-selective decoupling. *J. Magn. Reson. Ser. A.*, 102(3):364–369, 1993.

[106] Ē. Kupče, H. Matsuo, and G. Wagner. Homonuclear Decoupling in Proteins. In N.R. Krishna and L.J. Berliner, editors, *Modern Techniques in Protein NMR*, volume 16 of *Biological Magnetic Resonance*, pages 149–193. Kluwer Academic / Plenum Publishers, 1998.

[107] E.R. Rey Castellanos, D.P. Frueh, and J. Wist. Selective polarization transfer using a single rf field. *J. Chem. Phys.*, 129(1):014504, 2008.

[108] F. Bloch and A. Siegert. Magnetic resonance for nonrotating fields. *Phys. Rev.*, 57:522–527, 1940.

[109] L. Emsley and G. Bodenhausen. Phase shifts induced by transient Bloch-Siegert effects in NMR. *Chem. Phys. Lett.*, 168(3-4):297–303, 1990.

[110] H. Geen, X.L. Wu, P. Xu, J. Friedrich, and R. Freeman. Selective excitation at two arbitrary frequencies. The double-DANTE sequence. *J. Magn. Reson.*, 81(3):646–652, 1989.

[111] S.L. Patt. Single- and multiple-frequency-shifted laminar pulses. *J. Magn. Reson.*, 96(1):94–102, 1992.

[112] A.P.D.M. Espindola, R. Crouch, J.R. DeBergh, J.M. Ready, and J.B. MacMillan. Deconvolution of complex NMR spectra in small molecules by multi frequency homonuclear decoupling (MDEC). *J. Am. Chem. Soc.*, 131(44):15994–15995, 2009.

[113] B.L. Tomlinson and H.D.W. Hill. Fourier synthesized excitation of nuclear magnetic resonance with application to homonuclear decoupling and solvent line suppression. *J. Chem. Phys.*, 59(4):1775–1784, 1973.

[114] T.F. Segawa, D. Carnevale, and G. Bodenhausen. How to tickle spins with a Fourier transform NMR spectrometer. *ChemPhysChem*, 14(2):369–373, 2013.

[115] R.A. Hoffman and S. Forsén. High resolution nuclear magnetic double and multiple resonance. *Prog. Nucl. Magn. Reson. Spectrosc.*, 1(1):15–204, 1966.

[116] R. Freeman. *A Handbook of Nuclear Magnetic Resonance*. Longman, 2nd edition, 1997.

[117] R. Freeman. Freeman, Ray: Double resonance methods in high-resolution NMR. In R.K. Harris and R.E. Wasylishen, editors, *Encyclopedia of Magnetic Resonance*. John Wiley & Sons, Ltd, Chichester, 2007. http://dx.doi.org/10.1002/9780470034590.emrhp0060.

[118] M. Bak, J.T. Rasmussen, and N.C. Nielsen. SIMPSON: A general simulation program for solid-state NMR spectroscopy. *J. Magn. Reson.*, 147(2):296–330, 2000.

[119] E. Fermi. Über den Ramaneffekt des Kohlendioxyds. *Z. Phys.*, 71(3-4):250–259, 1931.

[120] F. Günther. Anwendung von Doppelresonanzmethoden in der Fourier-Transformations-spektroskopie der hochauflösenden NMR. *Ann. Phys.*, 482(4):396–408, 1972.

[121] A. Wokaun and R.R. Ernst. Multiple quantum double resonance. *Mol. Phys.*, 38(5):1579–1601, 1979.

[122] I.J. Colquhoun and W. McFarlane. Fourier transform heteronuclear magnetic tree resonance in complex spin systems: Tetramethylbiphosphine disulfide. *J. Magn. Reson.*, 31(1):63–67, 1978.

[123] R. Freeman and W.A. Anderson. Indirect detection of weak or hidden nuclear magnetic resonance signals. *J. Chem. Phys.*, 39(3):806–810, 1963.

[124] C. Bauer, R. Freeman, T. Frenkiel, J. Keeler, and A.J. Shaka. Gaussian pulses. *J. Magn. Reson.*, 58(3):442–457, 1984.

[125] J. Courtieu, P.E. Fagerness, and D.M. Grant. The elimination of degeneracies in spin systems of magnetically equivalent nuclei by nematic solvents and spin tickling. *J. Chem. Phys.*, 65(3):1202–1205, 1976.

[126] M.H. Levitt. Singlet and other states with extended lifetimes. In R. K. Harris and R. E. Wasylishen, editors, *Encyclopedia of Magnetic Resonance*. John Wiley & Sons, Ltd, Chichester, 2010. http://dx.doi.org/10.1002/9780470034590.emrstm1036.

[127] M.H. Levitt. Singlet nuclear magnetic resonance. *Annu. Rev. Phys. Chem.*, 63(1):89–105, 2012.

[128] P.E.S. Smith, G. Bensky, G.A. Álvarez, G. Kurizki, and L. Frydman. Shift-driven modulations of spin-echo signals. *Proc. Natl. Acad. Sci. U. S. A.*, 109(16):5958–5961, 2012.

Curriculum Vitae

Takuya Fabian SEGAWA

Personal Details

Date of birth	3rd of October 1984
Place of birth	Baden, Switzerland
Nationalities	Swiss and Japanese
Contact information	takuya.segawa@epfl.ch / takuya.segawa@alumni.ethz.ch

Education

EPF Lausanne (Switzerland) 2009-2013

PhD Thesis in the *Laboratory of Biomolecular Magnetic Resonance* of
Prof. Geoffrey Bodenhausen, *Institute of Chemical Sciences and Engineering*
Nuclear Magnetic Resonance (NMR) Spectroscopy

→ fundamental research on *spin echo* and *decoupling* sequences in the liquid state [3-14]

ETH Zürich (Switzerland)

Master of Science in Chemistry (emphasis on physical chemistry) 2007-2008
including research projects in the fields of

- Biological NMR (Prof. Roland Riek) [2]
- Laser Spectroscopy (Prof. Frédéric Merkt)

Bachelor of Science in Chemistry 2004-2007

- Erasmus exchange during the winter semester 06/07 to the
  Ecole Normale Supérieure in **Paris** (France)
  → research project in the NMR group of Prof. Geoffrey Bodenhausen [1]

Languages Skills

German – Mother tongue, **Japanese** – Fluent, **English** – Fluent, **French** – Fluent

Awards and Grants

→ * **Poster Prize** on the occasion of the EUROMAR conference 2011 in Frankfurt
→ **Best Teaching Prize** in 2012 from the Section of Chemistry and Chemical Engineering at EPFL
→ **Chemistry Travel Award** in 2011 from the Swiss Academy of Sciences and the Swiss Chemical Society
→ **AMPERE Grant** to attend the EUROMAR conference 2012 in Dublin

Memberships

Member of the *Schweizerische Studienstiftung (Swiss Study Foundation)*	2005-present
Member of the *Swiss Chemical Society*	2009-present

Personal Interests

Music	Playing viola and violin in chamber and symphonic orchestras

Scientific Publications

1. T. Segawa, F. Kateb, L. Duma, G. Bodenhausen, and P. Pelupessy, *Exchange Rate Constants of Invisible Protons in Proteins Determined by NMR Spectroscopy*, ChemBioChem, **2008**, *9*, 537.
2. B. Vögeli, T.F. Segawa, D. Leitz, A. Sobol, A. Choutko, D. Trzesniak, W. van Gunsteren, and R. Riek, *Exact Distances and Internal Dynamics of Perdeuterated Ubiquitin from NOE Buildups*, J. Am. Chem. Soc., **2009**, *131*, 17215.
3. B. Baishya, T.F. Segawa, and G. Bodenhausen, *Apparent Transverse Relaxation Rates in Systems with Scalar-Coupled Protons*, J. Am. Chem. Soc., **2009**, *131*, 17538.
4. T.F. Segawa, N. Aeby, and G. Bodenhausen, *Apparent Transverse Relaxation Rates in Systems with Coupled Carbon-13 Spins*, Phys. Chem. Chem. Phys., **2010**, *12*, 9772.
5. T.F. Segawa, B. Baishya, and G. Bodenhausen, *Transverse Relaxation of Scalar-Coupled Protons*, ChemPhysChem, **2010**, *11*, 3343.
6. S. Ulzega, N. Salvi, T.F. Segawa, F. Ferrage, and G. Bodenhausen, *Control of Cross Relaxation of Multiple-Quantum Coherences Induced by Fast Chemical Exchange under Heteronuclear Double-Resonance Irradiation*, ChemPhysChem, **2011**, *12*, 333.
7. B. Baishya, T.F. Segawa, and G. Bodenhausen, *Quenching Homonuclear Couplings in Magnetic Resonance by Trains of Non-Refocusing Pulses*, J. Magn. Reson., **2011**, *211*, 240.
8. T.F. Segawa, A. Bornet, N. Salvi, P. Miéville, V. Vitzthum, D. Carnevale, S. Jannin, M.A. Caporini, S. Ulzega, P.R. Vasos, M. Rey, and G. Bodenhausen, *Extending Timescales and Narrowing Linewidths in NMR*, Chimia, **2011**, *65*, 652.
9. T.F. Segawa, B. Baishya, and G. Bodenhausen, *Transverse Relaxation of Scalar-Coupled Protons in Magnetic Resonance of Non-Deuterated Proteins*, Appl. Magn. Reson., **2012**, *42*, 353.
10. S. Chinthalapalli, A. Bornet, T.F. Segawa, R. Sarkar, S. Jannin, and G. Bodenhausen, *Ultrahigh-Resolution Magnetic Resonance in Inhomogeneous Magnetic Fields: Two-Dimensional Long-Lived-Coherence Correlation Spectroscopy*, Phys. Rev. Lett., **2012**, *109*, 047602.
11. D. Carnevale, T.F. Segawa, and G. Bodenhausen, *Polychromatic Decoupling of a Manifold of Homonuclear Scalar Interactions in Solution-State NMR*, Chem. Eur. J., **2012**, *18*, 11573.
12. A. Bornet, J. Milani, S. Wang, D. Mammoli, R. Buratto, N. Salvi, T.F. Segawa, V. Vitzthum, P. Miéville, S. Chinthalapalli, A.J. Perez-Linde, D. Carnevale, S. Jannin, M. Caporini, S. Ulzega, M. Rey, and G. Bodenhausen, *Dynamic Nuclear Polarization and Other Magnetic Ideas at EPFL*, Chimia, **2012**, *66*, 734.
13. T.F. Segawa, D. Carnevale, and G. Bodenhausen. *How to Tickle Spins with a Fourier Transform NMR Spectrometer*, ChemPhysChem, **2013**, *14*, 369.
14. T.F. Segawa and G. Bodenhausen, *Modulations of Spin Echoes in Liquids*, Encyclopedia of Magnetic Resonance, eds-in-chief R.K. Harris and R.E. Wasylishen, John Wiley: Chichester, *accepted*.

Conference Contributions

- **EUROMAR 2012**, University College Dublin, Ireland, July 1-5, 2012, *How to Measure Transverse Relaxation of Protons?*, T.F. Segawa, D. Carnevale, and G. Bodenhausen (poster)
- *** EUROMAR 2011**, Goethe Universität, Frankfurt, Germany, August 21-25, 2011, *Pulse Trains with Variable Nutation Angles for Homonuclear Decoupling*, T.F. Segawa, P. Miéville, D. Carnevale, B. Baishya and G. Bodenhausen (poster)
- **EMBO Practical Course** in "Multidimensional NMR in Structural Biology", Il Ciocco, Italy, August 1-6, 2010, *Measuring Apparent Transverse Relaxation Rates in Homonuclear J-Coupled Systems*, T.F. Segawa, N. Aeby, B. Baishya, and G. Bodenhausen (poster)
- **Swiss Chemical Society – 2012 Fall Meeting**, ETH Zürich, September 13, 2012, *Can One Measure Transverse Relaxation Rates of Protons in NMR?*, T.F. Segawa, D. Carnevale, and G. Bodenhausen (talk)
- **XIXth Swiss NMR Symposium**, Universität Bern, January 17, 2012, *Homonuclear Decoupling in Time and Frequency Domain*, T.F. Segawa, D. Carnevale, and G. Bodenhausen (talk)
- **Swiss Chemical Society - 2010 Fall Meeting**, ETH Zürich, September 16, 2010, *New Methods in Nuclear Magnetic Resonance to Measure Transverse Relaxation Rates in Homonuclear J-coupled Systems*, T.F. Segawa, B. Baishya, N. Aeby, and G. Bodenhausen (talk)